

SOURCE OF THE CATALYTIC DIFFERENCES BETWEEN HUMAN CARBONIC
ANHYDRASES III AND II AS DETERMINED BY SITE-SPECIFIC
MUTAGENESIS

BY

PHILIP VICTOR LOGRASSO

A DISSERTATION PRESENTED TO THE GRADUATE SCHOOL
OF THE UNIVERSITY OF FLORIDA IN PARTIAL FULFILLMENT
OF THE REQUIREMENTS FOR THE DEGREE OF
DOCTOR OF PHILOSOPHY

UNIVERSITY OF FLORIDA

1992

To my father--for teaching me his principles: caring,
dedication, and honesty

To my mother--for her unconditional love

To my friends--for the good times

ACKNOWLEDGEMENTS

I am very grateful to many people for helping me in my work. Dr. David Silverman has been a true mentor. He has taught me to be a thorough and diligent scientist. The data analysis, writing, and organizational skills I have learned from him are invaluable.

Dr. C.K. Tu warrants a special mention because a great many problems were solved with a simple, "Hey Tu." I have learned a great deal about enzyme kinetics from Tu, but it is his generous spirit and willingness to help that I most hope I retain. Thanks Tu.

Three people have been a great help on the molecular biology aspect of this work: Drs. Phil Laipis, Susan Tanhauser, and David Jewell. Each has contributed to my knowledge in this field, and for that I am grateful.

George Wynns taught me a great deal about protein purification and deserves many thanks. Our conversations about baseball, Florida, and life always brightened the day. It was also a pleasure working with all of the staff in the Pharmacology Department. Special thanks go to Judy Adams for formatting this thesis and all her help.

Finally, no acknowledgement would be complete without thanking my parents and friends for their encouragement and love.

TABLE OF CONTENTS

	<u>page</u>
ACKNOWLEDGMENTS	iii
LIST OF TABLES	vi
LIST OF FIGURES	vii
LIST OF ABBREVIATIONS	ix
ABSTRACT	x
CHAPTER 1: INTRODUCTION	1
Investigating the Catalytic Mechanism of Carbonic Anhydrase using Site-Directed Mutagenesis	1
Genetic Differences and Tissue Distribution of Various Carbonic Anhydrase Isozymes	5
Biological Role of Carbonic Anhydrase III	7
Structure of Carbonic Anhydrase	8
General Shape of the Molecule	9
Secondary Structure	12
Catalytic Mechanism	18
Interconversion of CO ₂ and HCO ₃ ⁻	19
Proton Transfer	20
Dehydration	21
CHAPTER 2: THE MUTAGENESIS, EXPRESSION, PURIFICATION, AND KINETIC METHODS USED TO CREATE AND CHARACTERIZE HCA III MUTANTS	25
Mutagenesis	25
Growth of Phage	29
Isolation of ss template DNA	30
Phosphorylation and Hybridization of the Site-Specific Oligonucleotide	31
In Vitro Double Strand DNA Synthesis	32
Screening Potential Mutants	32
Cassette Mutagenesis	33
Creation of Remaining Mutants	35
Expression of HCA III Mutants in <i>E coli</i>	35
Purification of Human Carbonic Anhydrase Mutants Expressed in <i>E coli</i>	42
Steady-State Kinetic Methods	52
Stopped-Flow Spectrophotometry	52
4-Nitrophenyl Acetate Hydrolysis	54
Equilibrium Kinetic Methods	58

CHAPTER 3: CATALYTIC ENHANCEMENT OF HUMAN CARBONIC	
ANHYDRASE III BY REPLACEMENT OF PHE 198 WITH LEU	61
Introduction	61
Results	62
Discussion	77
Interconversion of CO ₂ and HCO ₃ ⁻	77
Proton Transfer	81
Inhibition	84
Conclusion	86
CHAPTER 4: EFFECTS OF THE MOLECULAR PROPERTIES OF	
RESIDUE 198 ON CATALYSIS AND INHIBITION OF HCA III	87
Introduction	87
Results	88
Discussion	98
Interconversion of CO ₂ and HCO ₃ ⁻	100
Proton Transfer	111
Inhibition	121
Conclusion	123
CHAPTER 5: DISCUSSION AND CONCLUSIONS	125
LIST OF REFERENCES	132
BIOGRAPHICAL SKETCH	138

LIST OF TABLES

<u>Table</u>	<u>Page</u>
1. Comparison of maximal steady-state rate constants and values of the apparent pK_a for the hydration of CO_2 and the hydrolysis of 4-nitrophenyl acetate catalyzed by HCA III and HCA II	3
2. Comparison of amino acid differences near the active sites of HCA III and HCA II	11
3. Maximal (pH-independent) steady-state constants and values of apparent pK_a for the hydration of CO_2 and the hydrolysis of 4-nitrophenyl acetate catalyzed by carbonic anhydrase and mutants	63
4. Inhibition constants K_I (micromolar) determined from R_1 , the catalyzed rate of interconversion of CO_2 and HCO_3^- at chemical equilibrium	75
5. Solvent hydrogen isotope effects on R_1 and R_{H_2O} catalyzed by HCA III, HCA II, and two mutants	76
6. Maximal (pH-independent) steady-state constants and values of the apparent pK_a for the hydration of CO_2 and rate of release of $H_2^{18}O$ catalyzed by mutant and wild-type carbonic anhydrases	89
7. Inhibition constants K_I (micromolar, ethoxzolamide), (millimolar, cyanate), determined from R_1 , the catalyzed rate of interconversion of CO_2 and HCO_3^- at chemical equilibrium	99

LIST OF FIGURES

<u>Figure</u>	<u>page</u>
1 Comparison of amino acid sequences for human CA II and CA III	10
2 X-ray crystal structure of part of the active site cavity of bovine carbonic anhydrase	13
3 Side-by-side representation of some of the amino acid side chains found in the active site cavity of carbonic anhydrase III and II	16
4 Oligonucleotide-directed mutagenesis using single-stranded template containing uracil residues	28
5 Location of key features on the pET81f1 HCA III expression vector	38
6 Time course of F198V HCA III synthesis after induction with 40 μ M IPTG	41
7 Flow chart detailing the purification of human carbonic anhydrase III mutants expressed in <i>E coli</i>	44
8 Elution profile of K64H-R67N HCA III after purification on DEAE-sephacel	48
9 UV absorbance spectrum for purified F198A HCA III	49
10 12% polyacrylamide gel detailing the levels of purity of K64H-R67N HCA III during the different stages of carbonic anhydrase purification	51
11 Typical data analysis used to calculate steady-state kinetic constants	56
12 Carbonic anhydrase catalyzed ^{18}O -exchange at chemical equilibrium	60
13 Comparisons of k_{cat}/K_m for hydration of CO_2 catalyzed by variants of HCA III obtained by site-directed mutagenesis at positions 64, 67, and 198 in the active site cavity of HCA III	66

14	The pH dependence of $R_{H_2O}/[E]$ for F198L HCA III; R67N-F198L HCA III; and K64H-R67N-F198L HCA III	69
15	Comparison of the water-off rates, $R_{H_2O}/[E]$ for variants of HCA III at positions 64, 67, and 198 in the active site cavity of HCA III	71
16	The dependence on the imidazole concentration of $R_{H_2O}/[E]$ and $R_1/[E]$ catalyzed by F198L HCA III; R67N-F198L HCA III; and K64H-R67N-F198L HCA III	73
17	The pH dependence of the logarithm of k_{cat}/K_m for the hydration of CO_2 catalyzed by F198D HCA III, and F198N HCA III	92
18	The pH dependence of the logarithm of k_{cat} for the hydration of CO_2 catalyzed by F198D HCA III, and F198N HCA III	94
19	The pH dependence of $R_{H_2O}/[E]$ for F198D HCA III, and F198N HCA III	97
20	Plot of the logarithm of k_{cat}/K_m for CO_2 hydration versus pK_a of zinc-bound water for six amino acid replacements at position 198 and for wild-type HCA III	102
21	Plot of the logarithm of k_{cat}/K_m for CO_2 hydration versus the logarithm of $K_I^{OCN^-}$ for six amino acid replacements at position 198 and for wild-type HCA III	107
22	Plot of the logarithm of k_{cat} versus ΔG transfer of the amino acid side chain from nonaqueous solution to water	118

LIST OF ABBREVIATIONS

BCA	bovine carbonic anhydrase
BSA	bovine serum albumin
CA	carbonic anhydrase
CD	circular dichroism
cDNA	complimentary DNA
CHES	2[N-cyclohexyl amino] ethanesulfonic acid
DEAE-sephacel	diethylaminoethyl sephacel
DNA	deoxyribonucleic acid
DNase	deoxyribonuclease
dsDNA	double-stranded DNA
DTT	dithiothreitol
EDTA	ethylenediaminetertaacetic acid
g	gravitational force
HCA	human carbonic anhydrase
HEPES	N-2-hydroxyethylpiperazine-N'- 2-ethanesulfonic acid
IPTG	isopropylthio- β -D-galatopyranoside
kDa	kilodalton
LB	Luria broth
MOPS	3-(N-morpholino)propanesulfonic acid
MW	molecular weight
NMR	nuclear magnetic resonance
OD	optical density
PEB	phenol extraction buffer
PEG	polyethylene glycol
SDS	sodium dodecyl sulfate
SSC	standard sodium citrate buffer
ssDNA	single-stranded DNA
TAPS	N-{[Tris(hydroxymethyl)methyl] amino} propane sulfonic acid
TBE	tris-borate EDTA
Tris	tris(hydroxymethyl)aminomethane

Abstract of Dissertation Presented to the Graduate School
of the University of Florida in Partial Fulfillment of the
Requirements for the Degree of Doctor of Philosophy

SOURCE OF THE CATALYTIC DIFFERENCES BETWEEN HUMAN CARBONIC
ANHYDRASES III AND II AS DETERMINED BY SITE-SPECIFIC
MUTAGENESIS

By

Philip V. LoGrasso

May, 1992

Chairman: David N. Silverman

Major Department: Pharmacology and Therapeutics

The objective of this work was to determine which of the unique amino acids near the active site of the low activity human carbonic anhydrase (HCA III) is the molecular source of the 500-fold difference in catalytic and inhibition properties between HCA III and human carbonic anhydrase II (HCA II).

Mutants of HCA III were made by oligonucleotide-directed mutagenesis replacing three residues near the active site with amino acids known to be at the corresponding positions in HCA II (Lys 64 → His, Arg 67 → Asn, and Phe 198 → Leu). Emphasis was placed on Phe-198 where replacement residues varied in size, charge, and hydrophobicity and were selected

to test how these physical properties would affect CO₂ hydration, 4-nitrophenyl acetate hydrolysis, and inhibitor binding. Catalytic properties were measured by stopped-flow spectrophotometry and ¹⁸O exchange between CO₂ and water using a mass spectrometer.

Replacing Phe-198 with Ala, Asn, Asp, Leu, Tyr, and Val caused an increase in k_{cat}/K_m with Phe 198 → Asp having the largest increase, approximately 130-fold greater than wild-type HCA III. In general, non-hydrogen bonding residues at position 198 (Ala, Val, Leu) had a maximal velocity 10-fold greater than hydrogen bonding residues (Asn, Asp, Phe, Tyr) where Phe 198 has been shown to be hydrogen bonded to active-site water. In addition, a correlation between hydrophobicity and the turnover number was found.

The triple mutant, with the replacements Lys 64 → His, Arg 67 → Asn, and Phe 198 → Leu had a CO₂ hydration activity, a turnover number for CO₂ hydration, and an activity for 4-nitrophenyl acetate hydrolysis which approximated within 5-fold that of HCA II in magnitude and pH profile.

These data suggest that Phe 198 is a major contributor to the low CO₂ hydration activity, the low pK_a of the zinc-bound water, and is a major interactive binding site of sulfonamides and cyanate in HCA III. Moreover, the correlation between the turnover number and hydrogen-bonding capability or hydrophobicity suggests an altered proton transfer pathway in the mutants.

CHAPTER 1 INTRODUCTION

Investigating the Catalytic Mechanism of Carbonic Anhydrase Using Site-Directed Mutagenesis

The carbonic anhydrases (CA) are zinc-containing metalloenzymes which catalyze the following reversible reaction: $\text{CO}_2 + \text{H}_2\text{O} \rightleftharpoons \text{HCO}_3^- + \text{H}^+$. Carbonic anhydrase is a relatively small protein existing as a monomer and having an approximate molecular weight of 30 kDa. It contains one zinc atom/molecule protein which is located at the bottom of a conical cavity 15 Å from the surface of the protein. The zinc ion is coordinated to the imidazole ring of three histidine residues, numbers 94, 96, and 119, in a slightly distorted tetrahedral geometry (Eriksson et al., 1988). A fourth coordination site harbors a water molecule. It is this metal center which is believed to be directly involved in the conversion of CO_2 to HCO_3^- . Accordingly then, the ionization of the zinc-water is critical in the catalytic pathway.

Of the eight genetically-distinct isozymes of carbonic anhydrase (Kato, 1990; Tashian, 1989) known to catalyze the above reaction, two of them, CA III and CA II found primarily in red skeletal muscle and red blood cells, respectively,

provide a useful venue for investigations of catalytic mechanism using site-directed mutagenesis because they have large differences in enzymatic activity with very similar backbone structures. The high activity form, isozyme II, has a steady-state turnover number for CO₂ hydration of $1.4 \times 10^6 \text{ s}^{-1}$ (Khalifah, 1971) and is indeed one of nature's most catalytically efficient enzymes. Conversely, isozyme III has a turnover number of $1 \times 10^4 \text{ s}^{-1}$ (Jewell et al., 1991; Silverman and Lindskog, 1988) that is approximately 140-fold smaller than that of CA II (Table 1). In conjunction with the sizable differences in turnover number between the two isozymes, they also show significantly different $k_{\text{cat}}/K_{\text{m}}$ values. For example, CA II has $k_{\text{cat}}/K_{\text{m}}$ at $1.5 \times 10^8 \text{ M}^{-1}\text{s}^{-1}$ (Khalifah, 1971) (Table 1), close to the diffusion controlled limit, whereas CA III has $k_{\text{cat}}/K_{\text{m}}$ at $3 \times 10^5 \text{ M}^{-1}\text{s}^{-1}$ (Jewell et al., 1991). To date, it remains unclear as to what primary structural features are the source for this large catalytic difference between these two isozymes. It is one purpose of this study to investigate which amino acids in the active-site of isozyme III may account for this considerable difference. Particular emphasis will be placed on phenylalanine (Phe) 198.

In addition to their different catalytic efficiencies, their ability to be inhibited by sulfonamides is different. The binding constant for inhibition by acetazolamide (Sanyal et al., 1982; Tu et al., 1983; Engberg et al., 1985; Karali and Silverman, 1985) is much weaker for isozyme III compared

Table 1. Comparison of maximal steady-state rate constants and values of the apparent pK_a for the hydration of CO_2 and the hydrolysis of 4-nitrophenyl acetate catalyzed by HCA III and HCA II.

Enzyme	$k_{cat}/K_m (M^{-1}s^{-1})$	$k_{cat} (s^{-1})$	$k_{enz} (M^{-1}s^{-1})$	pK_a	$K_I (\mu M)$
HCA III	$3 \times 10^5 (a)$	$1 \times 10^4 (a)$	11 (b)	<6.0	8.0 (e)
HCA II	$1.5 \times 10^8 (c)$	$1.4 \times 10^6 (c)$	$2.7 \times 10^3 (d)$	6.9 (d)	0.008 (e)

K_I values for ethoxzolamide were measured at chemical equilibrium. k_{enz} is k_{cat}/K_m for 4-nitrophenyl acetate hydrolysis. The precise pK_a of HCA III has not been determined, but is estimated to be < 6.0 (Engberg and Lindsog, 1984; Karali and Silverman, 1985; Ren et al, 1988). a = Jewell et al., 1991; b = Tu et al., 1986; c = Khalifah, 1971; d = Steiner et al., 1975; e = LoGrasso et al., 1991.

with isozyme II. Similarly, ethoxzolamide binds CA II more tightly than CA III (Table 1). A third major difference that exists between these two isozymes is in their ability to hydrolyze esters such as p-nitrophenyl acetate. CA II possesses considerable activity (Steiner et al., 1975) for this process while CA III has a negligible activity (Tu et al., 1986) (Table 1). Another major difference is the pK_a of the main activity-controlling group, which is zinc-bound water for both CO_2 hydration and ester hydrolysis. Isozyme III has a pK_a for zinc-bound water that is at least one pK_a unit lower than that of isozyme II (Engberg and Lindskog, 1984; Kararli and Silverman, 1985; Ren et al., 1988). Values for these pK_a s are given in Table 1.

Despite the considerable differences in catalytic and inhibition properties between CA III and CA II, the two isozymes have backbone conformations which are very similar. Comparison of the x-ray crystal structures from human carbonic anhydrase II (HCA II) and bovine carbonic anhydrase III (BCA III) shows a root mean square difference in location of main chain atoms of 0.92 Å (Eriksson, 1988). This difference is even lower for many residues near the active site. Since human carbonic anhydrase III (HCA III) is 89% identical in primary sequence to BCA III, it is believed that its structure is nearly identical to that of BCA III.

With these catalytic differences and structural similarities in mind, one intent of this study is to gain a mechanistic understanding of carbonic anhydrase using site-

specific mutants of isozyme III to determine the molecular source of these considerable differences.

Genetic Differences and Tissue Distribution of Various Carbonic Anhydrase Isozymes

Eight genetically distinct isozymes of carbonic anhydrase have now been identified in mammals (Tashian, 1989; Kato, 1990). Four of these (coding for CA I, CA II, CA III, and CA VII) have been fully or partially characterized (Venta et al., 1985; Lloyd et al., 1986; Brady et al., 1987; Yoshihara et al., 1987; Montgomery, 1988) with regard to their intron and exon structure. The human CA I, CA II, and CA III genes are linked on chromosome 8 (Davis et al., 1987) whereas the genes coding for CA VI and VII have been located on chromosomes 1 and 16, respectively. In addition, the nucleotide sequence of a full length cDNA clone which encodes the human muscle-specific carbonic anhydrase (CA III) has been reported (Lloyd et al., 1986). This cDNA identifies a 1.7-kb mRNA coding for the protein. To date, the chromosomal positions of CA IV and CA V have yet to be identified.

It has been demonstrated by a variety of biochemical methods (Siffert and Gros, 1982; Shima et al., 1983; Dermietzel et al., 1985) that at least three types of carbonic anhydrase are present in striated muscle. CA III is found in rather large quantities in the cytosol of red (i.e. predominantly slow-oxidative) skeletal muscle and can comprise as much as 20% of all cytosolic protein (Gros and

Dodgson, 1988). It is found in contrastingly low quantities in white (i.e. fast-glycolytic) muscles. In comparison, the high activity CA II isozyme is either absent or low in red muscles, exemplified by soleus and vastus intermedius, and high in white muscle such as tibialis anterior and gastronemius. In addition to isozymes II and III, a high activity CA, identified as CA IV, could be extracted from membrane fractions.

CA III is also found in liver of non-primates, salivary glands, red cells, lung, and kidney. CA I and CA II, on the other hand, are widely distributed in red blood cells (where CA I is the most abundant protein next to hemoglobin in these cells) and secretory tissues such as the lens and ciliary body of the eye. CA V is a mitochondrial carbonic anhydrase which has been found in the kidney and liver (Tashian, 1989).

Lastly, it has been shown (Carter et al., 1984; Jeffery et al., 1984; Jeffery et al., 1986) in rat liver that CA III is low in females and high in males and is apparently under control of growth hormone. However, there is no evidence to suggest that levels of CA III in muscle are different between males and females (Shiels et al., 1984). Moreover, Wistrand et al. (1987) using immunofluorescence microscopy showed that denervation of fibers of rat soleus, tibialis anterior, and exterior digitorum longus muscles markedly raised CA III levels in all three fibers, especially in type II fibers which normally lack CA III.

Biological Role of Carbonic Anhydrase III

Three primary biological activities of CA III have been studied. They include: CO₂ hydratase activity; ester hydrolysis activity; and a phosphatase activity. To date, the only one of these activities which is believed to have any physiological significance is the CO₂ hydratase activity.

In 1935, Roughton reasoned that carbonic anhydrase in the muscle would be an enemy to the cell rather than an aid due to its fast kinetics of CO₂ hydration (Roughton, 1935). Conversely, after the discovery of isozyme III, many questioned whether the role of CA III was as a CO₂ hydratase at all due to its low specific activity. In fact, it has been shown (Gros and Dodgson, 1988) that carbonic anhydrase in the muscle accelerates the rate of CO₂ hydration in the rabbit soleus by a factor of 400. This significant increase, in spite of the enzyme's low turnover number, can largely be attributed to the relatively high concentration of CA III in red muscle fibers which has been shown to be 0.5 mM in rat soleus (Carter et al., 1982). In addition, Gros et al. (1987) have shown that CO₂ diffusion in rat abdominal muscle can be suppressed if the muscle is incubated with acetazolamide concentrations which are high enough to indicate the involvement of the sulfonamide-resistant carbonic anhydrase (CA III). Thus, they concluded that the primary role of CA III is for the facilitation of CO₂ diffusion.

Tu et al. (1986) have shown that BCA III has a negligible esterase activity, which probably occurs at a site different than the active site of CO₂ hydration. This evidence comes from experiments in which the zinc atom was removed from the enzyme, and others in which high concentrations of known inhibitors of CA such as N₃⁻, CNO⁻, and some sulfonamides had no effect on the activity. Other reports (Engberg et al., 1985; Jewell et al., 1991) have also shown this to be the case for BCA III and HCA III, respectively.

There is also evidence for a phosphatase activity in CA III (Koester et al., 1981; Nishita and Deutsch, 1986). However, it has been suggested that the difference in pH dependence between the phosphatase activity and the CO₂ hydratase activity, and the difference in inhibition potency using phosphate, molybdate, fluoride, and acetazolamide for these two activities, are the active site is different for these two activities. Furthermore, and perhaps most importantly, no physiological substrate for the phosphatase activity is known (Gros and Dodgson, 1988).

Structure of Carbonic Anhydrase

Figure 1 presents a comparison of the amino acid sequences for human CA II, and CA III. Isozymes II and III show a 56% identity in their primary sequences (Tashian, 1989). Of the 36 residues postulated to occur within the active-site cavity of carbonic anhydrase (Tashian, 1989), 25

are invariant between HCA III and HCA II. Some notable differences of amino acids near the active sites of HCA III and HCA II are compared in Table 2. Three major differences which have been the focus of considerable work are the residues, lysine (Lys) 64, arginine (Arg) 67, and phenylalanine (Phe) 198. With the exception of horse CA III, which has Arg 64, the other isozymes of vertebrate carbonic anhydrase sequenced to date have these residues unique to isozyme III. In HCA II these residues are histidine (His) 64, asparagine (Asn) 67, and leucine (Leu) 198.

General Shape of the Molecule

The crystal structures for both HCA II (Liljas et al., 1972; Eriksson et al., 1988) and BCA III (Eriksson, 1988) have been determined at 2.0 Å resolution. The general shape of HCA II can be described as an ellipsoid with approximate dimensions 54x42x39 Å³ measured between extremes of the backbone. Since the structures of BCA III and HCA II are nearly identical (Eriksson, 1988), the dimensions for HCA II are an excellent approximation for BCA III. Indeed, Engberg et al. (1985) have shown that the hydrodynamic properties of isozyme III are very similar to isozymes I and II suggesting that isozyme III, like isozymes I and II, is a compact nearly spherical molecule.

	1	10	20	30	40	50	60	70
HUMCA2	MSHHWCYCKHNGPEHWHKDFPIAKGERQSPVDIDHTAKYDPSLKPLSVSYDQATSLRILNNGHAFNVEF							
	:	:	:	:	:	:	:	:
HUMCA3	MAKEWGYASHNGPDWHHELFPNAKGENQSPVELHTKDIRHDPQLQPSVSYDGGSAKTIILNNGKTCRVVF							
	:	:	:	:	:	:	:	:
	71	80	90	100	110	120	130	140
HUMCA2	DDSQDKAVLKGGLDGTYYRLIQFHFHWGSLDGQSEHTVDKKYAAELHLVHWNTKYGDFGKAVQQPDGL							
	:	:	:	:	:	:	:	:
HUMCA3	DDTYDRSMLRGGLPGPYRLRQFHLHWGSSDDHGSEHTVDGVKYYAAELHLVHWNPKNYTFKEALKQRDGI							
	:	:	:	:	:	:	:	:
	141	150	160	170	180	190	200	210
HUMCA2	AVLGIFLKVGSAPGLQKVVDVLDISIKTKGKSADFTNFDPRGLLPESLDYWTYPGSLTTPPLLECVTWIV							
	:	:	:	:	:	:	:	:
HUMCA3	AVIGIFLKIGHENGFEQIFLDALDKIKTKGKEAPFTKFDPSCLFPACRDYWTYQGSFTTPPCEECIVWLL							
	:	:	:	:	:	:	:	:
	211	220	230	240	250	260		
HUMCA2	LKEPISVSSEQLKFRKLNFNNGEPEELMVDNWRPAQPLKNRQIKASF							
	:	:	:	:	:	:	:	:
HUMCA3	LKEPMTVSSDQMAKRLSLLSSAENEPPVPLVSNWRPPQPINNRVVRASF							
	:	:	:	:	:	:	:	:

Figure 1. Comparison of amino acid sequences for human CA II and CA III.

The human sequence is derived from the nucleotide sequence for HCA III. (See Henderson et al., 1973; Lin and Deutsch, 1974; Lloyd et al., 1986). Dashed lines between residues in HCA II AND HCA III indicate amino acid identity between the two isozymes.

Table 2. Comparison of amino acid differences near the active sites of HCA III and HCA II.

Amino acid position	HCA III	HCA II
64	Lys	His
65	Thr	Ala
66	Cys	Phe
67	Arg	Asn
91	Arg	Ile
141	Ile	Leu
198	Phe	Leu
204	Glu	Leu
207	Ile	Val
211	Leu	Val

Secondary Structure

The high resolution x-ray data show the major secondary structure of HCA II to be a central β -pleated sheet made up of ten segments involving approximately 30% of the amino acid residues (Kannan, 1980). There are a number of minor pleated sheet structures as well as two well defined α -helical regions. Other α -helices are of the distorted 3_{10} type. Overall, the secondary structure of carbonic anhydrase has been shown to be 17% helix and 40% β -sheet. These estimations are in close agreement with Raman scattering studies (Craig and Garber, 1977) which indicate HCA I is 19% helix and 39% β -sheet. Moreover, infrared absorption spectra (Timasheff et al., 1967) and circular dichroism (CD) spectra (Beychok et al., 1966; Coleman, 1968) both confirm the presence of antiparallel β -structures in carbonic anhydrase.

The active site cavity of carbonic anhydrase lies on a β -pleated sheet structure consisting of four antiparallel strands designated γ , δ , ϵ , and ζ (Liljas et al., 1972). The active site is easily located by the presence of the essential zinc atom which is found at the apex of the conical active site cavity. Three histidyl residues, two of them His 94 and His 96 reside on the δ strand, and one His 119 resides on the ϵ strand of the β -structures, along with a water molecule ligand to the zinc forming a distorted tetrahedral geometry. Figure 2 presents the x-ray crystal structure of part of the active site of BCA III (Eriksson, 1988). The

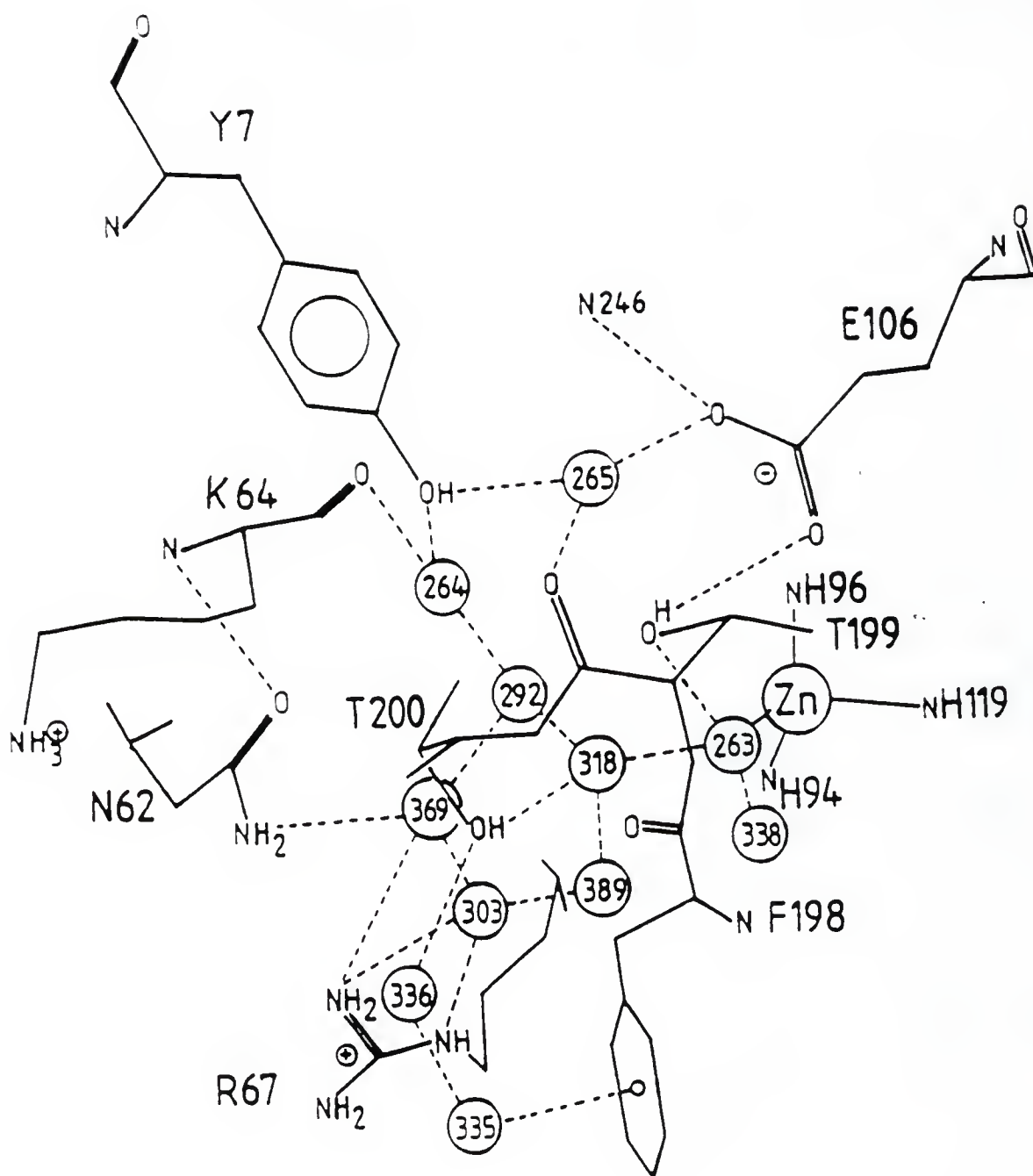


Figure 2. X-ray crystal structure of part of the active site cavity of Bovine Carbonic Anhydrase III (Eriksson, 1988).

water ligand (water #263) of the zinc is hydrogen bonded to the side-chain hydroxyl group of threonine (Thr) 199 which in turn is hydrogen bonded to the carboxylate of glutamate (Glu) 106. Other active site water molecules are presented as well as the unique residues Lys 64, Arg 67, and Phe 198.

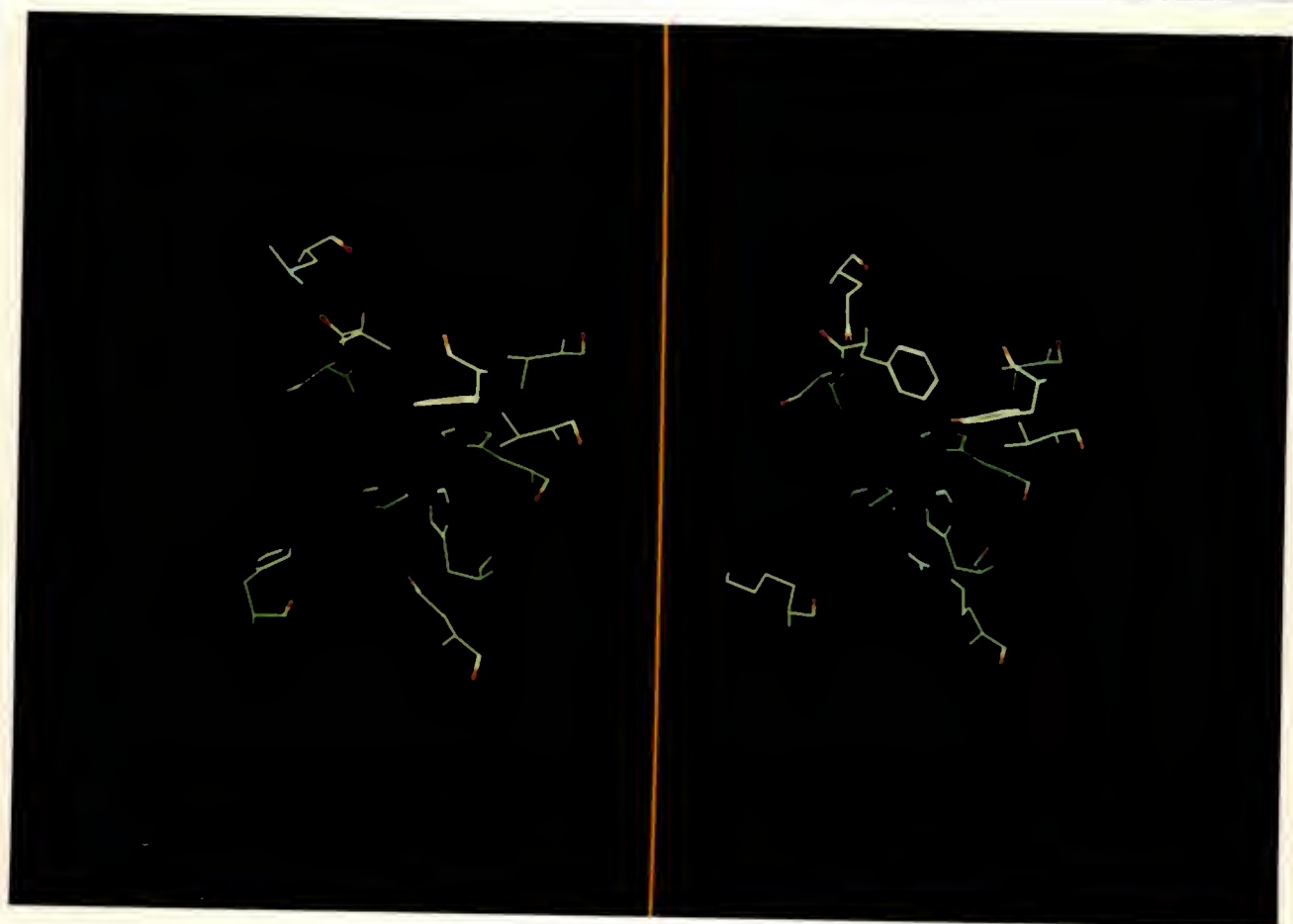
Aside from the central zinc atom the active site cavity of carbonic anhydrase can be characterized by its hydrophilic and hydrophobic portions. The hydrophilic region of isozyme III contains the unique residues Lys 64 and Arg 67 as well as the three His ligands (94, 96, 119) to the zinc. Additionally, Thr 199, Thr 200, and Tyr 7 are also found in this portion of the molecule. The most important residue in terms of this work that appears in the hydrophobic region of the active site cavity is Phe 198. Other potentially important residues that reside in this region are Arg 91, Val 121, Phe 131, Val 143, and Glu 204.

The closeness in backbone structures between BCA III and HCA II is illustrated in Figure 3 which presents the side-by-side structures of these two isozymes. The root mean square fit for 95 main chain residues situated in the central β -sheet structures of BCA III and HCA II (numbers 39-41, 89-98, 115-123, 140-149, 168-176, 187-218, and 256-260) was found to be 0.39 Å (Eriksson, 1988) indicating nearly identical structures for those residues.

Despite this closeness in backbone structure between BCA III and HCA II, the x-ray crystal data indicate that the

Figure 3. Side-by-side representation of some of the amino acid side chains found in the active site cavity of carbonic anhydrase III (right panel) and II (left panel).

The atoms are colored by type: oxygen is red; nitrogen is blue; and carbon is green. Due to film exposure, some carbon atoms photographed yellow. Central to the BCA III structure (right panel) are the three histidine ligands coordinated to the zinc (not pictured); and the unique residues Phe 198, Lys 64, and Arg 67. Additionally Tyr 131 can be found orthogonal to Phe 198. For comparison, the left panel shows the corresponding residues of HCA II which are Leu 198, His 64, Asn 67, and Phe 131. Both structures present identical molecular orientations. These structures are taken from the x-ray crystal data of Eriksson (1988) for BCA III and Eriksson et al.(1988) for HCA II.



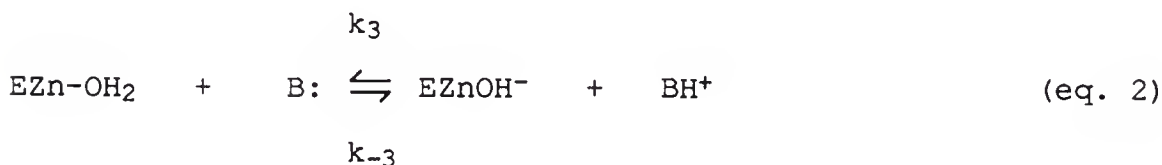
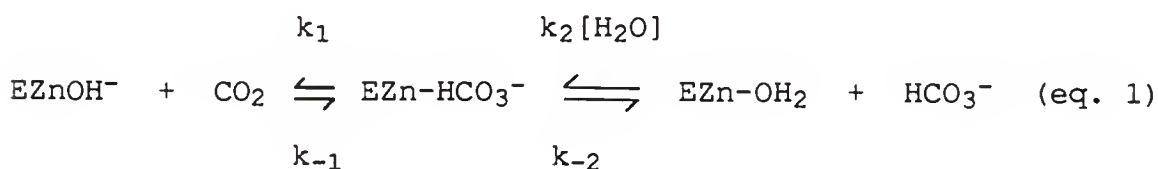
active site cavity of BCA III is much more sterically constrained than HCA II (Eriksson, 1988). This has largely been attributed to two residues in BCA III: Arg 67 and Phe 198. These residues are Asn and Leu respectively in HCA II. The distance between the N- ζ atom of Arg 67 and the zinc ion is 8.7 Å. The distance between the C- α atom of the Phe 198 side-chain and the zinc ion is 7.38 Å (Eriksson, 1988). Eriksson gives no quantitative measure as to how much the active site cavity volume is reduced by these unique residues, but comparison of the volumes of these two residues shows Phe to be 203.4 Å³ and Leu to be 167.9 Å³ (Richards, 1977).

Lastly, it should be noted that several other features of the Phe 198 side-chain could contribute to structural, catalytic and inhibition differences between the two isozymes. For example, water 335 has been shown to hydrogen bond to the π -electron system of the benzene ring of Phe 198. In turn water 335 is involved in a hydrogen bonding network through the hydroxyl group of Thr 200 and water 318 to the zinc-bound water of the active site (Eriksson, 1988) (Figure 2). Since no analogous pattern is possible for HCA II, which contains leucine at position 198, this unique water structure could be responsible for the unique catalytic properties of HCA III. Furthermore, Eriksson et al. (1988) have shown Leu 198 to be in van der Waals' contact with sulfonamide and anion inhibitors. Therefore, the steric bulk of Phe 198

could indeed be the reason why sulfonamides are such poor inhibitors of CA III.

Catalytic Mechanism

There is a wide body of evidence (Silverman et al., 1979; Simonsson et al., 1979; Tu et al., 1990; Rowlett et al., 1991) which supports a catalytic mechanism for carbonic anhydrase that occurs in two distinct and separate processes. The first stage of catalysis for hydration of CO₂ is the nucleophilic attack of EZnOH⁻ on CO₂ to yield HCO₃⁻. The release of HCO₃⁻ from the enzyme results in water bound to the metal (eq. 1). The second stage of catalysis involves a rate-contributing proton transfer from EZnOH₂ to buffer to regenerate the active form of the enzyme, EZnOH⁻, thus completing the catalytic cycle (eq. 2).



Interconversion of CO_2 and HCO_3^-

As seen in equation 1, the interconversion of CO_2 and HCO_3^- contains rate constants in the pathway up to and including release of HCO_3^- from the enzyme. In terms of the Briggs-Haldane steady-state approximation, the apparent second order rate constant, k_{cat}/K_m , is equal to $k_1k_2/(k_{-1} + k_2)$ for this simplified pathway. For HCA II, it has been shown that k_{cat}/K_m is dominated by k_1 (Lindskog, 1984). On the other hand, Rowlett et al. (1991) have shown that, unlike isozyme II, isozyme III probably has significant contributions for k_{cat}/K_m from all three constants, k_1 , k_{-1} , and k_2 .

For the hydration of CO_2 catalyzed by CA II, k_{cat}/K_m has been shown to have a pH-profile which can be described by a simple titration curve having a single ionization with a pK_a near 7 (Khalifah, 1971; Steiner et al., 1975). This pK_a has been attributed to zinc-bound water and has much experimental support (Simonsson and Lindskog, 1982). CA III, on the other hand, shows pH-profiles for k_{cat}/K_m which are independent of pH in the range of 6 to 9 (Tu et al., 1983; Engberg and Lindskog, 1984; Karali and Silverman, 1985; Ren et al., 1988).

Data from solvent hydrogen isotope effect studies on HCA II (Steiner et al., 1975; Venkatasubban and Silverman, 1980) in H_2O and D_2O show an isotope effect near unity for k_{cat}/K_m suggesting CO_2 and HCO_3^- interconversion occurs in a step independent of a rate-limiting proton transfer step. These

data, taken together with the pH-rate profile data, are highly indicative of two separate and independent processes for this catalytic mechanism. Further support for the veracity of these conclusions will be presented when the dehydration aspect of this mechanism is considered.

Proton Transfer

As described in equation 2, the catalyzed hydration of CO₂ requires that a proton be transferred from the active site of carbonic anhydrase to the surrounding medium. Since it was known that proton transfer from a group of pK_a 7 to water could be transferred at a maximal rate of 10³-10⁴ s⁻¹ (Eigen, 1964), it was initially a dilemma to explain how CA II could have a turnover number of 10⁶ s⁻¹. In 1973, several workers (Khalifah, 1973; Lindskog and Coleman, 1973) suggested that proton transfer was to buffer in solution rather than water.

For isozyme II, there are many studies (Steiner et al., 1975; Tu et al., 1989) which show that His 64 acts as a proton shuttle enhancing activity by increasing the rate described in equation 2. Data from solvent hydrogen isotope effects (Venkatasubban and Silverman, 1980) indicate that proton transfer proceeds through at least two hydrogen-bonded water molecules which are suggested to be the ones situated between the zinc-water and the imidazole of the side-chain of His 64.

For isozyme III, it has been observed that the turnover number is 10^3 - 10^4 s⁻¹ (Karali and Silverman, 1985; Jewell et al., 1991) consistent with proton transfer to water. However, Rowlett et al. (1991) and Jewell et al. (1991) have shown that HCA III is capable of intramolecular proton transfer at high pH through lysine 64. This approximate 5-fold increase in k_{cat} at pH values > 8 can be correlated with the pK_a of lysine. Moreover, Tu et al. (1990) have shown that proton transfer in catalysis by HCA III can be enhanced 6-fold by the addition of 100 mM imidazole. These data suggest that the imidazole side-chain of the buffer can act in lieu of the imidazole side-chain of His 64 which is naturally present in CA II, but absent in CA III.

Finally, it should be noted that there is a body of data from solvent hydrogen isotope effects for both isozymes (Steiner et al., 1975; Karali and Silverman, 1985; Tu et al., 1990) which indicate that the proton-transfer step described by k_{cat} is rate-limiting and separate from the steps involved in CO_2 and HCO_3^- interconversion.

Dehydration

The mechanism can also be studied in the dehydration direction at chemical equilibrium. In this method, the exchange of ^{18}O between CO_2 and H_2O , and between ^{12}C and ^{13}C labeled CO_2 can be followed (Silverman and Tu, 1975; Silverman et al., 1979). In these experiments, two rates for

catalysis at chemical equilibrium are determined. The first is R_1 , the rate of interconversion of CO_2 and HCO_3^- (eq. 3).



In this dehydration reaction (eq. 3), the ^{18}O -label from substrate bicarbonate transiently labels the active site of carbonic anhydrase. Since $^{13}\text{CO}_2$ is also present at chemical equilibrium, one possible fate of the ^{18}O -label is hydration of $^{13}\text{CO}_2$. (The experimental details of this method will be discussed in chapter 2). A second possible fate of this ^{18}O -label is release to water, a step which can occur independently of the first step. From these processes, two experimental rate constants can be determined. ϕ_{cat} is the rate constant which describes the exchange of ^{18}O between ^{12}C and ^{13}C species of CO_2 . θ_{cat} is the rate constant describing the loss of ^{18}O -label to water. (The rate of release of ^{18}O -labeled water, $R_{\text{H}_2\text{O}}$ will be discussed shortly.) Silverman et al. (1979) have described these rate constants in detail and have derived equations which express R_1 and $R_{\text{H}_2\text{O}}$ in terms of θ_{cat} and ϕ_{cat} .

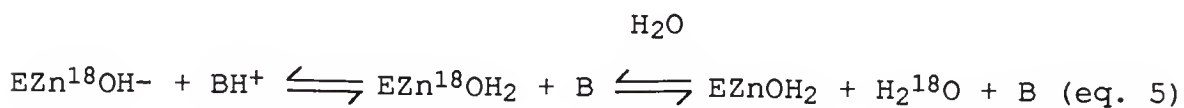
The measurement of ^{13}C NMR line widths also gives the catalytic rate at chemical equilibrium between CO_2 and HCO_3^- (Simonsson et al., 1979). These researchers found that the rate of CO_2 and HCO_3^- interconversion at chemical equilibrium can be expressed in the form of the Michaelis-Menten

equation. Similarly, Silverman et al. (1979) found that R_1 could also be expressed in this form (eq. 4):

$$R_1 = k_{\text{cat}}^{\text{exch}} [\text{S}_{\text{tot}}] [\text{E}_{\text{tot}}] / (K_{\text{eff}} + [\text{S}_{\text{tot}}]) \quad (\text{eq. 4})$$

where K_{eff} is the apparent binding constant between substrate and enzyme. Finally, $k_{\text{cat}}^{\text{exch}}/K_{\text{eff}}$ has been shown to be equivalent to k_{cat}/K_m .

As mentioned earlier, two rates for catalysis are measured at chemical equilibrium. The second of these two, $R_{\text{H}_2\text{O}}$, is the rate of release of ^{18}O -labeled water from the active site. This rate is given by equation 5:



In terms of the mechanism presented in equation 5, it is seen that $R_{\text{H}_2\text{O}}$ involves a proton transfer from BH^+ (which can be buffer in solution, water in the active site, or a group on the enzyme such as histidine) to the zinc-bound hydroxide in the active site. This forms a zinc-bound water which is readily exchangeable with solvent water (Tu and Silverman, 1985). Thus, $R_{\text{H}_2\text{O}}$ describes the proton transfer dependent rate of release of ^{18}O -labeled water from the active site of carbonic anhydrase.

Much experimental evidence exists for two distinct and separate aspects of catalysis by carbonic anhydrase at

chemical equilibrium. The bulk of this evidence comes from buffer dependence and solvent isotope experiments conducted by ^{13}C NMR (Simonsson et al., 1979) and ^{18}O -exchange using mass spectrometry (Silverman et al., 1979; Tu et al., 1990).

The ^{13}C NMR studies show that the exchange of CO_2 and HCO_3^- is equally rapid in H_2O and D_2O indicating this process is not dependent on, and separate from, a rate-contributing proton transfer step. Furthermore, they show that the exchange is equally rapid in the presence or absence of buffers indicating that no buffer dependent steps are located on the pathway of CO_2 and HCO_3^- exchange.

Similarly, the ^{18}O -exchange studies (Silverman et al., 1979; Tu et al., 1990) show that R_1 is independent of buffer indicating no buffer dependent steps for CO_2 and HCO_3^- exchange. Conversely, they found $R_{\text{H}_2\text{O}}$ was indeed dependent on buffer concentration indicating a proton transfer step facilitated by the presence of buffers.

Finally, it has been shown for both HCA III (Karali and Silverman, 1985) and HCA II (Tu and Silverman, 1982) that R_1 is essentially the same in H_2O and D_2O indicating that CO_2 and HCO_3^- interconversion is independent of a rate contributing proton transfer, whereas $R_{\text{H}_2\text{O}}$ is highly dependent (especially for HCA II) on this process.

Thus, just as in the case as the steady-state, there is a wealth of experimental evidence at chemical equilibrium which suggests that the catalytic mechanism of carbonic anhydrase occurs in two distinct and separate steps.

CHAPTER 2
THE MUTAGENESIS, EXPRESSION, PURIFICATION AND KINETIC METHODS
USED TO CREATE AND CHARACTERIZE HCA III MUTANTS

Mutagenesis

The molecular biological effort of this project is the creation and expression of site-specific mutants of human carbonic anhydrase III. Two primary means of mutagenesis were used. The first was an oligonucleotide-directed mutagenesis approach developed by Kunkel (1985) and Kunkel et al. (1987). The second was a cassette mutagenesis approach developed by Wells et al. (1985).

Kunkel (1985) and Kunkel et al. (1987) have described a method using the *E coli* strain BW313 (*dut*⁻ *ung*⁻) to create a DNA template which contains a small number of uracil residues in place of thymine. *E coli* *dut*⁻ mutants lack the enzyme dUTPase. This causes an elevation of dUTP levels allowing effective competition with TTP for incorporation into DNA. *E coli* *ung*⁻ mutants lack the enzyme uracil N-glucosylase which normally excises uracil from DNA. Thus, the combination of the two mutants allows successful incorporation of uracil into DNA in place of thymine. After the *in vitro* extension reaction, the double stranded plasmid composed of one uracil containing strand and one strand containing the introduced

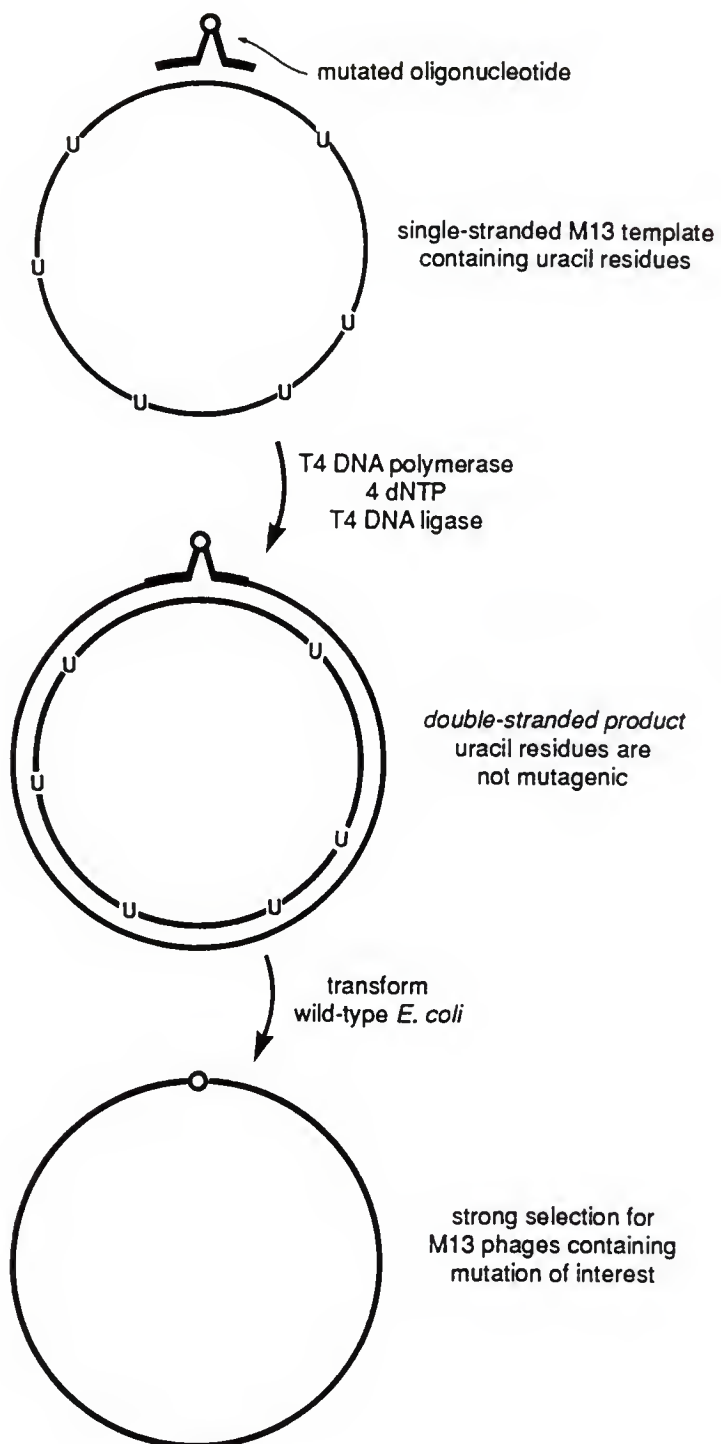
mutation, is transformed into a $\text{dut}^+ \text{ung}^+$ *E coli* host (TG-1) which selectively degrades the uracil containing strand. Upon subsequent bacterial replication a mutant plasmid is produced. This scheme is illustrated in Figure 4.

The mutants K64H-R67N HCA III, R67N-F198L HCA III, and R67N-F198A HCA III were created using the following procedure: Initially, 5 μl of a 50% glycerol stock of *E coli* BW313 were grown in 2 ml of Luria broth (LB). The media consists of 10.0 g tryptone (Difco Laboratories); 5.0 g yeast extract (Difco Laboratories); 5.0 g NaCl per liter of deionized water. The pH of this medium is raised from 7.2 to 7.4 with 12 M NaOH and the medium is autoclaved for sterility. All cultures were grown for 12 to 16 hours at 37°C and agitated for oxygenation at 280 rpm.

Competent *E coli* BW313 for transformation were prepared as follows: 1 ml of the overnight culture was transferred to 100 ml LB. The cells were grown until the $\text{OD}_{600} = 0.2-0.4$. Cells were centrifuged at 5000 x g for 10 minutes. The cells were resuspended in 1/2 volume (50 ml) of ice-cold 50 mM CaCl_2 and incubated on ice for 20 minutes. The cells were centrifuged as before and resuspended in 1/10 volume (1 ml) of ice-cold 50 mM CaCl_2 . These cells were incubated on ice for no less than 20 minutes and no more than 4 hours prior to transformation.

Figure 4. Oligonucleotide-directed mutagenesis using a single-stranded template containing uracil residues (Kunkel et al., 1987) is prepared from a *dut⁻ ung⁻ E coli* strain.

A synthetic oligonucleotide containing a desired mutation is annealed to the template and treated with T4 DNA polymerase and T4 DNA ligase to produce double-stranded product composed of one strand containing uracil residues. Transformation into a *dut⁺ ung⁺ E coli* host allows for recovery of mutant DNA containing only the desired mutation.



Transformation of competent *E coli* BW313 was carried out as follows: 1 μ l of pET81f1 HCA III R67N plasmid (these vectors containing an origin of replication for single strand (ss) DNA will be described in the section of this chapter on expression) was incubated with 0.1 ml of competent *E coli* BW313 on ice for 45 minutes. The cells were then heat shocked at 42°C for 2 minutes to maximize plasmid absorption. Two milliliters of LB media was added, and the cells were incubated for 1 hour at 37°C and 280 rpm. Plasmids were selected by plating on LB plates which contained 20 μ g/ml ampicillin (Amp).

Growth of Phage

E coli BW313 colonies selected from the LB/Amp plates were grown so that phage infection could be used to produce template DNA. Briefly, 20 ml of the transformed BW313 cells were grown to mid-log phase. Five milliliters of this culture was transferred to 100 ml LB/Amp containing 10 μ g/ml uridine and 10^8 - 10^9 plaque forming units (pfu) of the ss-DNA inducing helper phage R408 (Stratagene, La Jolla, CA), an M13 derivative, and grown at 37°C, 280 rpm for 18 hours. After incubation, the culture was centrifuged at 5000 x g for 30 minutes to collect the supernatant.

Isolation of ss Template DNA

Bacteriophage were precipitated from the clear supernatant by adding 1 volume of 5X PEG/NaCl (15% w/v Polyethylene glycol 8000; 2.5 M NaCl) to 4 volumes of supernatant. The solution was mixed well and incubated on ice for 1 hour. The precipitate was collected by centrifugation at 5000 x g for 15 minutes. The pellet was well-drained, and resuspended in 5 ml of phenol extraction buffer (PEB) (100 mM Tris-HCl, pH 8.0; 300 mM NaCl; 1 mM EDTA). This mixture was vortexed vigorously for resuspension, and incubated on ice for 1 hour. Next, the sample was centrifuged again as above and the previously described steps were repeated. At this point, the supernatant was extracted two times with 5 ml of phenol (which was equilibrated with PEB), centrifuged for 5 minutes at 5000 x g, and the aqueous layer was extracted 2X with 5 ml chloroform/amy1 alcohol (24:1). Next, the DNA was precipitated from the aqueous layer by adding 0.1 volume of 3 M sodium acetate (pH 5.0) and 2.5 volumes of 100% ethanol. After incubating the above mixture at -20°C for 20 minutes, the ssDNA was collected by centrifugation for 1 hour, dried under vacuum, and resuspended in 200 µl of water.

Phosphorylation and Hybridization of the Site-Specific Oligonucleotide

A 17-base oligonucleotide, complimentary to nucleotides 1145-1161 of the ssDNA template was synthesized for the creation of the mutant R67N-F198L HCA III. This 17-mer had the following nucleotide sequence:

5' G GGC TCA CTG ACC ACG C 3'

N -Gly-Ser-Leu-Thr-Thr- C

The two mutant nucleotides are underlined, and reside in the codon for amino acid 198. In the wild-type sequence, they would be T and C, respectively, and therefore code for Phe. In this mutant sequence, Leu is substituted for Phe at amino acid 198 and therefore the codon is CTG. The entire amino acid sequence coded for by the 17-mer is presented beneath the DNA sequence. (A similar approach was used to create the other mutants made in this manner.) Phosphorylation of the 5' hydroxyl group of the 17-mer was carried out in a 10 μ l reaction containing 50 mM Tris-HCl (pH 7.5); 10 mM $MgCl_2$; 5 mM dithiothreitol; 1 mM ATP; 2.0 μ g Bovine serum albumin (BSA); 2.0 μ g oligonucleotide; and 2 units T4 polynucleotide kinase (New England Biolabs). The mixture was incubated at 37°C for 1 hour and terminated by adding 3 μ l of 100 mM EDTA and heating to 65°C for 10 minutes.

The hybridization of the phosphorylated nucleotide to the ssDNA template was carried out in a primer:template molar

ratio of 10:1. The total volume of the reaction was 25 μ l and contained 1.2 μ l of 20X SSC (3 M NaCl; 300 mM sodium citrate). The annealing reaction mixture was incubated at 70°C for 10 minutes and allowed to cool slowly to room temperature.

In Vitro Double Strand DNA Synthesis

To create a covalently closed dsDNA molecule, 20 μ l of the above reaction was added to 10 μ l of the following buffer: 20 mM Hepes (pH 7.8); 2 mM dithiothreitol; 10 mM MgCl₂; 5 μ l each of 10 mM dATP, dTTP, dGTP, and dCTP; 10 μ l of 10 mM ATP; 36 μ l H₂O; 2 units (2 μ l) T4 DNA ligase (New England Biolabs) and 2.5 units T4 DNA polymerase (U.S. Biochemical). The reaction mixture was incubated at 0°C for 5 minutes, room temperature for 5 minutes, and then 37°C for 2 hours.

Screening Potential Mutants

Plasmid DNA was sequenced by the dideoxysequencing method developed by Sanger et al. (1977), using the Taq Track system of Promega. DNA sequencing reactions were subjected to electrophoresis on 0.05 cm thick gels, 54 x 33 cm, consisting of 6% (w/v) polyacrylamide, 7 M urea, and 0.05 TBE, pH 8.3. Gels were typically run at 1400 V for 7 hours. Upon completion of electrophoresis, the gel was transferred to 3 M paper and covered with saran wrap for autoradiography

on XAR film (Kodak) at -20°C . The film was generally exposed for 12 to 16 hours.

Cassette Mutagenesis

Wells et al. (1985) have described the use of cassette mutagenesis to create multiple mutations at defined sites. Briefly, this method introduces unique restriction sites into a plasmid using oligonucleotide mutagenesis. These sites are in close proximity to a target codon and often do not alter the final amino acid coding sequence. Thus, we are able to insert a mutagenic cassette into restriction sites flanking the region to be mutated, maintaining the wild-type coding sequence, and introducing a mutant codon at the desired codon or codons. Design of the restriction sites is also intended to eliminate one or in some cases both restriction sites. This facilitates selection of clones containing the mutagenic cassette because they can simply be screened by restriction digests.

The mutants F198D HCA III, F198N HCA III, F198V HCA III, and F198Y HCA III were created using the following procedure: Tanhauser et al. (unpublished) have created unique restriction sites for Nru I and Stu I in the pET81f1 HCA III expression vector (this vector will be discussed in the next section). The Nru I site was introduced at nucleotide 1126 and the Stu I site was introduced at Nucleotide 1160. This allows for mutants within a 34-base pair region.

For example, the mutant F198Y HCA III was created by synthesizing the following single-stranded oligonucleotides:

5' C GAC TAC TGG ACC TAC CAG GGC TCA TAC ACC ACG 3'

5' CGT GGT GTA TGA GCC CTG GTA GGT CCA GTA GTC G 3'

These two oligonucleotides were 5'-phosphorylated in separate 10 μ l reaction mixtures containing approximately 3 μ g ss-oligonucleotide; 1 mM ATP; 1.0 U T4 kinase (New England Biolabs); 70 mM Tris-HCl (pH 7.6), 10 mM MgCl₂, and 5 mM DTT, and then annealed by mixing, heating to boiling, and letting cool to room temperature.

The double-stranded 34-mer was ligated to a pET81f1 HCA III backbone which had the wild-type Nru I - Stu I cassette region excised. Ligation reactions typically used backbone:oligonucleotide molar ratios of 1:10 and were carried out at 14°C for 16 hours using 1 mM ATP; 1.0 U T4 DNA ligase (New England Biolabs); 70 mM Tris-HCl (pH 7.6), 10 mM MgCl₂, and 5 mM DTT. Ligation reactions were terminated with 25 mM EDTA. The ligation mixture was then transformed into competent *E coli* GM119 dcm⁻ for the purpose of screening for positive clones with Nru I and Stu I restriction digests.

Screening for potential positive clones was first accomplished by restriction digests using Nru I and Stu I. Creation of a positive clone which contains the desired mutation left the Nru I site intact but deletes the Stu I site. Thus, potential positive clones yielded a single

linear band after restriction with Nru I, but yielded a wild-type double-stranded DNA pattern when cut with Stu I. These results were then corroborated with DNA sequencing of the plasmid (Sanger et al., 1977). Positive clones had just the desired mutant sequence in the region of interest and the wild-type sequence everywhere else.

Creation of Remaining Mutants

The mutants F198A HCA III and F198L HCA III were made by recombination of DNA from wild-type HCA III expression vector backbone with a 625 base-pair fragment containing the 198 region excised and the 625 base-pair region containing the 198 region of R67N-F198A and R67N-F198L, respectively. K64H-R67N-F198L HCA III was made by recombination of the K64H-R67N backbone with a 625 base-pair fragment of the 198 region excised and the 625 base-pair region of F198L. Basically, this was accomplished by digesting both pET81f1 HCA III and pET81f1 HCA III mutants with BamH I and Bcl I. This removes a 625 base-pair region from nucleotides 866-1491. Religation of the proper fragments created the desired plasmid. Clones were then sequenced to confirm mutant assignment.

Expression of HCA III Mutants in *E coli*

The expression system used in this study was based on bacteriophage T7 RNA polymerase as first described by Studier and Moffatt (1986). This expression system has many advantages for it provides high-level transcription from the

T7 promoter and high selectivity due to the absence of a natural promoter in *E coli*.

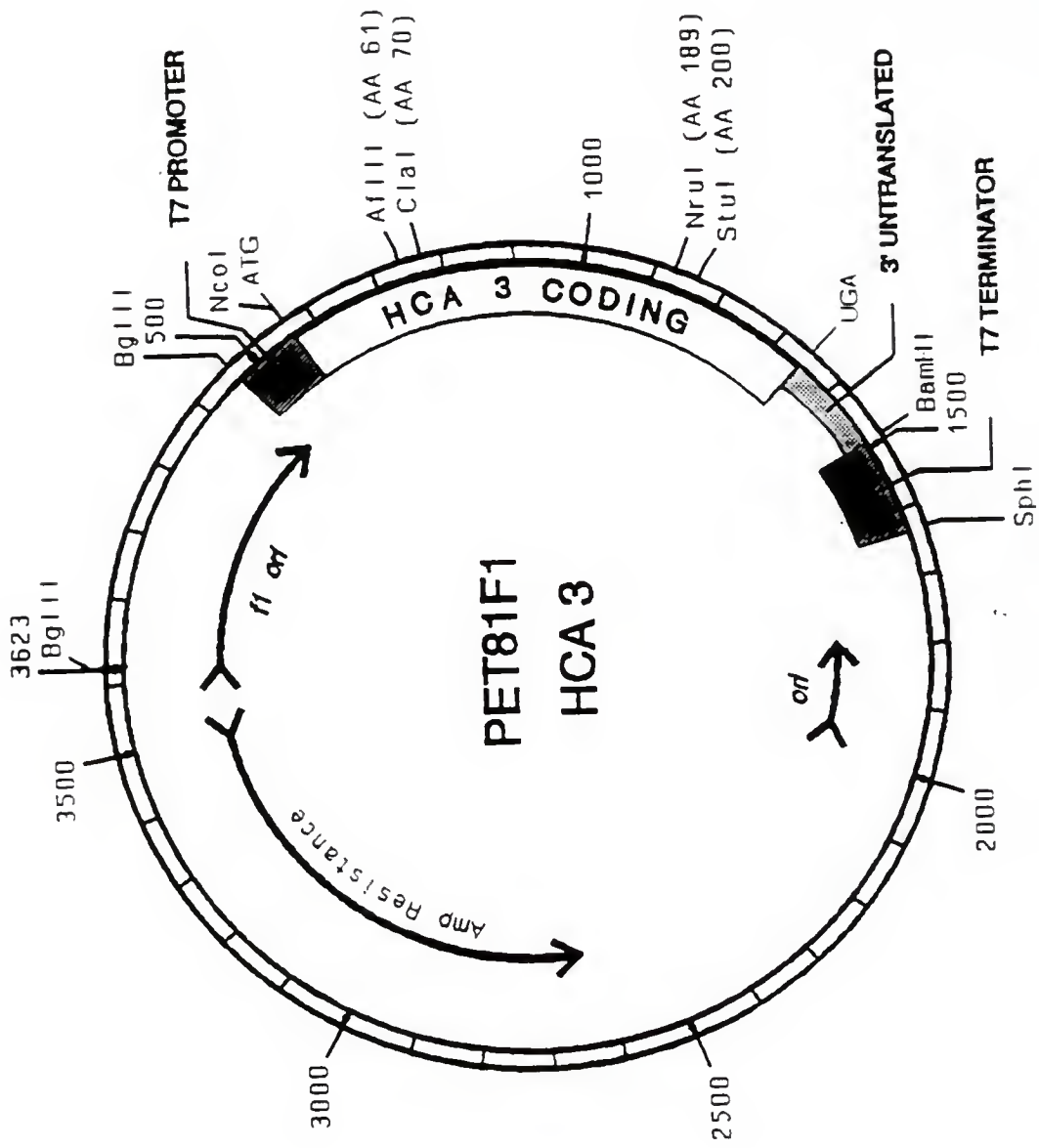
Figure 5 presents some key features of a modified form of this expression vector termed pET81f1 HCA III (Tanhauser et al., unpublished). Notable features include: an f1 origin for single-strand phage replication; T7 promoter and terminator regions; the HCA III gene which contains the unique Nru I and Stu I restriction sites; and a gene which confers ampicillin resistance.

Expression of the HCA III gene is carried out in the *E coli* lysogen BL21(DE3) which carries a λ lysogen encoding the gene for T7 RNA polymerase. This T7 RNA polymerase gene is under control of the lac UV5 promoter (Studier and Moffatt, 1986). Thus, upon induction of the culture with isopropyl- β -D-thiogalactopyranoside (IPTG), T7 RNA polymerase is synthesized with subsequent translation of the target HCA III gene.

The *E coli* strain BL21(DE3)plysS (chloramphenicol resistant) was transformed with the pET81f1 HCA III mutant plasmid. In addition to conferring chloramphenicol resistance, the plysS plasmid carries the gene for lysozyme. This is used as an aid for cell lysis in the purification procedure. Resultant cells which contained both plasmids were selected on LB plates containing both 200 mg/L ampicillin and 34 mg/L chloramphenicol. A single colony from this plate was used to inoculate 2 ml of LB containing the above concentrations of antibiotics. The 2 ml culture was

Figure 5. Location of key features on the pET81f1 HCA III expression vector.

Key features include: an f1 origin for ss-DNA replication; T7 promoter region; HCA III coding region; NRU I and STU I restriction sites; T7 terminator; and ampicillin resistance.



grown at 37°C, 280 rpm to log-phase. One ml of this culture was used to inoculate a 1 liter expression culture containing the above concentrations of antibiotics and 0.2% (w/v) glucose. This culture was grown at 37°C, 280 rpm in 2800 ml Fernbach flasks until the OD₆₀₀ = 0.2 to 0.4. At this time, the culture was induced for HCA III synthesis with 40 µM IPTG (Studier and Moffatt, 1986; Rosenberg et al., 1987). In addition, 2 µM ZnSO₄ was added. The cells were incubated an additional 3 hours after induction, pelleted at 5000 x g for 10 minutes, frozen at -70°C for 16 to 20 hours, and thawed at room temperature to allow cell lysis so that carbonic anhydrase activity could be tested.

The synthesis of carbonic anhydrase was monitored by taking one ml aliquots from the bacterial culture at hourly time points during expression. These 1 ml aliquots were centrifuged and the pellet was frozen for future SDS-PAGE analysis. The zero hour time point was just prior to induction with IPTG. Subsequent time points at 1, 2, and 3 hours were also taken.

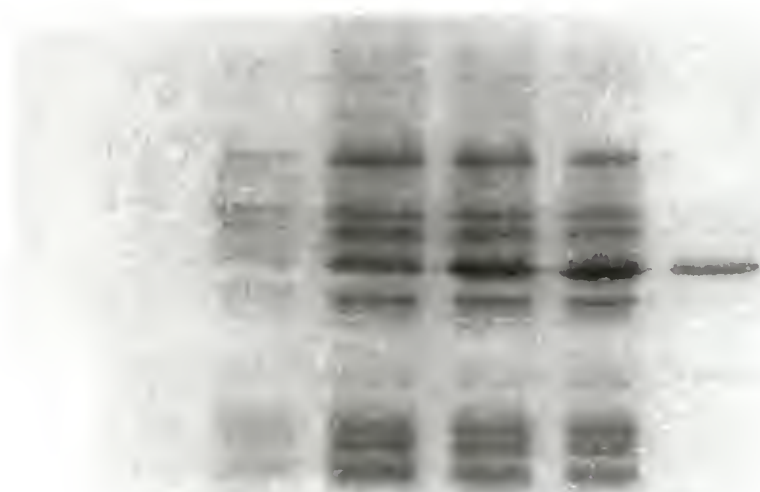
Figure 6 shows a typical time course of expression of HCA III. The 1 ml pellets were resuspended in 200 µl of SDS-reducing buffer (62.5 mM Tris-HCl, pH 6.8; 10% glycerol; 2% SDS; 0.05% bromophenol blue; and 5% (v/v) mercaptoethanol), heated to boiling for 3 minutes, and loaded in 20 µl aliquots on a 12% polyacrylamide mini-gel. The samples were electrophoresed at 200 V for 45 minutes. The gel was stained with 0.1% Comassie Blue R-250 containing 40% methanol, 10%

Figure 6. Time course of F198V HCA III synthesis after induction with 40 μ M IPTG.

One milliliter aliquots were taken from the *E coli* expression culture at 0, 1, 2, and 3 hours after IPTG induction (Lanes 1-4, respectively). Lane 5 is a standard sample of Bovine carbonic anhydrase from Sigma Chemical Company used as a molecular weight marker (MW = 30 kDa). Samples were electrophoresed for 45 minutes at 200 V on a 12% SDS-polyacrylamide gel and stained with Coomassie blue.

Time (hours)

0 1 2 3



MW

30 kDa

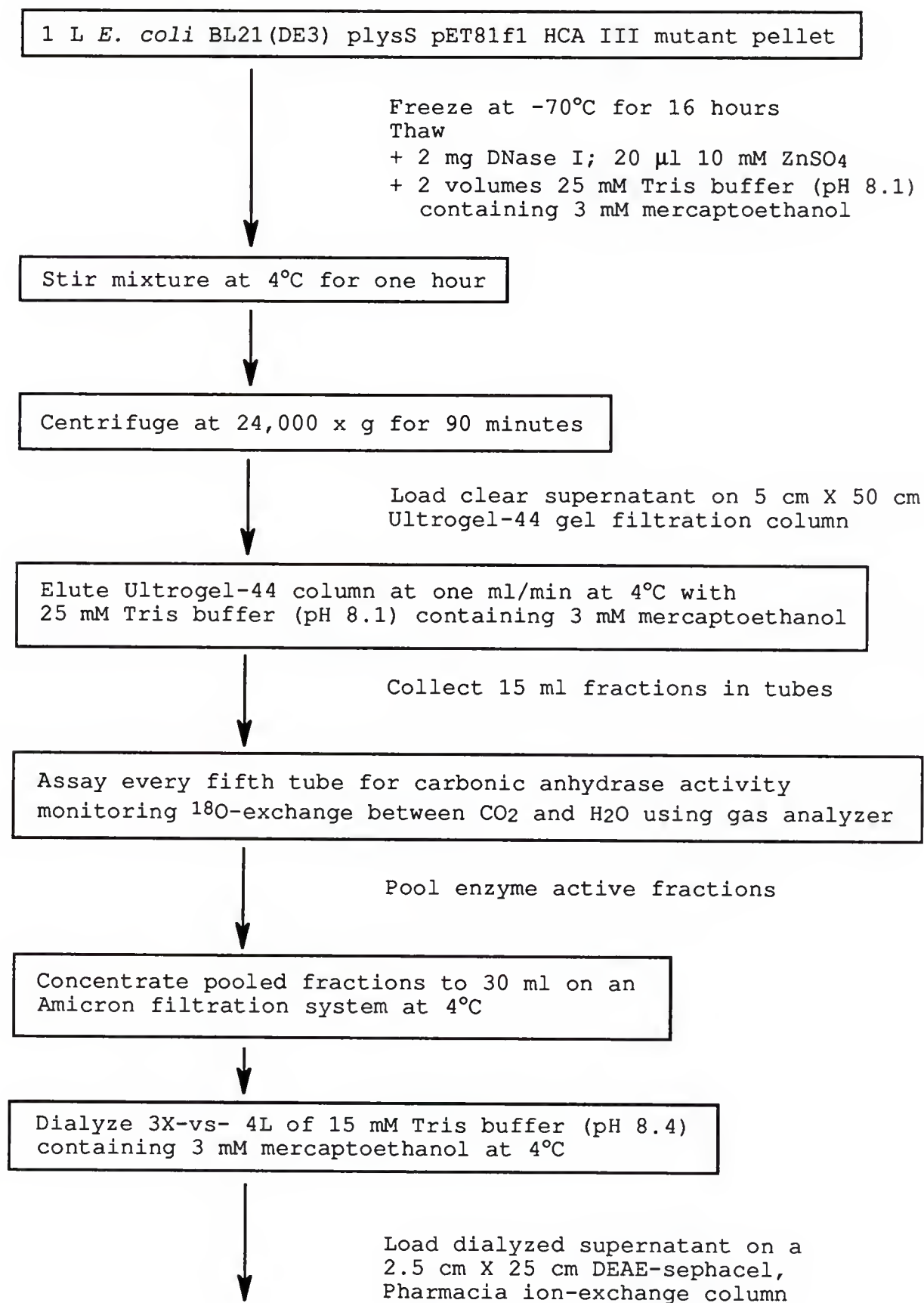
acetic acid for 16 hours. Gels were destained in 10% acetic acid and 40% methanol solutions.

Purification of Human Carbonic Anhydrase Mutants
Expressed in *E. coli*

The method used for purification of HCA III mutants created for our studies was based on that of Tu et al. (1986). However, it is important to note that many modifications of their procedure were necessary due to the unique properties of each of the mutant enzymes. This statement particularly applies to the steps involved in ion-exchange chromatography where Tris buffer concentration and pH varied depending on the mutant being purified.

Figure 7 presents a flow chart outlining the overall purification scheme of HCA III mutants. Cells were freeze-thawed for lysis and then treated with 1 mg/20 ml DNase I for digestion of nucleic acid. Centrifugation at 24,000 x g removed cell debris from the supernatant. Elution on the Ultrogel-44 column separated approximately 20% of all proteins from carbonic anhydrase. Cation exchange chromatography on DEAE-sephacel separated carbonic anhydrase based on its unique pI from all other proteins in the mixture. It is important to note that 15 mM Tris buffer (pH 8.4) was used for dialysis and DEAE-sephacel elution of all mutants except: F198D HCA III which needed 0.1 M Tris (pH 8.0); and K64H-R67N-F198L HCA III which needed 75 mM Tris (pH

Figure 7. Flow chart detailing the purification of human carbonic anhydrase III mutants expressed in *E coli*



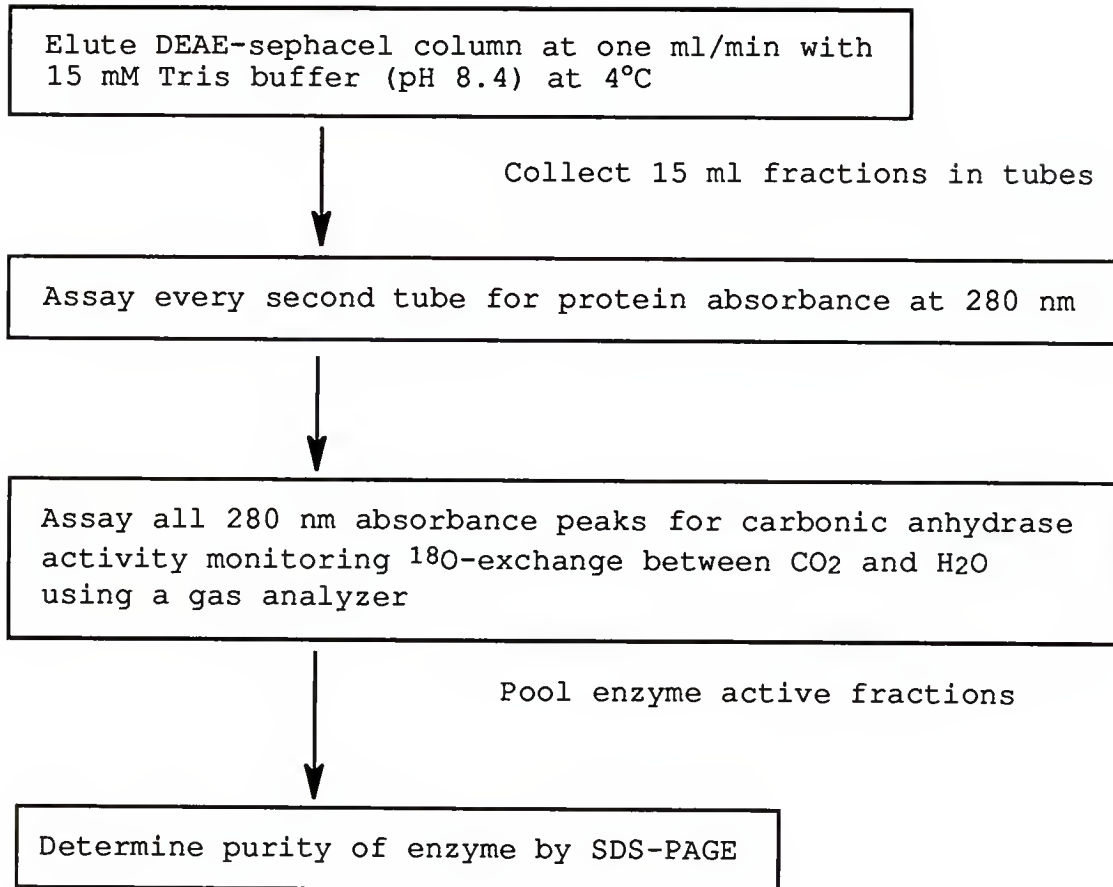


Fig. 7 Cont.

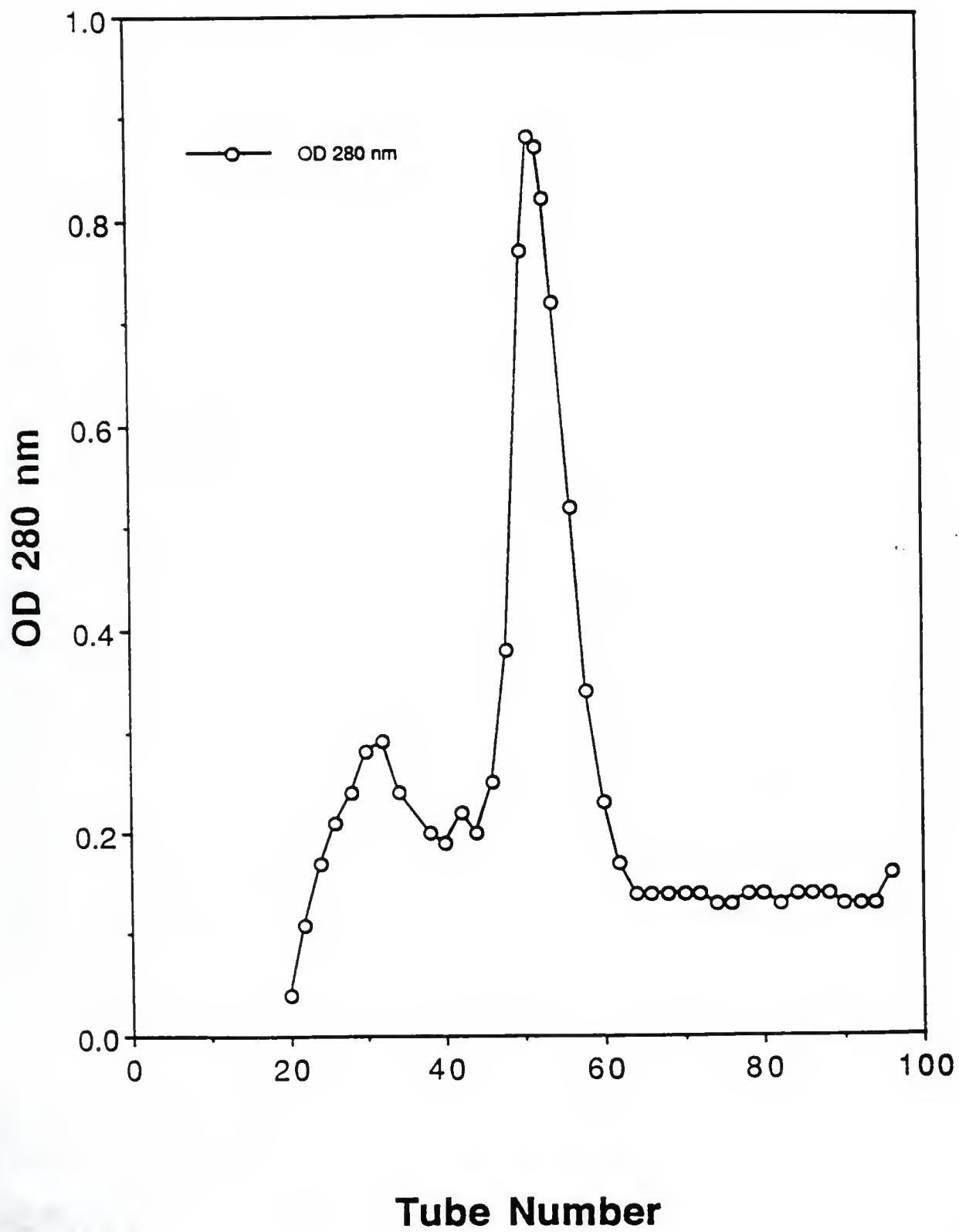
8.1). Figure 8 presents a typical elution profile of K64H-R67N HCA III after DEAE-sephacel purification.

Figure 9 shows a typical UV spectrum recorded in the range of 310 to 210 nm of purified F198A HCA III. The concentration of human carbonic anhydrase III mutants was determined from the molar absorptivity of $6.2 \times 10^4 \text{ cm}^{-1}$ at 280 nm (Sanyal et al., 1982). For the mutants F198L, R67N-F198L, and K64H-R67N-F198L HCA III, this molar absorptivity was confirmed by titration with the tight binding inhibitor ethoxzolamide by estimating the active-site concentration using a Henderson plot (Segel, 1975). The two methods yielded an enzyme concentration which differed by approximately 10-15%. Furthermore, for the triple mutant K64H-R67N-F198L HCA III we were able to corroborate the enzyme concentration determined from the Henderson plot with the Bradford assay. The calculated enzyme concentration from these two methods differed by less than 5% suggesting that all of the protein present is pure, active carbonic anhydrase.

Figure 10 presents a 12% polyacrylamide gel which follows the entire purification scheme. Lane 4 shows the final purified carbonic anhydrase which is estimated to be greater than 98% pure. Further description of other lanes is found in the legend to Figure 10. For the single mutants F198V and F198D HCA III this enzyme purity was verified with silver staining. Enzyme purity was estimated to be greater than 95% pure by this method (data not shown). Finally, in

Figure 8. Elution profile of K64H-R67N HCA III after purification on DEAE-Sephacel.

The column was eluted at a flow rate of 1 ml/min with 15 mM Tris (pH 8.4) at 4°C. Fractions were collected in a volume of 15 ml/tube. Enzyme activity was found in tubes 46-61. These fractions were pooled for use in kinetic experiments.



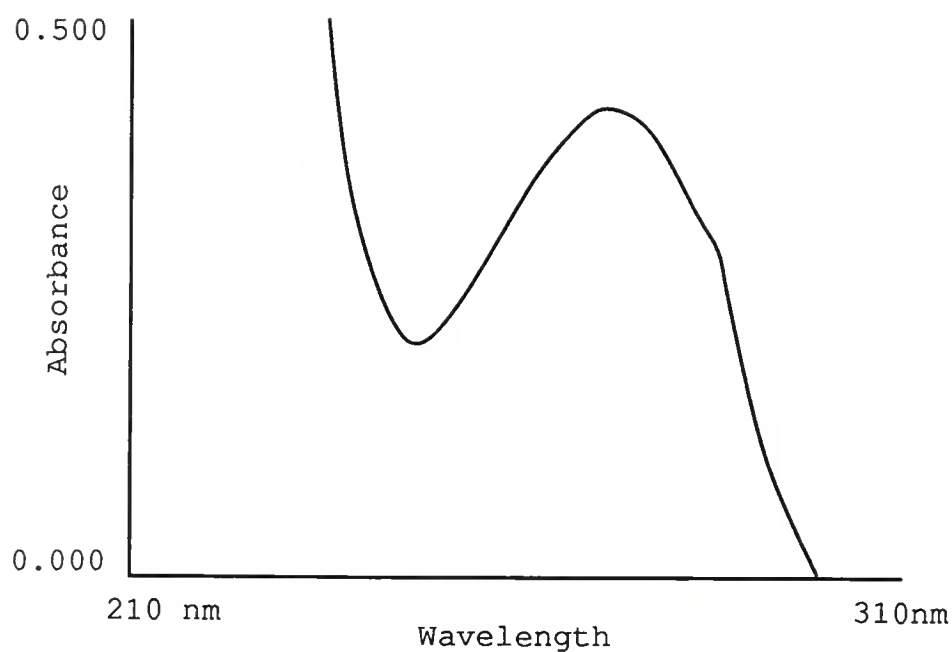


Figure 9. UV absorbance spectrum for purified F198A HCA III.

Spectra were recorded on a Beckman DU-7 spectrophotometer in the range of 310-210 nm. The spectrophotometer was blanked with 15 mM Tris (pH 8.1).

Figure 10. 12% polyacrylamide gel detailing the levels of purity of K64H-R67N HCA III during the different stages of carbonic anhydrase purification.

Lane 1: 1 ml crude cell lysate of *E coli* BL21(DE3) plysS pET81f1 HCA III pellet

Lane 2: Supernatant after centrifugation at 24,000 x g

Lane 3: Pooled enzyme active tube fractions after Ultrogel-44 gel filtration chromatography

Lane 4: Pooled enzyme active tube fractions after DEAE-Sephacel cation exchange chromatography

Lane 5: Standard sample of bovine carbonic anhydrase from Sigma Chemical Co. used as a molecular weight marker (MW= 30 kDa)

Lanes 1 2 3 4 5



MW

30 kDa

the substantial history of carbonic anhydrase literature there are no published or anecdotal reports for HCA II, HCA III, or any mutants of these two isozymes which show any evidence for the isolation of non-active enzyme fractions or inclusion bodies. Thus, it is most likely that our measures of enzyme concentration reflect solely on pure, fully active HCA III mutants. Any trace of inactive enzyme would result in an active enzyme concentration which is lower than reported. Thus, the reported enzyme concentrations reflect a lower limit for enzyme concentration.

Steady-State Kinetic Methods

Stopped-Flow Spectrophotometry for CO₂ Hydration

Saturated solutions of CO₂ were prepared by bubbling CO₂ gas into deionized water contained in a vessel maintained at 25°C. Dilutions were prepared in the absence of air by coupling two syringes as described by Khalifah (1971). CO₂ concentrations were calculated based on a saturated CO₂ solution concentration of 33.8 mM at 25°C (Poker and Bjorkquist, 1977). After dilutions were made, final CO₂ concentrations ranged from 0.85 to 17 mM.

Initial velocities for CO₂ hydration were determined by stopped-flow spectrophotometry (carried out on an Applied Photophysics stopped-flow spectrophotometer) using a pH-indicator method (Khalifah, 1971). The pH-indicator method takes advantage of buffer-indicator pairs which have nearly

identical pK_a values. The buffer-indicator pairs used in this study, their pK_a values, and the wavelength observed were as follows: Mops{3-(N-morpholino)propanesulfonic acid} (pK_a 7.2) and p-nitrophenol (pK_a 7.1, 400 nm); Taps {N-tris[hydroxymethyl]methyl-3-amino propanesulfonic acid} (pK_a 8.4) and m-cresol purple (pK_a 8.3, 578 nm); Ches {2[N-cyclohexyl amino] ethanesulfonic acid} (pK_a 9.3) and thymol blue (pK_a 8.9, 590 nm). The difference in molar extinction coefficients between the acid and base forms of the indicator was determined by spectrophotometric titration at the buffer concentration, ionic strength, temperature, and wavelength used in the stopped-flow experiments. Final buffer concentrations were 50 mM. All steady-state experiments were performed at 25°C with a total ionic strength of the solution maintained at a minimum of 0.1 M using Na_2SO_4 .

To record the initial velocity of hydration (v), the rate of change of the absorbance of indicator versus time was measured by rapidly mixing the contents of two syringes. One drive syringe contained a CO_2 solution, and the second contained enzyme, buffer and indicator. The initial velocity of hydration was determined by least-squares analysis of a minimum of six traces of indicator absorbance versus time, each comprising less than 10% of the complete reaction (Rowlett and Silverman, 1982). Initial velocities were corrected for by subtracting the uncatalyzed rate for CO_2 hydration.

The initial velocity (v) can be calculated as described by Rowlett and Silverman (1982) and is related to the buffer factor, Q , described by Khalifah (1971). Briefly, Q is a function of the state of ionization of the buffer and indicator, and relates changes in absorbance in indicator to changes in concentration of H^+ . It is calculated as described by Khalifah (1971).

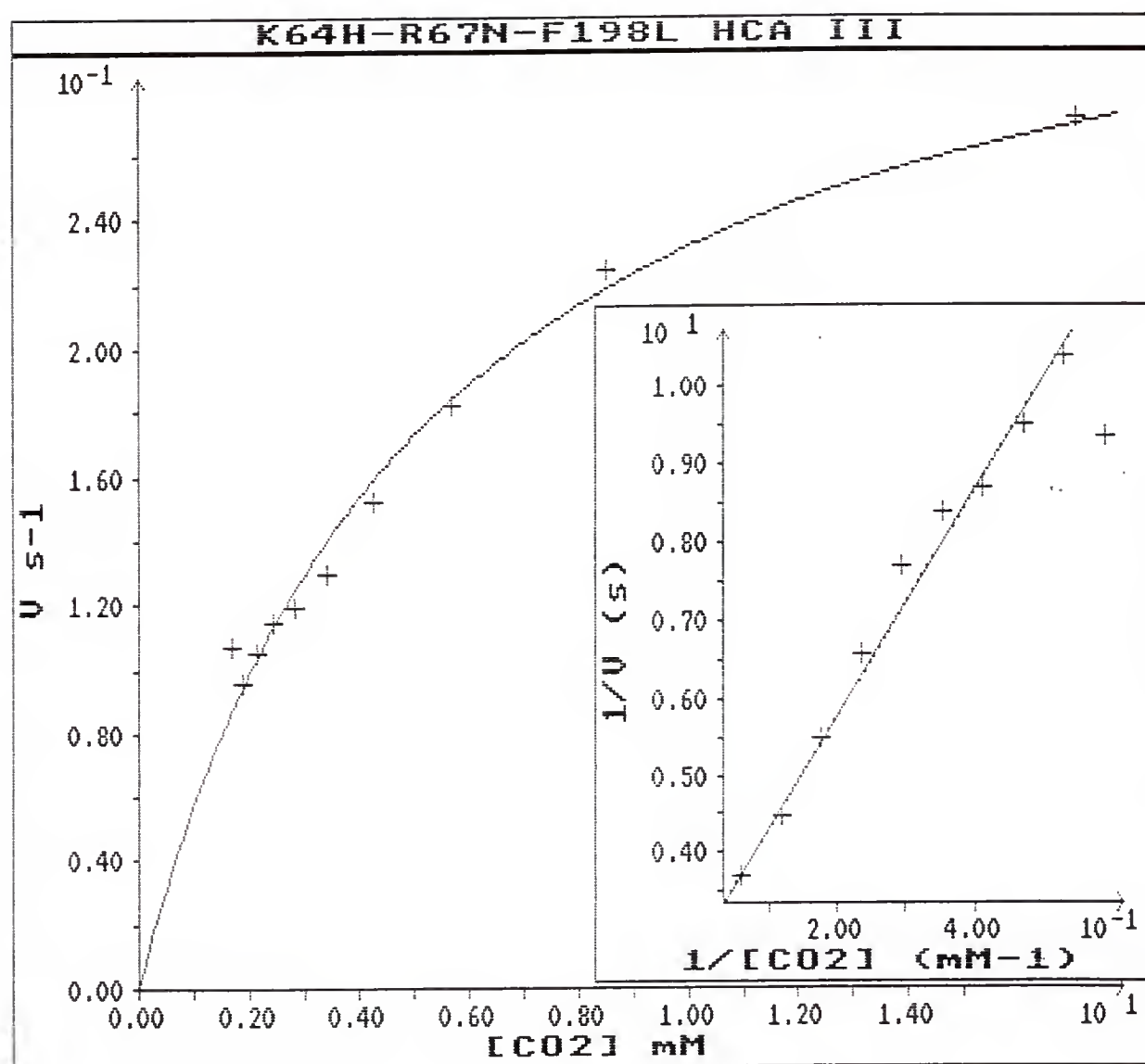
The main panel of Figure 11 presents a typical Michaelis-Menten, velocity-vs-substrate profile for CO_2 hydration catalyzed by the mutant K64H-R67N-F198L HCA III. The inset shows the Lineweaver-Burke plot for these data. The program Enzymatic Analysis in Enzfitter (Elsevier Biosoft, Cambridge, UK) was used to calculate steady-state constants from these data. The enzyme concentrations used in these studies varied depending on the CO_2 hydration activity of the enzyme but were generally in the range of 93 nM to 1 μM .

4-Nitrophenyl Acetate Hydrolysis Kinetics

Initial velocities of the hydrolysis of 4-nitrophenyl acetate catalyzed by carbonic anhydrase III mutants were measured (using a Beckman DU7 Spectrophotometer) by the method of Verporte et al. (1967) in which the increase in absorbance was followed at 348 nm. Absorbance-vs-time traces were recorded for 3 minutes. To investigate the hydrolysis activity over a range of pH values, solutions containing the

Figure 11. Typical data analysis used to calculate steady-state kinetic constants.

The main panel shows a plot of the velocity-vs-substrate curve for the hydration of CO_2 catalyzed by the mutant K64H-R67N-F198L HCA III at pH 6.35 and 25°C. The reaction was carried out in 50 mM MOPS, ionic strength 0.1 M. The inset shows a double-reciprocal plot of these data.



following buffers were used: Mes (2-N[morpholino]ethanesulfonic acid); Mops; Hepes (N-2-Hydroxyethylpiperazine-N'-2-ethanesulfonic acid); and Taps. Reaction solutions contained 33 mM of one of the above buffers whose total ionic strength was maintained at 0.1 M with Na₂SO₄. All measurements were made at 25°C.

The molar absorptivity for 4-nitrophenyl acetate is $5.4 \times 10^3 \text{ M}^{-1}\text{cm}^{-1}$ (Verporte et al., 1967). The cell path length was 1 cm and the final substrate concentration in the reaction mixture was 1 mM. Enzyme concentrations varied depending on the catalytic activity of the mutant being studied (the general range was from 0.5 μM to 5 μM). The enzyme catalyzed rate was determined by subtracting the uncatalyzed rate of hydrolysis from the catalyzed rate. The steady-state rate constant, k_{cat}/K_m , termed k_{enz} , for 4-nitrophenyl acetate hydrolysis was calculated using the following equation (eq. 6):

$$k_{\text{enz}} = k_{\text{cat}}/K_m = \frac{\Delta R}{(\epsilon) (b) [S] [E]} \quad (\text{eq. 6})$$

where ΔR = catalyzed rate - uncatalyzed rate of 4-nitrophenyl acetate hydrolysis, b = path length, ϵ = molar absorptivity of 4-nitrophenol, $[S]$ = substrate concentration, and $[E]$ = enzyme concentration.

Equilibrium Kinetic Methods

^{18}O -Exchange at Chemical Equilibrium

The measurement of the rate of hydration-dehydration cycles of CO_2 by the exchange of ^{18}O between CO_2 and water is based on the method of Mills and Urey (1940). Oxygen-18 labeled bicarbonate and carbon-13 labeled bicarbonate were prepared as described by Silverman et al. (1979). Isotope exchange experiments were performed on a Dycor N-100 residual gas analyzer at 25°C in the pH range 6 to 9. Adjustments in pH were made with NaOH and H_2SO_4 . In all experiments, the total ionic strength of solution was maintained at 0.2 M by the addition of Na_2SO_4 .

Each experiment was started by placing into the vessel 8.0 ml of 100 mM Hepes (pH 7.5 to 7.7) in which ^{18}O - and ^{13}C -labeled bicarbonate had been dissolved. A period of several minutes elapsed to allow approach to chemical equilibrium. At this point, measurements of the isotopic content of CO_2 were taken. The uncatalyzed rate of CO_2 and HCO_3^- inter-conversion was subtracted from the enzyme catalyzed rate for all experiments.

The fate of the ^{18}O - ^{12}C -labeled bicarbonate atoms and the ^{16}O - ^{13}C -labeled bicarbonate atoms for carbonic anhydrase catalyzed ^{18}O -exchange at chemical equilibrium is illustrated in Figure 12. ^{18}O -labeled atoms are represented by the filled oxygens. This technique allows the measurement of the atom fraction of ^{18}O in all CO_2 . Silverman and Tu (1976) and Silverman et al. (1979) have described in detail how the rate

constant, θ , describing the exchange of ^{18}O between CO_2 and H_2O , and the rate constant, ϕ , describing the exchange of ^{18}O between ^{12}C - and ^{13}C -containing CO_2 species can be obtained from experiment. These rate constants, in turn, describe R_1 and $R_{\text{H}_2\text{O}}$ (see Chapter 1). The standard deviations in $R_{\text{H}_2\text{O}}$ were 10 to 25% with the poorest precision at higher values of $R_{\text{H}_2\text{O}}$. The standard deviations in R_1 were less than 10%.

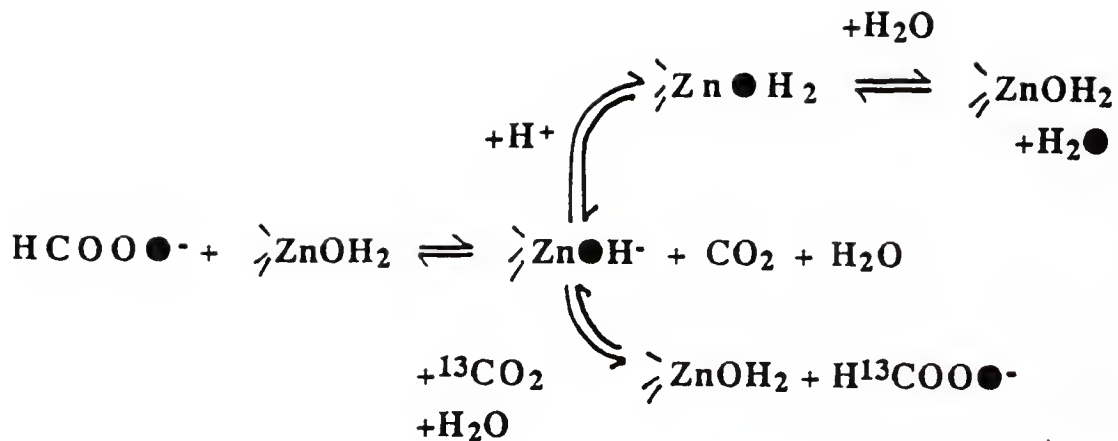


Figure 12. Carbonic anhydrase catalyzed ^{18}O -exchange at chemical equilibrium.

This technique allows for the measurement of ^{18}O in all CO_2 species, and thus R_1 and RH_2O . The ^{18}O -label is designated by the filled oxygen atoms.

CHAPTER 3
CATALYTIC ENHANCEMENT OF HUMAN CARBONIC
ANHYDRASE III BY REPLACEMENT OF PHE 198 WITH LEU

Introduction

The replacements Lys 64 → His and Arg 67 → Asn in HCA III, as reported by Jewell et al. (1991), result in mutants with modest (3-fold or less) enhancement in k_{cat}/K_m for hydration of CO_2 . Neither of these replacements at positions 64 and 67 causes the pK_a for the zinc-bound water to increase into the pH range above 6 or to enhance the very weak catalytic hydrolysis of 4-nitrophenyl acetate. Histidine at position 64, which occurs naturally in HCA II and has been placed in HCA III, is necessary for maximal turnover in the hydration of CO_2 by providing a pathway for proton transfer between zinc-bound water and buffers in solution (Tu et al., 1989; Jewell et al., 1991).

There have been no previous kinetic experiments that reflect on the specific function or role of Phe 198 in catalysis by HCA III. We have approached this problem using the site-specific mutant in which Phe 198 is replaced with Leu, the residue that appears in this position in HCA II. In addition, the double and triple mutants with replacements also at positions 64 and 67 were studied to detect

interactions between these positions in catalysis. Catalysis of the hydration of CO_2 was measured by stopped-flow spectrophotometry and the exchange of ^{18}O between CO_2 and water by mass spectrometry. The replacement Phe 198 \rightarrow Leu in HCA III caused major increases in kinetic constants for CO_2 hydration and 4-nitrophenyl acetate hydrolysis and in the tightness of binding of some sulfonamide inhibitors. Thus, Phe 198 is a significant contributor to some of the unique properties of carbonic anhydrase III.

Results

The steady-state parameters for the hydration of CO_2 catalyzed by mutants of HCA III with replacements at positions 64, 67, and 198 were measured by stopped-flow spectrophotometry. The pH dependence of k_{cat}/K_m could be described by a single ionization with a maximum at high pH; values of this ratio measured by ^{18}O exchange at low total substrate concentration were identical to values measured at steady state. The replacement Phe 198 \rightarrow Leu resulted in a large enhancement of k_{cat}/K_m for the hydration of CO_2 , about 20-fold compared with wild-type HCA III (Table 3). The further replacement Arg 67 to form the double mutant R67N-F198L HCA III resulted in a 70-fold increase compared with the value of $3 \times 10^5 \text{ M}^{-1}\text{s}^{-1}$ for wild-type HCA III. There was no further enhancement in this parameter caused by the replacement Lys 64 \rightarrow His to form the triple mutant (Table 3).

Table 3. Maximal (pH-independent) steady-state constants and values of apparent pK_a for the hydration of CO_2 and hydrolysis of 4-nitrophenyl acetate catalyzed by carbonic anhydrase and mutants^a

Enzyme	CO_2 Hydration			4-Nitrophenyl Acetate Hydrolysis	
	k_{cat} ($\times 10^{-4} s^{-1}$)	k_{cat}/K_m ($\times 10^{-6} M^{-1}s^{-1}$)	pK_a	k_{cat}/K_m ($\times 10^{-3} M^{-1}s^{-1}$)	pK_a
Wild-type HCA III ^b	0.2	0.3	<6.0	0.01	---
F198L HCA III	2.2 ± 0.3	7.4 ± 0.3	6.9	1.0 ± 0.1	6.4
R67N-F198L HCA III	2.1 ± 0.4	21 ± 1	6.9	2.1 ± 0.1	6.6
K64H-R67N-F198L HCA III	220 ± 16	18 ± 2	6.8	2.1 ± 0.1	6.6
Wild-type HCA II ^c	140	156	7.0	2.7	6.9

^aSteady-state constants were obtained as described in the text. Values of apparent pK_a were determined from k_{cat}/K_m with standard errors in pK_a of 0.2 for CO_2 hydration and 0.1 for ester hydrolysis

^bThe value of k_{cat} for CO_2 hydration omits values at $pH > 8$ which approached $1 \times 10^4 s^{-1}$ (Jewell et al., 1991). The very small value for ester hydrolysis may not occur at the active site for CO_2 hydration (Tu et al., 1986).

^cKhalifah (1971) for CO_2 hydration and Steiner et al. (1979) for 4-nitrophenyl acetate hydrolysis

Maximal values of k_{cat}/K_m for these and two additional mutants are given in Figure 13. Each of the mutants containing Leu 198 showed changes in k_{cat}/K_m consistent with an ionization of pK_a near 7, assumed to be that of the zinc-bound water with similarities to HCA II (Table 3; Khalifah, 1971).

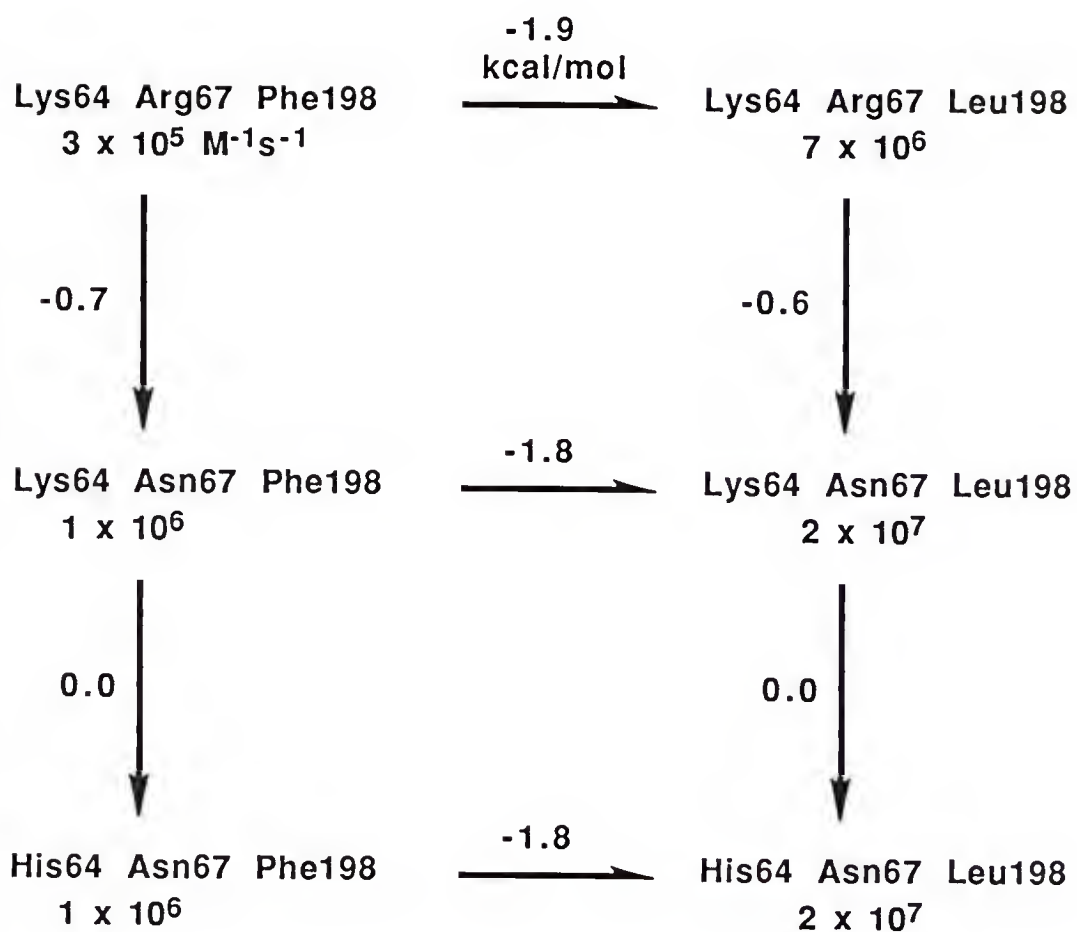
The presence of an ionization affecting catalysis was confirmed by the measurement of catalytic hydrolysis of 4-nitrophenyl acetate. The resulting pH-rate profiles can be described as dependent on a single ionization with values of pK_a between 6.4 and 6.9 (Table 3). The catalytic rate of this hydrolysis by the wild-type bovine isozyme III is very small (the maximal value of k_{cat}/K_m is $11 \text{ M}^{-1}\text{s}^{-1}$, Tu et al., 1986). By this measure, the double and triple mutants of HCA III listed in Table 3 have activity nearly equivalent to that of isozyme II.

The steady-state turnover number k_{cat} for hydration catalyzed by the single mutant F198L (Table 3) did not vary in the pH range 6.5 to 8.5 and was approximately 10-fold higher than the wild-type HCA III which is $2 \times 10^3 \text{ s}^{-1}$ in this pH range (Jewell et al., 1991). The double mutant R67N-F198L HCA III had values of k_{cat} similar to the single mutant, except at $\text{pH} > 8.5$ for which k_{cat} increased with pH. This effect may be caused by proton transfer involving Lys 64. A similar effect was observed in the single mutant R67N HCA III (Jewell et al., 1991). There was further enhancement

Figure 13. Comparisons of k_{cat}/K_m for hydration of CO_2 catalyzed by variants of HCA III obtained by site-directed mutagenesis at positions 64, 67, and 198 in the active site cavity of HCA III.

Values of k_{cat}/K_m in $\text{M}^{-1}\text{s}^{-1}$ appear beneath each designated mutant. The values in kcal/mol adjacent to the arrows are the changes in free energy barriers for the catalysis corresponding to the designated mutations. Free energy changes are determined using $\Delta G = -RT \ln[(k_{\text{cat}}/K_m)_{\text{mut2}} / (k_{\text{cat}}/K_m)_{\text{mut1}}]$.

(kcat/Km)CO₂



observed for the triple mutant for which k_{cat} attained values comparable to those for HCA II of $1.4 \times 10^6 \text{ s}^{-1}$ (Khalifah, 1971).

The proton transfer-dependent rate of release of water from the active site, $R_{\text{H}_2\text{O}}/[\text{E}]$, was measured in the absence of buffers other than the substrate itself, CO_2 and its hydrated forms. $R_{\text{H}_2\text{O}}/[\text{E}]$ varied with pH for the triple mutant (Figure 14) in a manner similar to HCA II (Tu and Silverman, 1985). The maximal value of $R_{\text{H}_2\text{O}}/[\text{E}]$ for the triple mutant, $9 \times 10^4 \text{ s}^{-1}$, can be compared to the maximal value, near $5 \times 10^5 \text{ s}^{-1}$, for HCA II. The values of $R_{\text{H}_2\text{O}}/[\text{E}]$ for F198L and R67N-F198L HCA III are similar near 10^4 s^{-1} and rather independent of pH (Figure 14). For wild-type HCA III, the values of $R_{\text{H}_2\text{O}}/[\text{E}]$ are independent of pH at $2 \times 10^3 \text{ s}^{-1}$. Maximal values of $R_{\text{H}_2\text{O}}/[\text{E}]$ for additional mutants are given in Figure 15.

Upon addition of the buffer imidazole, there was considerable enhancement of $R_{\text{H}_2\text{O}}/[\text{E}]$ for the single and double mutants (Figure 16). Enhancement of $R_{\text{H}_2\text{O}}$ by addition of imidazole is a characteristic of HCA III and the K64H and R67N single mutants (Tu et al., 1990) as well as HCA II and some mutants (Tu et al., 1989). This has been interpreted as evidence for proton transfer from the imidazolium cation to the zinc-hydroxide increasing the rate of release of H_2^{18}O as shown in equation 4. For three mutants of isozyme III containing the replacement Phe 198 \rightarrow Leu, the rate R_1 of

Figure 14 The pH dependence of $R_{H_2O}/[E]$ for (▲) F198L HCA III; (■) R67N-F198L HCA III; (●) K64H-R67N-F198L HCA III. The values for HCA II are represented by the solid line (see Tu and Silverman, 1985).

Solutions contained 100 mM total concentration of CO_2 and HCO_3^- and no buffers were used. Experiments were carried out at 25°C with the total ionic strength of solution maintained at 0.2 M with Na_2SO_4 .

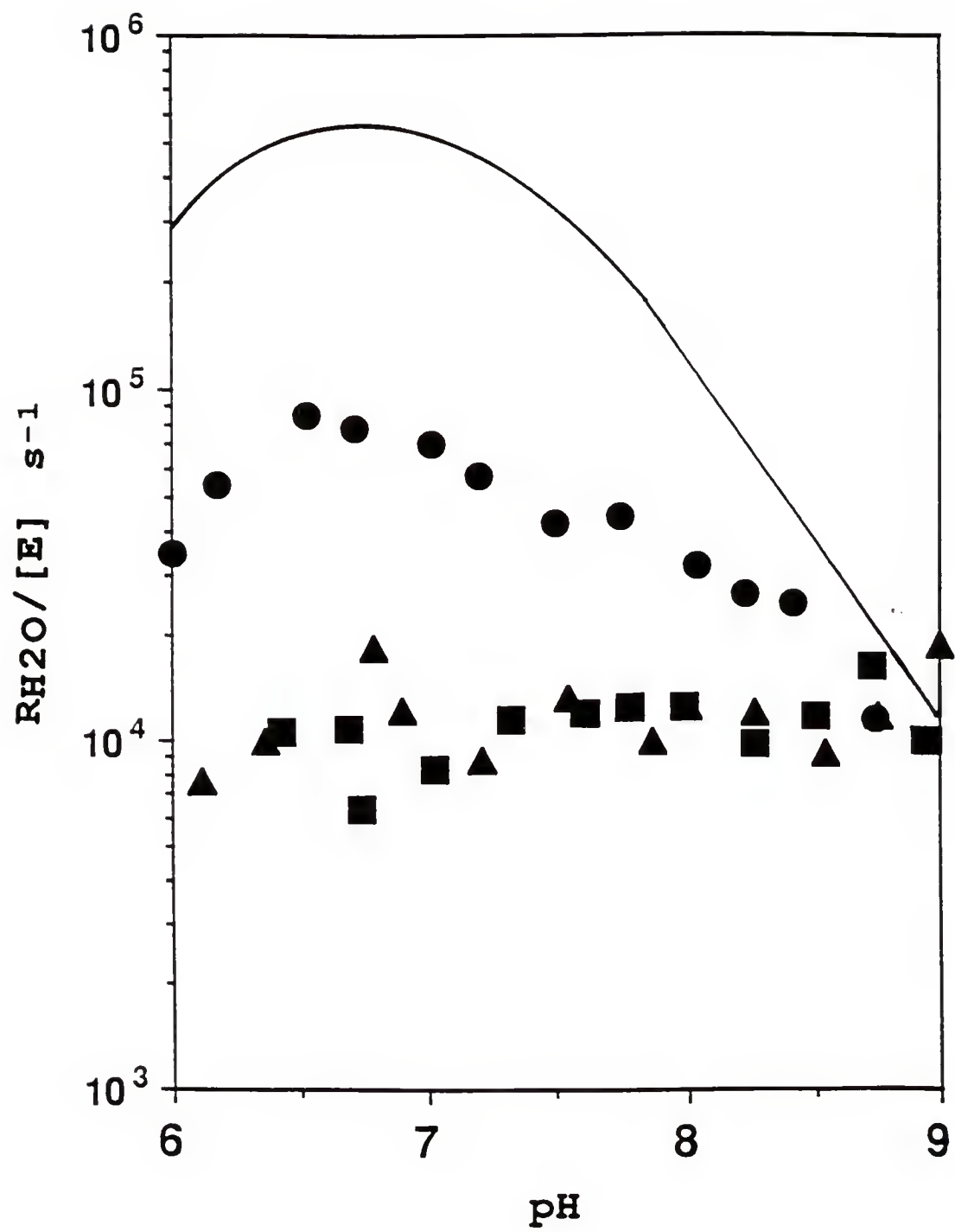


Figure 15. Comparisons of the water-off rates $R_{H_2O}/[E]$ (maximal values under the conditions of Figure 14) for variants of HCA III at positions 64,67, and 198 in the active site cavity of HCA III.

Values of $R_{H_2O}/[E]$ in s^{-1} appear beneath each designated mutant and the values in kcal/mol adjacent to the arrows are the free energy changes for the barriers in catalysis for the corresponding variants.

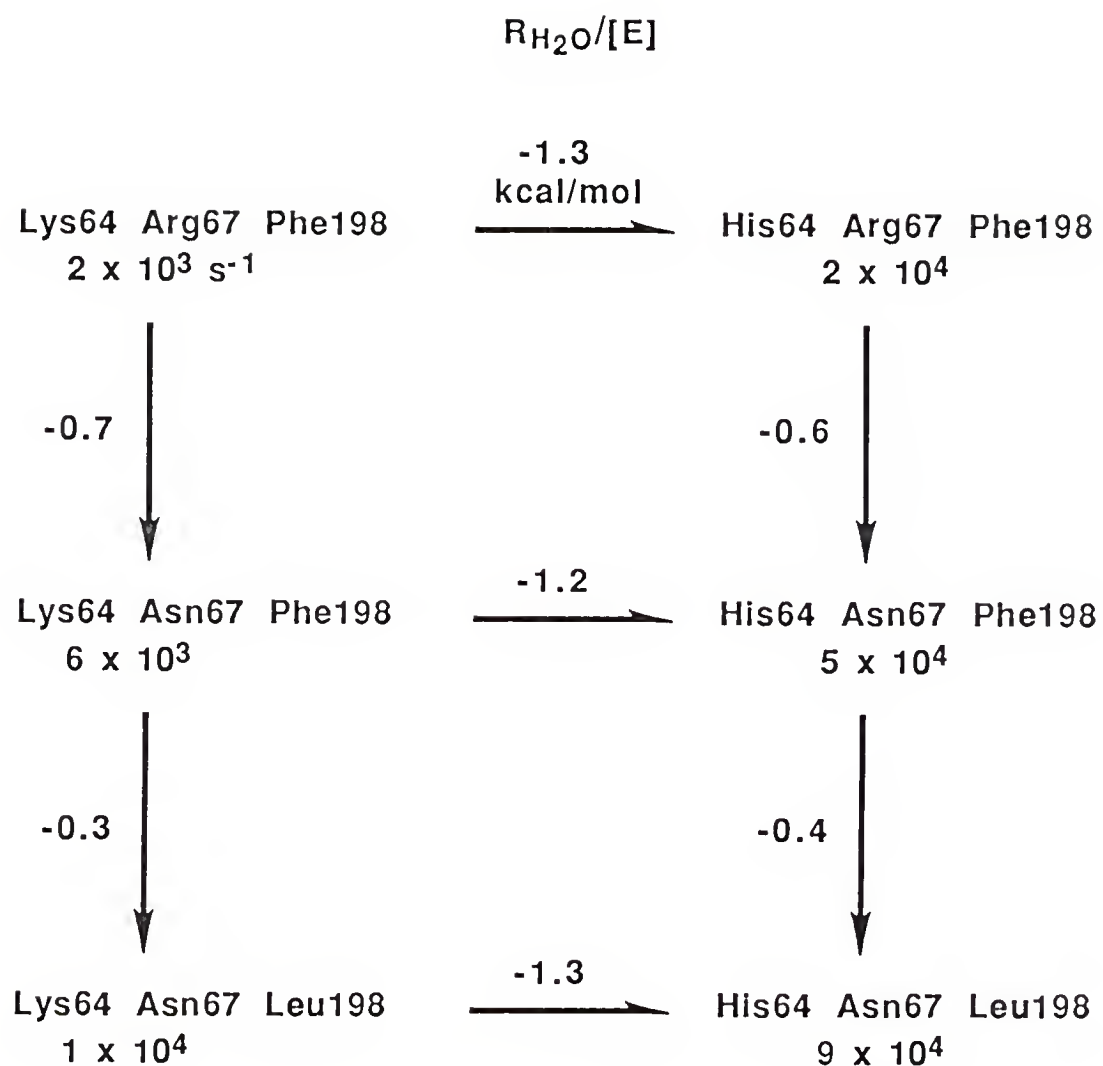
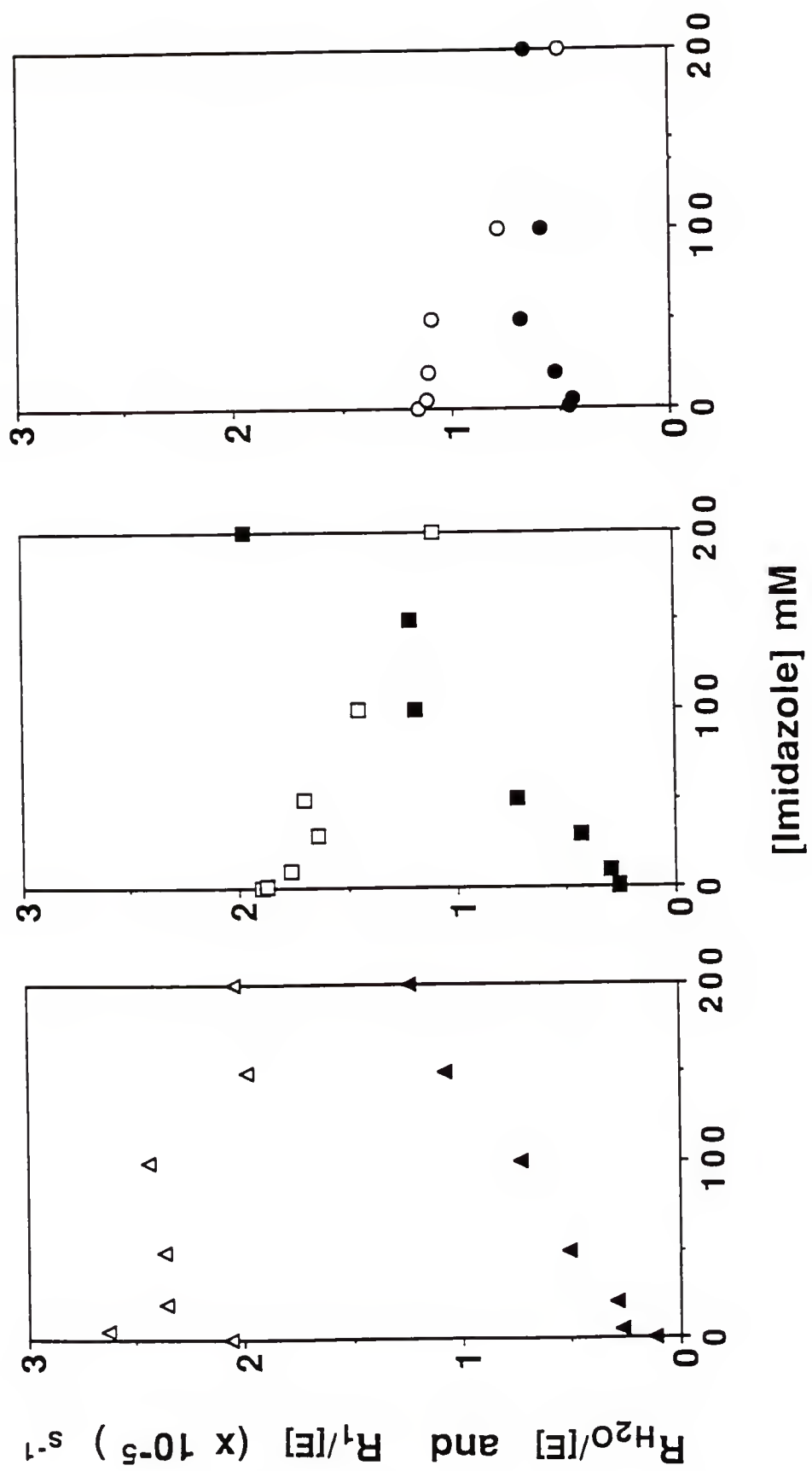


Figure 16. The dependence on the imidazole concentration of (filled symbols) $R_{H_2O}/[E]$ and (open symbols) $R_1/[E]$ catalyzed by (left) F198L HCA III; (middle) R67N-F198L HCA III; and (right) K64H-R67N-F198L HCA III.

The pH was 7.2 at 25°C with the total concentration of all species of CO_2 at 100 mM. The total ionic strength of solution was maintained at 0.2 M by addition of Na_2SO_4 .



interconversion of CO_2 and HCO_3^- at chemical equilibrium appears to be slightly inhibited by the addition of imidazole, as determined from the negative slopes of the plots in Figure 16.

The inhibition of two mutants and wild-type carbonic anhydrases II and III by two anions and the sulfonamides acetazolamide and ethoxzolamide are compared in Table 4. The reported values of K_I were obtained from ^{18}O -exchange experiments and are the concentrations of inhibitor required to reduce R_1 to 50% of its uninhibited value under the condition that the total substrate concentration ($[\text{CO}_2] + [\text{HCO}_3^-] = 25 \text{ mM}$) is much less than the apparent binding constant for substrate K_{eff} . At the pH of these experiments, 7.2, K_{eff} is about 200 mM for HCA II (Simonsson et al., 1979) and greater than 200 mM for HCA III and the two mutants in Table 3 as determined by substrate dependence studies (data not shown). The values of K_I determined from $R_{\text{H}_2\text{O}}$ in the same manner agreed within experimental uncertainty ($\pm 25\%$) with the values determined from R_1 . For the tightly bound inhibitors ethoxzolamide and acetazolamide, we accounted for the mutual depletion of free enzyme and inhibitor (Segel, 1975).

Solvent hydrogen isotope effects (SHIE) observed for $R_1/[E]$ are unity for isozymes II and III and two mutants of HCA III (Table 5). This is consistent with a wide body of data indicating no rate-contributing proton transfer in the steps of the interconversion of CO_2 and HCO_3^- shown in

Table 4. Inhibition constants K_I (micromolar) were determined from R_1 , the catalyzed rate of interconversion of CO_2 and HCO_3^- at chemical equilibrium. Measurements were made at pH 7.2 with conditions as described in the legend to Figure 14. No buffers were used.

Inhibitor	K_I			
	HCA III	F198L HCA III	R67N-F198L HCA III	HCA II
	μM			
Acetazolamide	40 (0.4) ^a	0.6 (0.08)	0.03 (0.007)	0.06 (0.02)
Ethoxzolamide	8 (0.08)	0.1 (0.02)	0.004 (0.0007)	0.008 (0.003)
OCN^-	30 (0.3)	50 (7)	30 (7)	30 (10)
I^-	30,000 (300)	30,000 (5,000)	30,000 (6,000)	30,000 (9,000)

^a Values in parenthesis are the estimated, pH-independent values for K_I describing the binding of inhibitors to the zinc-bound water form of the enzymes. These values were calculated as explained in the text using the values of pK_a determined from the esterase activities (Table 3). For HCA III these values were calculated assuming a pK_a of 5.2 for the zinc-bound water.

Table 5. Solvent hydrogen isotope effects on R_1 and R_{H_2O} catalyzed by HCA III, HCA II, and two mutants. Data were obtained at an uncorrected pH meter reading of 7; other conditions were as described in the legend to Figure 14.

	HCA III	F198L HCA III	K64H-R67N- F198L-HCA III	HCA II
$\frac{(R_1)_{H_2O}}{(R_1)_{D_2O}}$	1.03 ± 0.05^a	0.96 ± 0.08	1.05 ± 0.07	1.05 ± 0.03^b
$\frac{R_{H_2O}}{R_{D_2O}}$	2.4 ± 0.4^a	2.7 ± 0.7	4.5 ± 0.5	8.0 ± 0.7^b

^a Kararli and Silverman (1985).

^b Tu and Silverman (1982), this measurement at an uncorrected pH meter reading of 6.6.

equation 1 (Silverman and Lindskog, 1988). The SHIE for $R_{H_2O}/[E]$ are greater than 2.0 for each case in Table 5, consistent with proton transfer as a rate-contributing step in the pathway for the release of water from the active site (eq. 4). For comparison, k_{cat} for hydration of CO_2 has a SHIE of 3.8 and 2.5 for HCA II and III, respectively (Steiner et al., 1975; Kararli and Silverman, 1985).

Discussion

The most significant structural differences near the active sites of isozymes II and III of human carbonic anhydrase are at positions 64, 67, and 198. We have prepared mutants of isozyme III in which each of these residues is replaced by the amino acid present at the corresponding position of isozyme II. The aim of this work is to determine the catalytic role of these residues and the source of the large differences in catalytic and inhibition properties between HCA II and III.

Interconversion of CO_2 and HCO_3^-

The replacements Arg 67 \rightarrow Asn and Phe 198 \rightarrow Leu affected k_{cat}/K_m independently; the lowered energy barrier for the double mutant was the algebraic sum of the energy changes for each of the single mutants. This is demonstrated in Figure 13 in which the change in energy barriers for k_{cat}/K_m of the catalysis is given by the value adjacent to the arrows, in the manner described by Carter et al. (1984). The

replacement Lys 64 \rightarrow His had no effect on k_{cat}/K_m (except at pH > 8, see Jewell et al., 1991). These results can be understood by the rather widely separated positions of these residues in the active site cavity of isozyme III (Right panel of Figure 3). Phe 198 is on the hydrophobic side of the active-site cavity and Lys 64 and Arg 67 are on the hydrophilic side. Moreover, these two positively charged residues are separated by 8.8 Å, the distance between the side-chain N- ζ of Lys 64 and the C- ζ of Arg 67 in the crystal structure of bovine CA III (Eriksson 1988). The distance between these positions and the zinc is 12.6 and 9.2 Å, respectively.

We have also observed a pH dependence in k_{cat}/K_m for hydration of CO₂ in the HCA III mutants containing the Phe 198 \rightarrow Leu replacement. This is in contrast to the values of k_{cat}/K_m for wild-type CA III which are independent of pH in the range of pH 6 to 8 (Tu et al., 1983; Engberg et al. 1985; Kararli and Silverman, 1985). The lack of a pH dependence is attributed to the low pK_a of the zinc-bound water. The visible absorption spectrum of Co(II)-substituted bovine CA III (Engberg and Lindskog, 1984) provides additional evidence that for wild-type HCA III the pK_a of the zinc-bound water is less than 6.0. The pH dependence of k_{cat}/K_m in the Leu 198-containing mutants suggests that the pK_a of the zinc-water is above 6 and closer to the value of pK_a 7 for HCA II.

The pH dependence of catalysis for the Leu 198-containing mutants was supported by observation of the

hydrolysis of 4-nitrophenyl acetate in which the effect of an ionization with pK_a near 6.5 is apparent. There is very strong evidence that the pK_a obtained from ester hydrolysis reflects the ionization of the catalytically important metal-bound water (Pocker and Sarkanen, 1978; Simonsson and Lindskog, 1982). We conclude that the Phe 198 \rightarrow Leu replacement has increased the pK_a of the zinc-bound water from a value below 6.0 in wild-type HCA III (the exact value has not been determined because the enzyme denatures before the ionization is reached) to a value near 6.5 for the Leu 198-containing mutants. The values of pK_a from the esterase data are a more precise estimate than those obtained from k_{cat}/K_m for CO_2 hydration.

The increases in k_{cat}/K_m for the mutants of HCA III containing Leu 198 (Table 3 and Figure 13) can be attributed to the steps in equation 1. The ratio k_{cat}/K_m for hydration of CO_2 contains rate constants in the pathway up to and including the release of HCO_3^- from the enzyme; in terms of the simplified pathway of equation 1, $k_{cat}/K_m = k_1k_2/(k_{-1} + k_2)$. This ratio is unaffected by the intra- and inter-molecular proton transfer steps described in equation 2 (see for example Jonsson et al., 1976; Tu et al., 1990). Unlike HCA II in which k_{cat}/K_m is dominated by k_1 (Lindskog, 1984), isozyme III probably has significant contributions to k_{cat}/K_m of all three constants k_1 , k_{-1} , and k_2 (Rowlett et al., 1991). Thus, the Phe 198 \rightarrow Leu replacement could enhance k_{cat}/K_m at one or more of three steps: CO_2 binding, the interconversion

on the enzyme, and the dissociation rate of product HCO_3^- . To emphasize the complexity in explaining these changes, we note that the mutant of the efficient carbonic anhydrase II made by the replacement Leu 198 \rightarrow Phe (that is, L198F HCA II) has a value of k_{cat}/K_m that is about as great as that observed for wild-type HCA II (Ren et al., 1991; Taoka et al., 1991).

The increased value of the apparent pK_a of the catalysis upon the replacement Phe 198 \rightarrow Leu is not due significantly to changes involving the two positively charged side chains of Lys 64 and Arg 67 which have minor effects on this pK_a (Table 3). It is interesting that this increase is caused by the replacement of a hydrophobic residue by another hydrophobic residue. This increase in pK_a is very difficult to explain since it could arise, for example, from rather small conformational changes that affect the alignment or distance of the hydrogen bonds to zinc-bound water and that stabilize the zinc-bound water over zinc-bound hydroxide (see for example Scheiner and Hillenbrand, 1985). It is known from the structures of isozymes II and III that the zinc-bound hydroxide (and zinc-bound water in the low pH form) is hydrogen bonded with the side chain of Thr 199 and with two water molecules in the active site forming part of a partially ordered network of at least nine hydrogen-bonded waters (Eriksson et al., 1988). One of these waters forms a hydrogen bond with the π -electron cloud of the phenyl ring of Phe 198 in HCA III (Eriksson, 1988) suggesting that the Phe 198 \rightarrow Leu mutation may affect this water structure.

Proton Transfer

The replacement Phe 198 \rightarrow Leu caused up to 10-fold increases in k_{cat} for hydration (Table 3) and $R_{\text{H}_2\text{O}}$, the proton transfer-dependent rate of release of water from the active site (Figure 14) without introducing a residue capable of proton transfer. For the single mutant F198L and the double mutant R67N-F198L HCA III the values of k_{cat} are the same and generally independent of pH at $2 \times 10^4 \text{ s}^{-1}$, except at pH > 8.5 for the double mutant which may be due to the ionization of Lys 64. The values of $R_{\text{H}_2\text{O}}/[\text{E}]$ are also the same for this single and double mutant at about $1 \times 10^4 \text{ s}^{-1}$, again independent of pH. These properties of k_{cat} and $R_{\text{H}_2\text{O}}/[\text{E}]$ are similar to those observed for H64A HCA II, a mutant of the efficient isozyme in which the internal proton transfer group of His 64 is replaced with alanine, a side chain which cannot transfer protons. For H64A HCA II, k_{cat} is near $1 \times 10^4 \text{ s}^{-1}$ (pH 7.2 with a noninteracting buffer such as Mops; Tu et al., 1989), and $R_{\text{H}_2\text{O}}/[\text{E}]$ is independent of pH near $1 \times 10^4 \text{ s}^{-1}$. The solvent hydrogen isotope effects of Table 5 are consistent with a rate-contributing proton transfer in $R_{\text{H}_2\text{O}}$ catalyzed by two mutants of HCA III containing Leu 198. A reasonable hypothesis is proton transfer between the zinc-water and water in the active site.

Both k_{cat} and $R_{\text{H}_2\text{O}}/[\text{E}]$ were further increased for the triple mutant; k_{cat} increased to a value near $1 \times 10^6 \text{ s}^{-1}$ and $R_{\text{H}_2\text{O}}/[\text{E}]$ to $1 \times 10^5 \text{ s}^{-1}$ (Table 3, Figure 14). This triple

mutant contains His 64 which increases these parameters because of the introduction of an internal proton shuttle, the imidazole of the side chain, to facilitate proton transfer between zinc-water and solution. This is supported not only by the increased values of k_{cat} and $R_{\text{H}_2\text{O}}/[\text{E}]$ in Table 3 and Figure 14 but also roughly by the pH dependence of these parameters (Steiner et al., 1975; Tu et al., 1989; Jewell et al., 1991). The solvent hydrogen isotope effect in $R_{\text{H}_2\text{O}}$ for the triple mutant, Table 5, indicates a considerable contribution of proton transfer to the overall rate of $R_{\text{H}_2\text{O}}$.

We give, in Figure 15, the changes in energy barriers for $R_{\text{H}_2\text{O}}/[\text{E}]$ upon mutations in HCA III. Each of the enzymes in the first column contains Lys 64 and each in the second column contains His 64; therefore, the energy changes associated with the horizontal arrows of Figure 15 pertain to the introduction of the internal proton shuttle. This decrease in the energy barrier of 1.3 kcal/mole is independent of the replacements we made at positions 67 and 198. The intramolecular proton transfer between His 64 and the zinc-bound hydroxide is believed to occur through intervening hydrogen-bonded water (Venkatasubban and Silverman, 1980), and our results suggest that the replacements Arg 67 \rightarrow Asn and Phe 198 \rightarrow Leu do not influence this process. The measurements of $R_{\text{H}_2\text{O}}$ were made in the absence of added buffers so that the additional pathway for proton transfer involving buffer in solution (Tu et al., 1989) is avoided in these measurements.

Both k_{cat} and $R_{\text{H}_2\text{O}}$ for isozyme III are believed to be dominated by proton transfer to water (Kararli and Silverman 1985; Rowlett et al. 1991). Proton transfer energetics involving water are sensitive to changes in the distance of the hydrogen bond and deformations of the O-H ...O angle. For example, increasing the O ... O distance by 0.1 Å can increase the energy barrier for the proton transfer ($\text{H}_2\text{O}-\text{H}-\text{H}_2\text{O})^+$ by as much as 5 kcal/mole (Hillenbrand and Scheiner 1986). One other consideration is the frequent observation that the energy barrier for proton transfer is directly related to the difference in pK_a of the proton donor and acceptor groups. On this basis alone, we would predict that the mutants containing Leu 198 would have k_{cat} for hydration less than for wild type because of the greater proton affinity of the zinc-bound water in the mutants ($\text{pK}_a = 6.5$) compared with the wild type ($\text{pK}_a < 6.0$). However, the opposite was observed (Table 3). Consequently, changes in the structure of hydrogen-bonded water caused by the different side chains in the mutants may be more important than the initial and final energy levels in explaining the proton transfer rate between zinc-bound water and water in the active site.

Another effect of the Phe 198 → Leu replacement in HCA III is to enhance the apparent second-order rate constant $k_{\text{H}_2\text{O}}^{\text{B}}/K_{\text{eff}}^{\text{B}}$ (see Tu et al., 1990) for the transfer of protons from imidazole in solution to the enzyme. For F198L HCA III this constant is $5 \times 10^5 \text{ M}^{-1}\text{s}^{-1}$, obtained from Figure 16, and

for the double mutant R67N-F198L HCA III it is $9 \times 10^5 \text{ M}^{-1}$. The constant $k_{\text{H}_2\text{O}}^{\text{B}}/K_{\text{eff}}^{\text{B}}$ for the triple mutant is difficult to estimate because of experimental scatter, but is quite low, presumably because this enzyme has the internal proton transfer group of His 64. The value of $k_{\text{H}_2\text{O}}^{\text{B}}/K_{\text{eff}}^{\text{B}}$ for wild type HCA III is $1 \times 10^5 \text{ M}^{-1}\text{s}^{-1}$ (Tu et al., 1990). The increase in $k_{\text{H}_2\text{O}}^{\text{B}}/K_{\text{eff}}^{\text{B}}$ caused by the replacement Phe 198 \rightarrow Leu could be due to enhanced accessibility of the small buffer imidazole to the active site caused by the removal of the steric hindrance of Phe 198 or to some more subtle structural change. It is possible that proton transfer between imidazole and zinc-water occurs through the intervening water structure just as proposed for His 64 (Silverman and Lindskog, 1988).

Inhibition

Table 4 presents the apparent inhibition constants K_{I} at pH 7.2 for two sulfonamides and two anions determined by inhibition of ^{18}O exchange catalyzed by HCA II, HCA III, and two mutants. It is known that anions such as SCN^- and halides bind directly to the metal in carbonic anhydrase, displacing water or forming a fifth ligand (Lindskog, 1982; Eriksson et al., 1988). The binding of anions to the zinc-hydroxide form of isozyme II is very weak compared with that of the zinc-water form (approximately 100-fold weaker; Tibell et al., 1984). This has not been shown specifically for

isozyme III but is almost certainly the case. The pH dependence of the binding of acetazolamide indicates that a similar situation pertains (Lindskog and Thorslund, 1968).

We can convert the apparent values of K_I in Table 4 to pH-independent binding constants for the zinc-water form of the enzymes by dividing each value of the apparent K_I by $(1 + K_a/[H^+])$ using the values of pK_a determined from the hydrolysis of 4-nitrophenyl acetate (Table 3). These estimates of pH-independent K_I are given in parentheses in Table 4. The replacement Phe 198 \rightarrow Leu caused a considerable increase in tightness of binding for both acetazolamide and ethoxzolamide, resulting in values of K_I closer to that for HCA II. Eriksson et al. (1988) have shown that the thiadiazole ring of acetazolamide bound to HCA II is in van der Waals' contact with the side chain of Leu 198. It is most likely an unfavorable steric interaction between the thiadiazole ring and Phe 198 that contributes to the weak binding of acetazolamide to HCA III. On the other hand, the Phe 198 \rightarrow Leu replacement in HCA III caused a weaker binding of OCN^- and I^- , consistent with the known weaker binding of anions to HCA II compared with HCA III (Table 4; Sanyal et al., 1982).

Conclusion

It was previously suggested (Kararli and Silverman, 1985) that Lys 64 and Arg 67 were responsible for the unique catalytic and inhibition properties of carbonic anhydrase III, specifically its low activity in CO₂ hydration and ester hydrolysis, low pK_a for zinc-bound water, and weak binding of sulfonamides. The present work complements Jewell et al. (1991) in showing that Lys 64 and Arg 67 have relatively minor roles in determining these properties, but that Phe 198 can be identified as a major contributor to these unique features of carbonic anhydrase III.

CHAPTER 4

EFFECTS OF THE MOLECULAR PROPERTIES OF RESIDUE 198 ON CATALYSIS AND INHIBITION OF HCA III

Introduction

The previous chapter illustrated the important role Phe-198 plays in the catalytic hydration of CO₂, hydrolysis of 4-nitrophenyl acetate, and the binding of inhibitors by HCA III. This chapter focuses on how the molecular properties of residue 198 affect catalysis and inhibition, and what consequences this has on the two-stage catalysis.

Six replacement residues (Ala, Asn, Asp, Leu, Tyr, and Val) were introduced at position 198 which differ in size, charge, hydrogen bonding capability, and hydrophobicity. These residues were selected in part based on the surrounding active-site cavity environment. Unique to this active site is its water structure (Figure 2). For example, water 335 has been shown to hydrogen bond to the π -electron system of the benzene ring of Phe 198. In turn, water 335 is involved in a hydrogen bonding network through the hydroxyl group of Thr 200 and water 318 to the zinc-bound water of the active site (Eriksson, 1988). Since no analogous pattern is possible for HCA II, this unique aspect of the water structure could contribute to the catalytic properties of HCA III.

Indeed we have found that all of the replacements caused an increase in CO_2 and HCO_3^- interconversion. Non-hydrogen bonding residues (Ala, Val, Leu) had k_{cat} for hydration 10-fold greater than hydrogen bonding residues (Asn, Asp, Phe, Tyr). In addition, a correlation between hydrophobicity and the turnover number was found. These data suggest an altered proton transfer pathway in these mutants.

Results

The steady-state rate constant, k_{cat}/K_m for the hydration of CO_2 catalyzed by HCA III and six mutants at position 198 was measured by stopped-flow spectrophotometry and ^{18}O exchange between CO_2 and water. It is an interesting observation that every replacement made at this position resulted in a mutant with k_{cat}/K_m for CO_2 hydration greater than that of wild-type HCA III (Table 6). The largest changes were observed with the replacement Phe 198 \rightarrow Asp which resulted in a 130-fold enhancement of k_{cat}/K_m compared to wild-type HCA III (Table 6). The replacement Phe 198 \rightarrow Tyr caused the least effect. Two of the mutants, F198Y and F198V HCA III, were similar to wild-type in that no pH dependence of k_{cat}/K_m for hydration was observed in the range of our measurements (pH 6 to 9). However, the pH dependence of k_{cat}/K_m for the mutants F198A, F198D, F198L, and F198N HCA III could be described by a single ionization with a maximum at high pH (Table 6). Here the largest change was for F198D HCA III which had the apparent pK_a for catalysis increased to

Table 6. Maximal (pH-independent) steady-state constants and values of the apparent pK_a for the hydration of CO_2 and rate of release of $H_2^{18}O$ catalyzed by mutant and wild-type carbonic anhydrases^a

Enzyme	k_{cat}/K_m ($\times 10^{-6} M^{-1} s^{-1}$)	k_{cat}^b ($\times 10^{-4} s^{-1}$)	pK_a	$R_{H_2O}/[E]$ ($\times 10^{-4} s^{-1}$)
wild-type HCA III ^c	0.3	0.2	<6.0	0.3
F198Y HCA III	0.5	0.2	<6.0	0.2
F198V HCA III	1.6	1.0	<6.0	0.3
F198N HCA III	6.2	0.2	7.1	d
F198A HCA III	6.5	2.5	6.5	1.5
F198L HCA III	7.4	2.2	6.9	1.0
F198D HCA III	43	0.2	9.2	d
wild-type HCA II ^e	150	140	7.0	60

^a Values of apparent pK_a for catalysis were determined from k_{cat}/K_m for the hydration of CO_2 with standard errors in the pK_a of 0.2. Values of k_{cat} had standard errors less than 20% and k_{cat}/K_m less than 12%.

^b These values omit an increase at $pH > 8$ which has been attributed to the ionization of Lys 64 (Jewell et al., 1991).

^c From Jewell et al. (1991).

^d pH-dependence not described by a single ionization. See Figure 19.

^e From Khalifah (1971).

9.2 compared to wild-type HCA III which has been estimated at 5 (Ren et al., 1988). Figure 17 compares the pH-dependence of k_{cat}/K_m for the mutants F198D and F198N HCA III. Values of this ratio measured by ^{18}O -exchange at low total substrate concentration were identical with values measured at steady state. For the mutant F198D HCA III the maximal value of k_{cat}/K_m was 3-fold less than that for wild-type HCA II (Khalifah, 1971; Steiner et al., 1975).

A range of effects was also seen on the steady-state turnover number, k_{cat} for CO_2 hydration catalyzed by six mutants of HCA III at position 198 (Table 6). The replacement of Phe 198 with residues capable of hydrogen bonding (Asn, Asp, and Tyr) left k_{cat} unchanged in the low pH region. The replacements Phe 198 \rightarrow Ala and Phe 198 \rightarrow Leu increased k_{cat} approximately 12-fold. The values of k_{cat} for hydration of CO_2 catalyzed by HCA III and the mutants F198A, F198L, F198V, and F198Y HCA III of Table 6 were observed to be independent of pH in the range 6 to 8. Above pH 8, we observed a slight increase in k_{cat} for these mutants similar to that observed by many workers for wild-type CA III and consistent with the effect on catalysis of the ionization of Lys 64 (Karali and Silverman, 1985; Jewell et al., 1991; Rowlett et al., 1991). This effect was most dramatic for the mutants F198D and F198N HCA III. Enhancement of activity was maximal at high pH for both mutants, and for F198D HCA III the activity could be described by a single ionization having a pK_a value of 9.6 ± 0.3 (Figure 18). For the mutant F198D

Figure 17. pH dependence of the logarithm of k_{cat}/K_m ($\text{M}^{-1} \text{s}^{-1}$) for the hydration of CO_2 catalyzed by (\blacktriangle) F198D HCA III, and (Δ) F198N HCA III.

The buffers used in the experiments were: from pH 6.0 to pH 7.5, MOPS; from pH 7.8 to 8.8, TAPS; from pH 8.9 to pH 10.3, CHES. All buffer concentrations were 50 mM, the temperature was 25°C , and the total ionic strength of solution was maintained at a minimum of 0.1 M by the addition of Na_2SO_4 . The solid lines were calculated from the data using a pK_a determination in the program Enzfitter (Elsevier Biosoft, Cambridge, UK). The following pK_a values were calculated: F198D HCA III, 9.2 ± 0.2 ; F198N HCA III, 7.1 ± 0.04 . The maximal fitted values of k_{cat}/K_m ($\text{M}^{-1} \text{s}^{-1}$) for F198D HCA III and F198N HCA III were: $(4.3 \pm 0.3) \times 10^7$ and $(6.2 \pm 0.1) \times 10^6$, respectively.

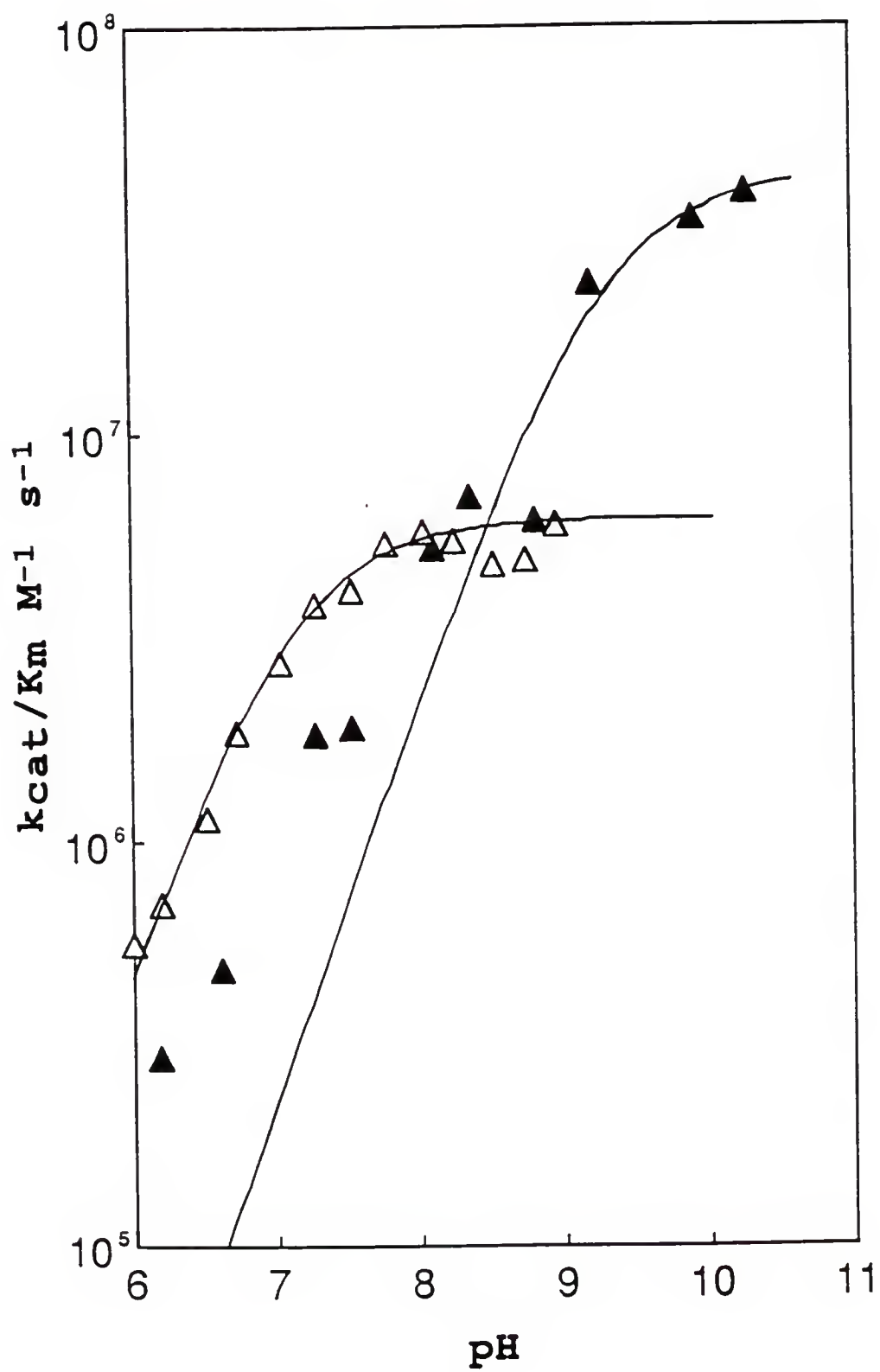
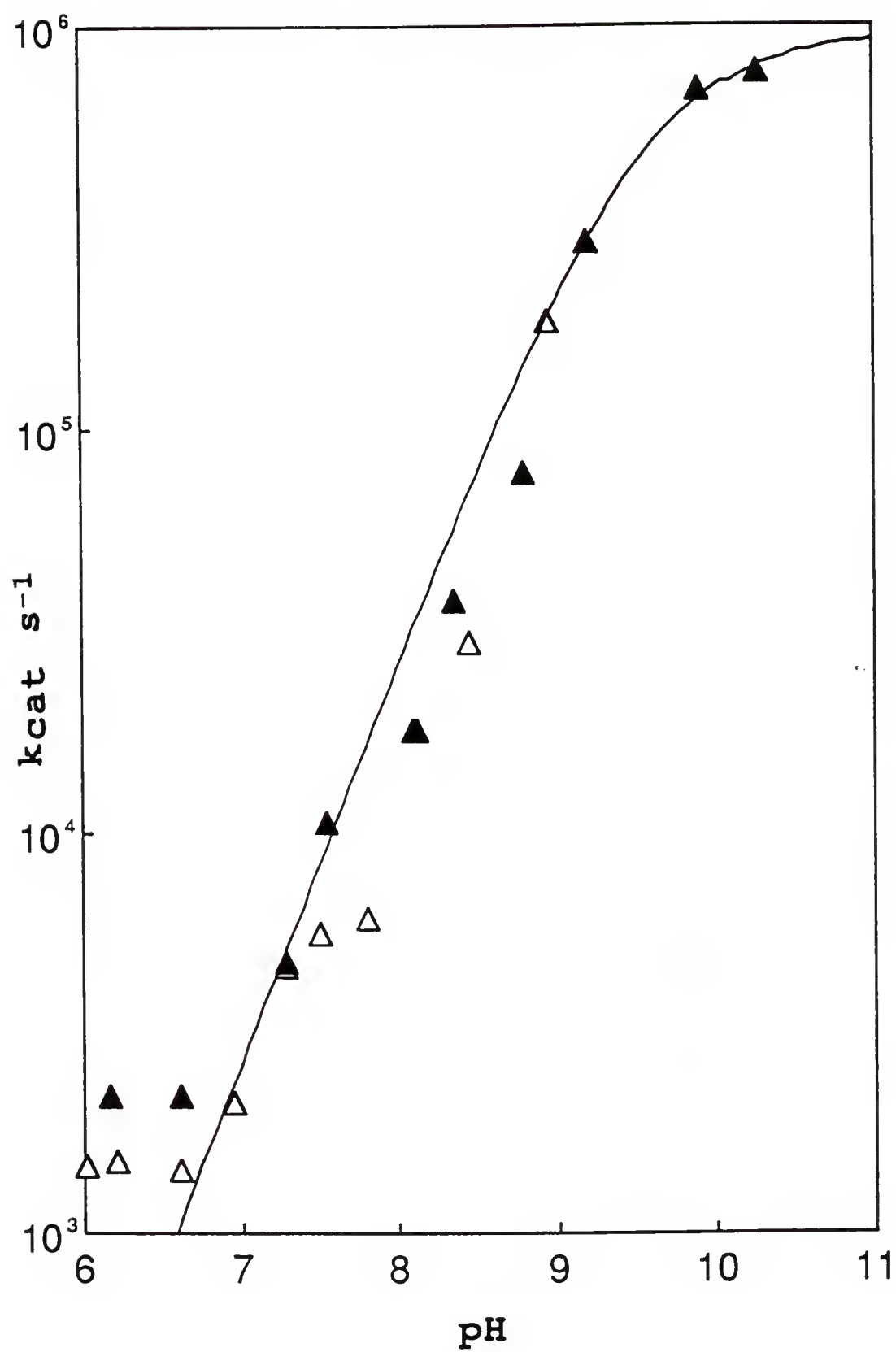


Figure 18. pH dependence of the logarithm of k_{cat} (s^{-1}) for the hydration of CO_2 catalyzed by (\blacktriangle) F198D HCA III, and (Δ) F198N HCA III.

Experimental and fitting conditions were identical to those in Figure 19. The following pK_a value was calculated: F198D HCA III, 9.6 ± 0.1 . The maximal fitted value of k_{cat} (s^{-1}) for F198D HCA III was $(9.5 \pm 0.5) \times 10^5$.



HCA III, maximal turnover approached $1 \times 10^6 \text{ s}^{-1}$. This value is in close agreement with the maximal turnover for wild-type HCA II (Khalifah, 1971; Steiner et al., 1975).

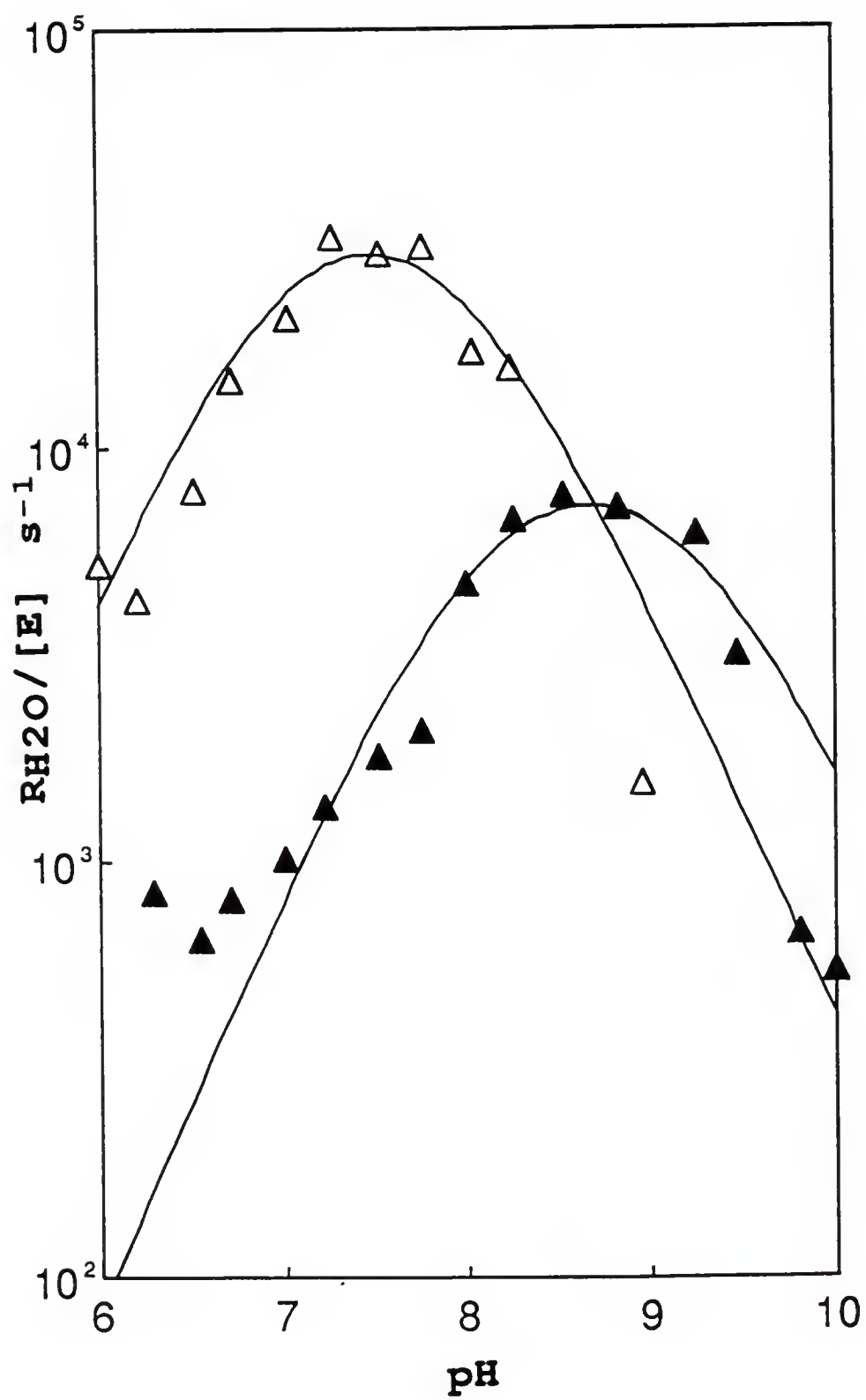
Only two of the mutants of HCA III listed in Table 6 had maximal values of k_{cat}/K_m for the catalytic hydrolysis of 4-nitrophenyl acetate greater than that of wild-type: F198A and F198L HCA III had k_{cat}/K_m at 60 and 1000 $\text{M}^{-1}\text{s}^{-1}$, respectively. The values of the apparent pK_a for this catalysis (6.0 ± 0.2 and 6.4 ± 0.2 for F198A and F198L, respectively) were somewhat lower than but in rough agreement with the values determined from CO_2 hydration and given in Table 6. These activities in ester hydrolysis catalyzed by F198A and F198L HCA III were inhibited by addition of 10^{-5} M ethoxzolamide.

The proton transfer dependent rates of release of H_2^{18}O from the active site, $R_{\text{H}_2\text{O}}/[\text{E}]$, for the F198A, F198L, F198V, and F198Y mutants of HCA III are listed in Table 6. $R_{\text{H}_2\text{O}}/[\text{E}]$ showed very little pH dependence over the range of pH 6 to 8 for these four mutants. F198A HCA III and F198L HCA III were enhanced approximately 10-fold and 5-fold, respectively, compared with wild-type HCA III, whereas F198V HCA III and F198Y HCA III were virtually unchanged compared with wild-type HCA III. For the mutants F198D and F198N HCA III, there was a pH-dependence of $R_{\text{H}_2\text{O}}/[\text{E}]$ with maximal enhancement at high pH (Figure 19).

Figure 19. pH dependence of $R_{H_2O}/[E]$ for (▲) F198D HCA III, and (Δ) F198N HCA III.

Solutions contained 25 mM total concentration of CO_2 and HCO_3^- for measurements in the pH range 6.0 to 8.5 and 100 mM for measurements in the pH range of 8.5 to 10.5, and no buffers were used. Experiments were carried out at 25°C with the total ionic strength of the solution maintained at 0.2 M with Na_2SO_4 . The curves drawn through the data points were calculated for two pK_a 's with the fitting program RS1 (BBN Software Products, Cambridge, MA). The pK_a of zinc-bound water measured from CO_2 hydration for F198D HCA III and F198N HCA III was set at 9.2 (Table 6, Figure 17) and 7.1 (Table 6, Figure 17), respectively. The pK_a of the proton donor group of F198D HCA III was 8.2 ± 0.1 , with the maximal fitted value, k_H (s^{-1}) = $(1.4 \pm 0.3) \times 10^5$. The pK_a for the proton donor group of F198N HCA III was 7.9 ± 0.1 , with the maximal fitted value, k_H (s^{-1}) = $(5.7 \pm 0.6) \times 10^4$. The maximal fitted value k_H is given in the following equation:

$$R_{H_2O} = k_H[E] / [(1 + 10^{(pH-pK_1)}) [1 + 10^{(pK_2-pH)}]]$$



The inhibition of the mutants and wild-type HCA III by ethoxzolamide and cyanate were determined using ^{18}O exchange at chemical equilibrium. The values of K_I in Table 7 are the concentrations of inhibitor required to reduce R_1 to 50% of its uninhibited value under the conditions that the total substrate concentration ($[\text{CO}_2] + [\text{HCO}_3^-] = 25 \text{ mM}$) is much less than the apparent binding constant for substrate K_{eff} . At the pH of these measurements, 7.3 to 7.5, K_{eff} is greater than 200 mM for wild-type HCA III and the mutants. Values in parentheses are the pH-independent binding constant.

Discussion

The replacement of Phe 198 in HCA III with Leu (previous chapter), the residue found at the corresponding position in isozyme II, results in a mutant that approaches HCA II in several properties. Compared with wild-type HCA III, the mutant F198L HCA III has significant enhancement (up to 25-fold) in catalytic hydration of CO_2 and 100-fold in hydrolysis of 4-nitrophenyl acetate, has an increase of at least one unit in the pK_a of the zinc-bound water, and has 80-fold increased inhibition by ethoxzolamide. The current study was designed to take advantage of the sensitivity of catalysis and inhibition to position 198 in HCA III and to understand the features of the active site that affect the mechanism.

Table 7. Inhibition constants determined from R_1 , the catalyzed rate of interconversion of CO_2 and HCO_3^- at chemical equilibrium^a

Enzyme	Ethoxzolamide (μM)	Cyanate (mM)
wild-type HCA III ^b	8.1 (0.05) ^c	0.03 (0.0002)
F198Y HCA III	8.9 (0.06)	0.03 (0.0002)
F198V HCA III	2.4 (0.02)	0.4 (0.003)
F198N HCA III	0.26 (0.09)	1.5 (0.5)
F198A HCA III	0.18 (0.02)	d
F198L HCA III	0.11 (0.03)	0.05 (0.02)
F198D HCA III	140 (130)	11 (11)
R67N-F198A HCA III		0.7 (0.08) ^e
wild-type HCA II ^f	0.008 (0.003)	30 (12)

^a Measurements were made at pH 7.3 to 7.5 with the conditions described in the legend to Figure 19. No buffers were used.

^b From Sanyal et al. (1982).

^c Values in parentheses are the estimated, pH-independent values for K_I describing the binding of inhibitors to the zinc-bound water form of the enzymes. These values were calculated as explained in the text using the values of pK_a determined from CO_2 hydration (Table 6). For HCA III, F198V HCA III, and F198Y HCA III, these values were calculated by assuming a pK_a of 5.2 for zinc-bound water.

^d Measurement not made.

^e Used as the Ala point in Figure 21.

^f From LoGrasso et al. (1991).

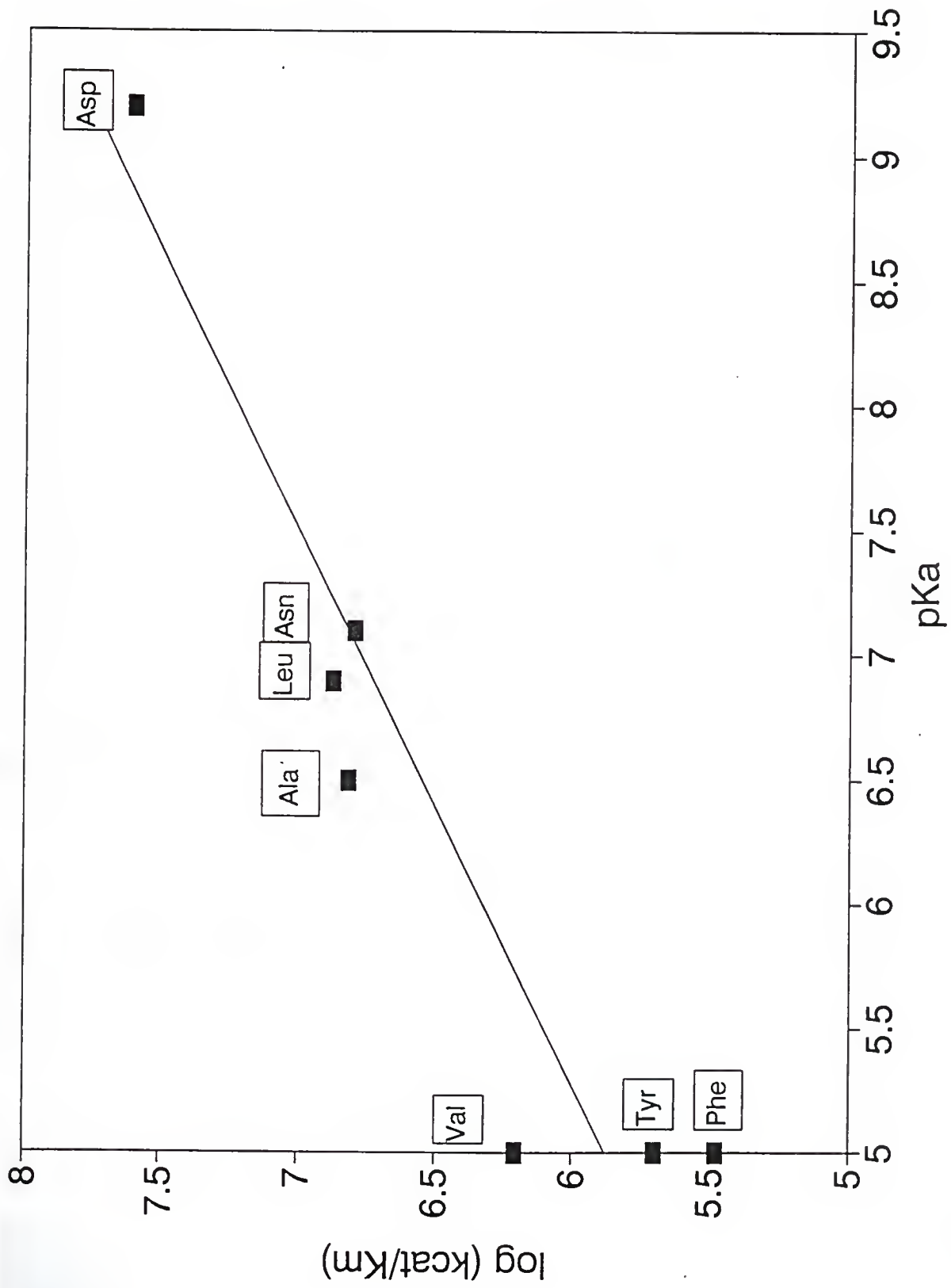
Interconversion of CO_2 and HCO_3^-

In the two-stage mechanism of catalysis of the hydration of CO_2 by carbonic anhydrase, the ratio k_{cat}/K_m contains rate constants for the steps up to and including the release of the first product, HCO_3^- ; these are the steps of the interconversion of CO_2 and HCO_3^- shown in equation 1. Increases of 20-fold or greater were observed for the mutants F198A, F198D, F198L, and F198N HCA III, and were accompanied by an increase in the pK_a of zinc-bound water from what is estimated to be near 5.0 (Tu et al., 1983; Engberg and Lindskog, 1984; Karali and Silverman, 1985; Ren et al., 1988) in wild-type isozyme III to 6.5 or greater in the above mutants (Table 6; Figure 17).

The dependence of $\log(k_{\text{cat}}/K_m)$ for CO_2 hydration on pK_a is presented in Figure 20. This Bronsted plot shows a linear correlation (correlation coefficient 0.88) between $\log(k_{\text{cat}}/K_m)$ and pK_a , and has a slope of 0.45 ± 0.08 . For wild-type HCA III and the mutants F198V and F198Y, it was not possible to make a precise measurement of the pK_a of the zinc-bound water due to denaturation of the enzyme at the low pH values required to make this measurement. Ren et al. (1988) have estimated a pK_a near 5 for HCA III based on spectrophotometric data and we have used this value in Figure 20. If the pK_a of the F198Y and F198V HCA III mutants are lower than estimated by Ren et al. (1988), then the slope for the Bronsted plot would be slightly lower. Therefore, the

Figure 20. Plot of the logarithm of k_{cat}/K_m ($M^{-1}s^{-1}$) for CO_2 hydration versus pK_a of zinc-bound water for six amino acid replacements at position 198 and for wild-type HCA III.

The residue substituted at position 198 is given near the data point. The data are fit to a line using a least-squares analysis: slope = 0.45 ± 0.08 ; correlation coefficient = 0.88. When Phe and Tyr are omitted from the plot, the correlation coefficient = 0.98. Standard errors in k_{cat}/K_m were generally under 10%. Standard errors in pK_a values were generally ± 0.1 .



Bronsted plot of Figure 20 most likely represents a maximum value for this slope. These increases in activity are a direct reflection of the increased base strength of zinc-bound hydroxide, and are a common observation for nucleophilic attack on a carbonyl (Fersht, 1985). While there is much precedence for Bronsted analysis in organic reactions, the application to enzyme catalyzed reactions has been difficult because of chemical and structural constraints imposed at the active site. Our mutagenesis studies have for the first time made such analysis for carbonic anhydrase catalysis possible. While Rowlett and Silverman (1982) were able to obtain a Bronsted plot for intermolecular proton transfer between buffers in solution and His 64 of HCA II, our data are the first to show that mutations in the active-site cavity can alter the pK_a of a catalytic center of carbonic anhydrase and consequently alter catalytic rate. Indeed, most structure-reactivity studies with enzymes focus on substrate changes rather than on changes in the enzyme (Fersht, 1985). Since the Bronsted analysis is solely based on the basicity of the nucleophile, it is likely that nucleophilic attack on CO_2 has some rate contributing effects towards catalysis. However, for wild-type HCA III and F198Y HCA III we can not rule out contributions from steric effects since the pK_a of zinc-bound water for these enzymes is not precisely known, but has been shown to be less than 5.5 (Ren et al., 1988).

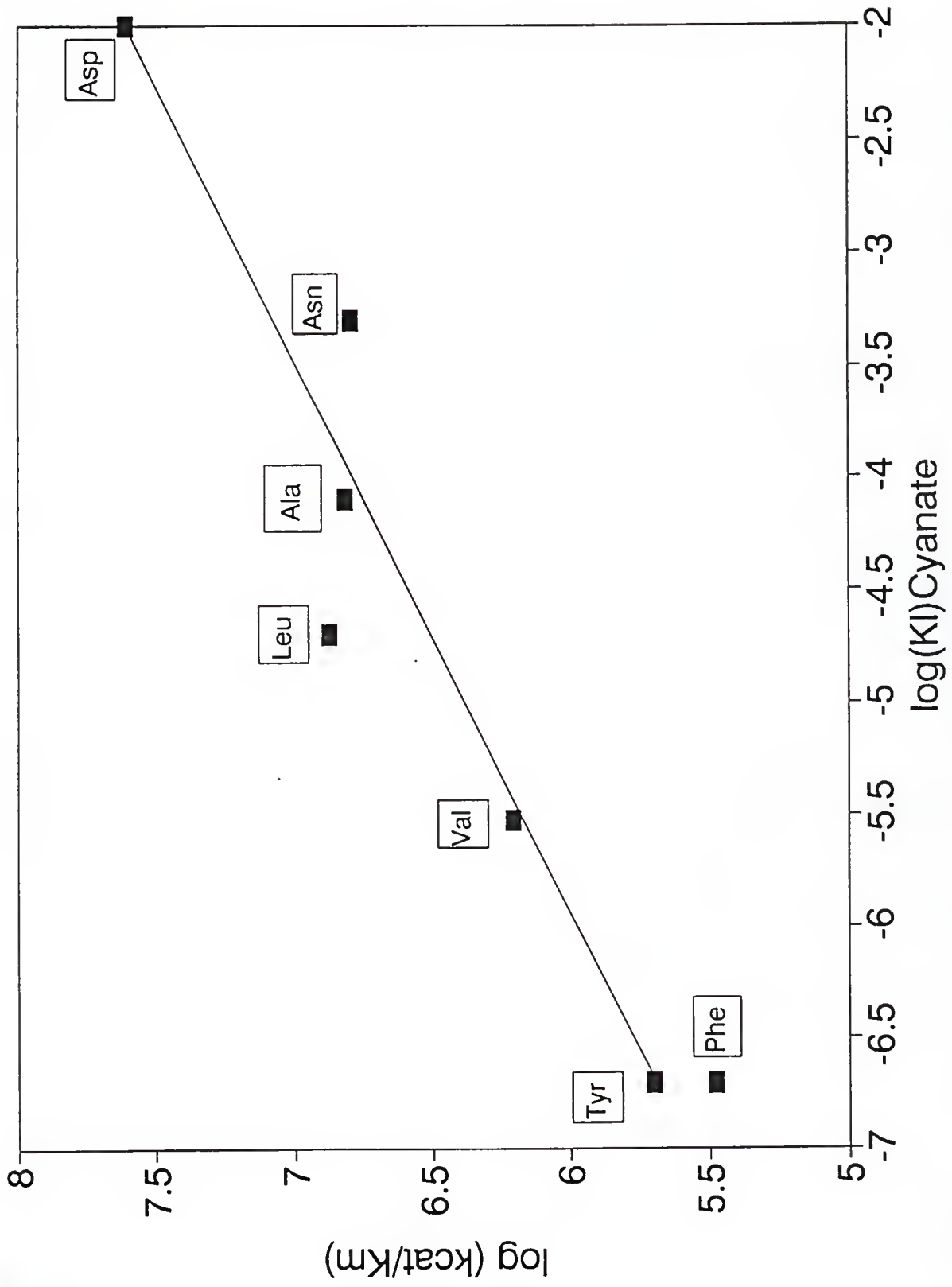
This increased base strength of the nucleophile gives information concerning the charge distribution in the transition state. For the case of a single rate-limiting step, the slope of 0.45 for the Bronsted plot indicates a structure for the transition state that is intermediate between the structure of the reactants and the structure of the products. However, it may be that no single step is completely rate limiting. Since k_{cat}/K_m contains rate constants up to and including the release of HCO_3^- (eq. 1), enhancement by replacements at position 198 could effect one or more of three possible steps: CO_2 binding, the interconversion on the enzyme, and the dissociation rate of HCO_3^- . Calculation of $\Delta\Delta G$ ($\Delta G_{\text{mutant}} - \Delta G_{\text{wild-type}}$) based on k_{cat}/K_m for CO_2 hydration for F198D HCA III and F198N HCA III is -2.90 kcal/mole and -1.80 kcal/mole, respectively. This difference of 1.1 kcal/mole between two mutants whose residues differ mainly in their charge indicates that the difference in charge between these two mutants may cause HCO_3^- release to have considerable rate-limiting contributions, especially for F198D HCA III. Furthermore, it may suggest that nucleophilic attack is only partially rate limiting for these mutant enzymes and that the rate-limiting contribution of nucleophilic attack for F198D HCA III is less than it is for F198N HCA III.

Substantial contributions from the binding of substrate or the dissociation of products or both could also have rate determining effects. This comment is based in part on the

known tight binding of anions (Sanyal et al., 1982) and the estimated tight binding of HCO_3^- (Silverman and Tu, 1986) to the active site of CA III. Behravan et al. (1990) have suggested based on derived free-energy profiles that the replacement Thr 200 \rightarrow His in HCA II stabilizes the enzyme- HCO_3^- complex by 1.79 kcal/mole caused by a substantial contribution from HCO_3^- release to the rate-determining step. In a similar manner the 1.1 kcal/mole decrease in energy barrier between F198D and F198N HCA III, could possibly be due to an increased rate of release of HCO_3^- in the case of F198D HCA III caused by the proximity of the carboxylate of Asp 198 to zinc-bound HCO_3^- . Figure 21, which shows a linear correlation (correlation coefficient 0.92) between $\log(k_{\text{cat}}/K_m)$ and $-\log(K_I)$ for cyanate gives further support to this argument. This correlation suggests that the binding of cyanate to HCA III is much weaker when charged or polar groups are present at position 198. In an analogous manner, HCO_3^- , may be more weakly bound to the enzyme when these groups are present, and consequently has a rapid release from the enzyme that results in enhanced values of k_{cat}/K_m . Calculation of $\Delta\Delta G$ ($\Delta G_{\text{mutant}} - \Delta G_{\text{wild-type}}$) between F198D HCA III and F198N HCA III based on the binding of cyanate is -1.78 kcal/mole and is on the same order as $\Delta\Delta G$ based on activity (-1.1 kcal/mole) suggesting that cyanate binding is a reasonable model for HCO_3^- binding. Indeed, Eriksson (1988) has suggested that the orientation which thiocyanate adopts in BCA III would also be the case for HCO_3^- . Finally, the complexity of these issues is illustrated in the work of

Figure 21. Plot of the logarithm of k_{cat}/K_m ($\text{M}^{-1}\text{s}^{-1}$) for CO_2 hydration versus the logarithm of $K_{\text{I}^{\text{OCN}^-}}$ (mM) for six amino acid replacements at position 198 and for wild-type HCA III.

The residue substituted at position 198 is given near the data point. The data are fit to a line using a least-squares analysis: slope = 0.41 ± 0.05 ; correlation coefficient = 0.92.



Rowlett et al. (1991) who found from simulations of catalysis that isozyme III probably has significant contributions to k_{cat}/K_m from all three constants k_1 , k_{-1} , and k_2 of equation 1.

Our primary evidence that the measured pK_a of 9.2 (Table 6; Figure 17) for F198D HCA III is that of zinc-bound water rather than the carboxylate of Asp 198 comes from two separate experimental measurements: stopped-flow spectrophotometry and ^{18}O exchange between CO_2 and water. Both of these techniques have in past experiments done by many researchers (Khalifah, 1971; Steiner et al., 1975; Silverman et al., 1979) measured a pK_a of zinc-bound water that corroborates the pK_a of zinc-bound water obtained from 4-nitrophenyl acetate hydrolysis experiments. Since the esterase measurement has been shown to be a measure of the pK_a of zinc-bound water (Lindskog, 1966; Simonsson and Lindskog, 1982), it is likely that both the steady state and equilibrium technique provide direct measurement of the pK_a of zinc-bound water as well. This interpretation is a reasonable one considering that a pK_a of 9.2 is close to expected (Martin, 1974) for a zinc-bound water moiety. On the other hand, Asp is known to have a pK_a between 2 and 5.5 in most proteins (Fersht, 1985). Thus, it is rather unlikely that Asp 198 would have a pK_a near 9.0. Additionally, it is known that anions bind the zinc-water, rather than the zinc-hydroxide from of carbonic anhydrase (Sanyal et al., 1982; Tibell et al., 1984). The closeness in magnitude of the $\Delta\Delta G$

($\Delta G_{\text{mutant}} - \Delta G_{\text{wild-type}}$) values based on ΔpK_a (5.5 kcal/mole) and $\Delta K_I^{\text{OCN}^-}$ (6.4 kcal/mole) between F198D HCA III and wild-type HCA III bear out this fact further indicating a pK_a of 9.2 for zinc-bound water rather than Asp 198.

Finally, it should be noted that we would not expect Asp 198 to form a salt bridge with any other active-site residues. The two most likely candidates, Lys 64 and Arg 67 lie on the hydrophilic side of the active-site cavity whereas position 198 is on the hydrophobic side of the cavity. The distance between the C- α atom of Lys 64 and the C- α atom of Phe 198 is 13.3 Å and the distance between the C- α atom of Arg 67 and the C- α atom of Phe 198 is 14.6 Å. Even total maximal extension of the Lys 64 side chain (6.7 Å from C- α to N- ζ) and Arg 67 (8.0 Å from C- α to N- ζ) and total maximal extension of Asp 198 would not span a large enough distance to allow formation of a direct salt bridge.

From our data it appears that most of the enhancement in CO_2 hydration activity comes from increased nucleophilic attack on CO_2 (Figure 20) and from electrostatic effects which promote HCO_3^- release (Figure 21). Indeed, we did not find any substantial correlations of k_{cat}/K_m for CO_2 hydration with the hydrophobicity of the residue at position 198 and only a marginal correlation with the volume of the side chain at residue 198, indicating that nonpolar and steric factors do not predominate. Since all of our mutations at position 198 are to smaller residues than Phe (except for Tyr, which is approximately the same size), we would not expect large

changes in structure as evidenced by Alexander et al. (1991). When they made mutations to smaller residues at position 143 in HCA II, minor structural changes were observed and, consequently, little effect was seen on activity due to the decreased volume of that residue. It was only when they made mutations to larger residues at position 143 that they observed significant structural changes which affected activity. By analogy, we would not expect steric factors to predominate in our studies.

Our hydrophobic correlation is different from the recent findings of Nair et al. (1991) in which correlations were found between k_{cat}/K_m for the hydration of CO_2 with the hydrophobicity of the side-chain at position 121 in HCA II. This site is valine in wild-type HCA II and the correlation caused enhanced activity with increased hydrophobicity at this site. However, our results are similar to recent findings of Fierke et al. (1991) in which no correlation was found between k_{cat}/K_m for hydration of CO_2 and the hydrophobicity of the side-chain at position 143 in HCA II. A reasonable hypothesis which could account for these observations revolves around the CO_2 binding site. Eriksson et al. (1988) have shown that thiocyanate bound to HCA II displaces the "deep water" molecule situated at the mouth of the hydrophobic pocket and interacts with Val 143 and Leu 198. This interaction is believed to mimic CO_2 binding. Moreover, Merz (1991) from theoretical calculations has described a binding site for CO_2 in HCA II which contains

among other residues, Val 121, Val 143, and Leu 198. Nair et al. (1991), using site-directed mutagenesis studies of Val 121 HCA II, have suggested that the side-chain of Val 121 plays only a minor role in orienting and stabilizing CO₂ during catalysis. Conversely, the x-ray crystallography experiments of Alexander et al. (1991) and the site-directed mutagenesis studies of Fierke et al. (1991) have suggested that Val 143 in HCA II plays a major role in influencing the proposed CO₂ binding site. Thus, the similarities in the hydrophobicity correlations between our results at position 198 in HCA III and that of Fierke et al. (1991) at position 143 in HCA II could reflect a common role these two residues play in CO₂ binding. It is important to stress that all three studies are investigating different residues (198, 143, and 121) using different carbonic anhydrase isozymes (HCA III for 198 and HCA II for 121 and 143), and therefore comments on these differences and similarities remain speculative until a definitive CO₂ binding site in both isozymes is determined.

Proton Transfer

The wide range of effects on the turnover number, k_{cat} indicates the strong influence residue 198 has on proton transfer (Table 6; Figure 18). There is a large body of evidence which suggests a rate-limiting proton transfer step in the turnover number for CO₂ hydration catalyzed by HCA II

and HCA III (Silverman and Lindskog, 1988). For HCA II, the pH dependence of k_{cat} is consistent with proton transfer from zinc-bound water to histidine 64 (Steiner et al., 1975; Tu et al., 1989). In HCA III, proton transfer is believed to be between zinc-bound water and water, although it has been suggested that Lys 64 in HCA III is capable of the same role at high pH (> 9.0) as His 64 in HCA II (Karali and Silverman, 1985; Jewell et al., 1991). In addition, the mutant F198D HCA III shows a solvent-hydrogen isotope effect (SHIE) of 3.27 ± 0.33 for $R_{\text{H}_2\text{O}}/[E]$ indicating a rate-limiting proton transfer in the pathway for the release of water from the active site (eq. 4). This same rate-limiting proton transfer has been shown for wild-type isozyme III (Karali and Silverman, 1985), as well as for F198L HCA III (previous chapter).

Our results for F198D and F198N HCA III confirm this role for Lys 64 in HCA III (Figure 18). The enhancement of k_{cat} to approximately $1 \times 10^6 \text{ s}^{-1}$ at high pH (> 9.0) for the mutant F198D HCA III is consistent with proton transfer from zinc-bound water to Lys 64, or some other residue with a pK_a near 9.5. The pH-dependence of k_{cat} follows a titration curve having a single ionization ($\text{pK}_a = 9.6 \pm 0.1$). This ionization is presumably that of Lys 64 and is in close agreement with a microscopic pK_a of 9.0 for Lys 64 as determined by computer simulations (Rowlett et al., 1991). Moreover, this pK_a is within one pK unit of the pK_a (8.5) determined for Lys 64 in wild-type HCA III as reported by

Jewell et al. (1991). Furthermore, Jewell et al. (1991) have shown a strong pH-dependence of k_{cat} for the mutant H64K HCA II which is qualitatively very similar to our results for F198D and F198N HCA III supporting the claim that Lys 64 is the proton acceptor group in these mutants. However, we cannot rule out the possibility that another active-site residue, such as Tyr 7 which presumably has a pK_a near 9.5 is acting as a proton acceptor.

When k_{cat} is not enhanced by the ionization of lysine 64, as is the case for the mutants F198A, F198L, F198V, and F198Y HCA III, no pH-dependence of k_{cat} is observed. However, an approximate 10-fold enhancement of k_{cat} from wild-type HCA III is seen for the mutants F198A, F198L, and F198V HCA III. These mutants have a pH-profile that nearly mirrors that of H64A HCA II in magnitude and pH-dependence (Tu et al., 1989). For H64A HCA II, Tu et al. (1989) concluded that proton transfer was between zinc-bound water and water in the active site. The data for the mutants F198A, F198L, and F198V HCA III which are similar to the data for H64A HCA II are also consistent with proton transfer between zinc-bound water and water.

In general, the transfer of protons from the active site of carbonic anhydrase to solution during the catalysis of the hydration of CO_2 is expected to follow the Bronsted relation in which the rate of proton transfer is proportional to the difference in pK_a s of zinc-bound water as donor and buffer or water as acceptor. For HCA III, we would anticipate that

this proton transfer must occur between the zinc-bound water ($pK_a < 5.5$, Ren et al., 1988) and water in solution ($pK_a = -1.7$). With the mutant of HCA III containing replacements at position 198, we observed significantly different values of the apparent pK_a for catalysis of CO_2 hydration, both by initial velocity and equilibrium methods, and for two mutants (F198A and F198L HCA III) were able to confirm these values of pK_a by observation of the catalyzed hydrolysis of 4-nitrophenyl acetate. These values of apparent pK_a are accurate representations of the ionization of the zinc-bound water (Lindskog, 1966; Simonsson and Lindskog, 1982). In fact, we did not observe adherence to the Bronsted relation in k_{cat} for CO_2 hydration catalyzed by mutants of HCA III with replacements at position 198; for example, the mutants F198D and F198Y HCA III had similar low pH values for k_{cat} although the pK_a of zinc-bound water is greater for F198D by at least three pK_a units (Table 6).

This indicates that some other feature of the active site cavity is altered in these mutants in a way to affect k_{cat} for CO_2 hydration. For k_{cat} values at low pH, where proton transfer occurs presumably between zinc-bound water and bulk water and is not influenced by the effects of lysine 64, our mutants fall into two groups: (1) At k_{cat} near $10^3 s^{-1}$ are those residues at 198 that have a hydrogen-bonding capability, Asn, Asp, Phe, and Tyr. The x-ray crystal structure of BCA III (Eriksson, 1988) shows a water molecule hydrogen-bonded to the π -system of the phenylalanine ring

illustrating it as part of a chain of hydrogen-bonded water molecules that extends to zinc-bound water. (2) At k_{cat} near 10^4 s^{-1} are those residues with no hydrogen bonding capability, Ala, Val, Leu. This 10-fold difference in k_{cat} may well be due to this difference in hydrogen bonding capability and a resultant alteration in the proton transfer pathway. Indeed, Venkatasubban and Silverman (1980) have shown from hydrogen solvent isotope effects that proton transfer proceeds through at least two hydrogen bonded water molecules extending from the zinc-bound water. It is also interesting to note that the replacements at residue 198 which have k_{cat} near 10^3 s^{-1} differ in their charge and size. These properties appear to have little effect on proton transfer. This suggests that the common thread of hydrogen bonding capability and its affect on active site water have a substantial influence on the rate of proton transfer. Similarly, the replacements at residue 198 that are hydrophobic and have no hydrogen bonding capability also effect proton transfer. However, little influence on proton transfer based on the size of the replacement residue is observed.

Another possibility which could cause an altered proton transfer pathway and is associated with the hydrogen bonding network revolves around effects the 198 replacements have on Thr 199 whose hydroxyl side chain is hydrogen bonded directly to the zinc-bound water. Hillenbrand and Scheiner (1986) have shown that changes as large as 5 kcal/mole in the energy

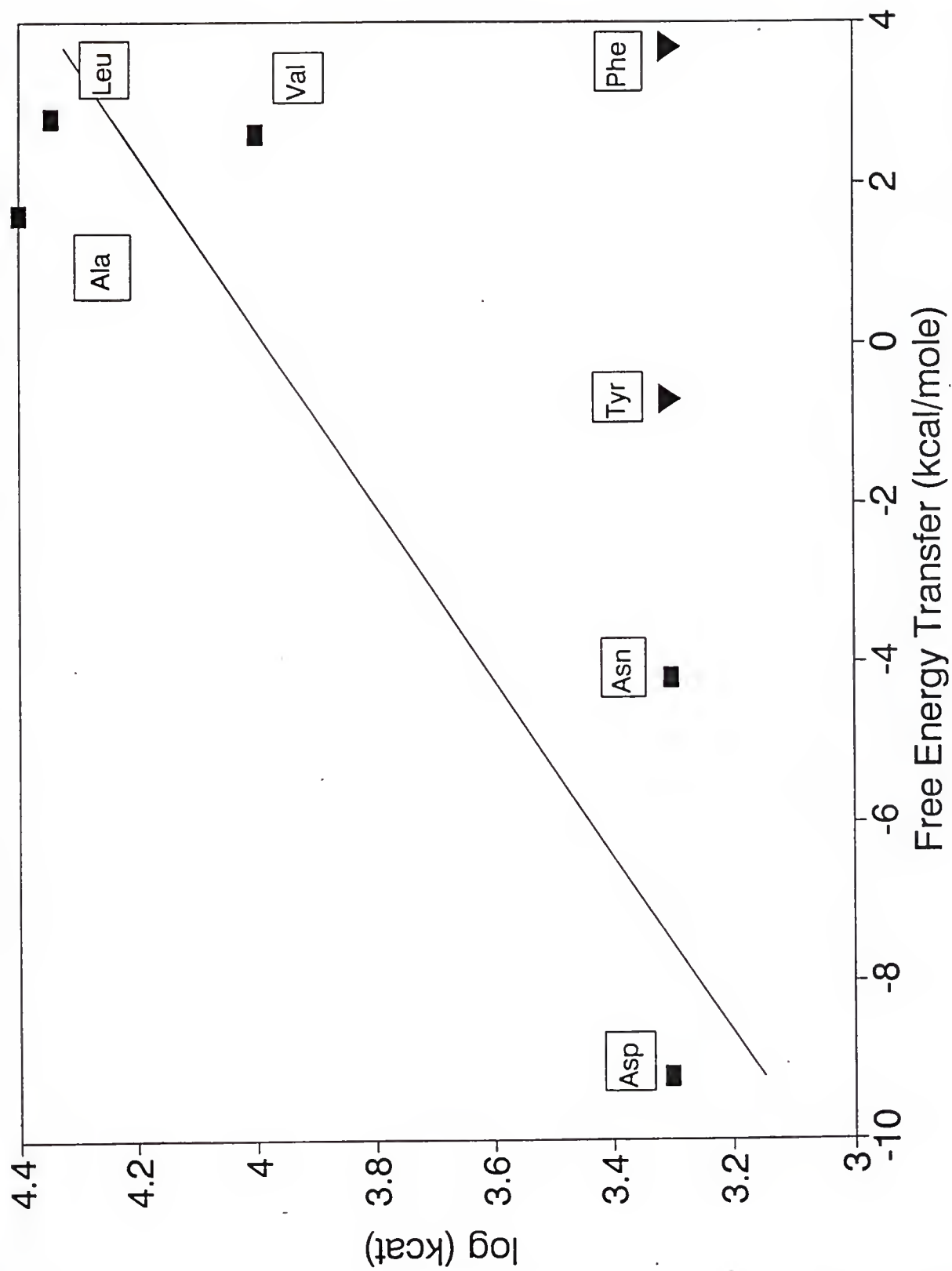
barrier for proton transfer involving water can result from changes as small as 0.1 Å in the distance of the hydrogen bond. Thus, small changes in hydrogen-bond distances in the active site as a result of replacements at residue 198 may well contribute to the observed variance in k_{cat} .

A third, but less likely explanation is illustrated in Figure 22 which presents a correlation between $\log(k_{\text{cat}})$ for hydration of CO_2 and the hydrophobicity of the side-chain present at position 198 in mutants of HCA III. The correlation is most apparent using the hydrophobicity scale of Engelman et al. (1986) (Figure 22) in which k_{cat} for wild-type HCA III and F198Y HCA III are aberrant and omitted from the correlation (slope, standard error, and correlation coefficient are 0.09 ± 0.03 , 0.79 in Figure 22). It is to be noted that this hydrophobicity scale includes the energy required to protonate the Asp side-chain. Poorer correlations were observed using other hydrophobicity scales; this includes the scale of Fauchere and Pliska (1983) (0.42 ± 0.23 , 0.46) and the scale of Sharp et al. (1991) (0.14 ± 0.13 , 0.23).

It is clear that among the hydrophobic residues at 198 the wild-type residue, Phe has a low value of k_{cat} and does not adhere to the correlations with hydrophobicity described in the previous paragraph. It is likely that such a hydrogen bond also exists in the mutant F198Y and could be the reason for their anomolous behavior. This result is different from

Figure 22. Plot of the logarithm of k_{cat} (s^{-1}) versus ΔG transfer (kcal/mole) of the amino acid side-chain from nonaqueous solution to water (Engelman et al., 1986).

The residue substituted at position 198 is given near the data point. The data are fit to a line using a least-squares analysis (the wild-type residue, Phe and the Tyr substitution were omitted from this calculation): slope = 0.09 ± 0.03 ; correlation coefficient = 0.79. Standard errors in k_{cat} were generally under 20%.



that found by Fierke et al. (1991) where they made substitutions at Val 143 in HCA II and Nair et al. (1991) where they made substitutions at Val 121 in HCA II. Their results showed no correlation of k_{cat} with hydrophobicity for substitutions of Val 143 HCA II and Val 121 HCA II leading them to conclude that the hydrophobic pocket plays an insignificant role in ordering the active-site water chain involved in transferring a proton from zinc-bound water to His 64. One possibility for the difference in our results and those of Fierke et al. (1991) and Nair et al. (1991) is that the disruption of the hydrogen-bonded molecule to Phe 198 in HCA III caused by our mutations may significantly alter active-site water structure. Since HCA II contains Leu at position 198, no analogous hydrogen-bonded water structure is present at that site (Eriksson et al., 1988) and therefore no similar change in the extended water network towards zinc-bound water is anticipated. This claim is supported by the results of Ren et al. (1991) and Taoka et al. (unpublished) in which they found little change in k_{cat} for the mutant L198F HCA II compared to wild-type HCA II. Even the double mutant, H64K-L198F HCA II had only a 3-fold reduction in k_{cat} compared to wild-type HCA II.

Thus, these rough correlations of k_{cat} with hydrophobicity most likely suggest a relation between the rate of proton transfer and the status of water in the active-site cavity of HCA III such that proton transfer is facilitated

when the more hydrophobic non-hydrogen bonding residues are present.

In a similar manner to k_{cat} , mutations at position 198 in HCA III affected R_{H_2O} . The pH-dependence of $R_{H_2O}/[E]$ for F198D and F198N HCA III could be fit quite well (correlation coefficient = 0.96 and 0.98, respectively) to a curve with two pK_a s (Figure 19). The pK_a of zinc-bound water measured from CO_2 hydration for F198D and F198N HCA III (Table 6, Figure 17) was set at 9.2 and 7.1, respectively. The pK , for the proton donor group of F198D and F198N HCA III was 8.2 ± 0.1 and 7.9 ± 0.1 , respectively. A pH profile having a maximal value at high pH and ionizations in the above range is consistent with proton transfer from lysine 64 to zinc-bound hydroxide. One possible reason why these values were between one and two pK units lower than that found in the steady state (9.6) is that in the equilibrium experiment many different ionization forms of the enzyme exist. Thus, the pK_a is a microscopic pK_a which is influenced by the different acid forms of the enzyme. Nevertheless, the above values are in fair agreement with the pK_a (8.5) determined for Lys 64 by Jewell et al. (1991).

The pH-independence (pH range 6 to 8.5) of k_{cat} seen for the mutants F198A, F198L, F198V and F198Y HCA III is also demonstrated in $R_{H_2O}/[E]$. These values ranged between 1×10^3 s^{-1} and 1.5×10^4 s^{-1} (Table 6). With respect to the pH-dependence and magnitude of $R_{H_2O}/[E]$, these mutants are

similar to R67N HCA III (Jewell et al., 1991), R67N-F198L HCA III (previous chapter), and H64A HCA II (Tu et al., 1989) indicating a proton transfer from water to zinc-bound hydroxide. Once again, this is the same interpretation as reached from the steady-state data.

Finally, it should be noted that no correlation between $R_{H_2O}/[E]$ and hydrophobicity was found (the slope, standard error, and correlation coefficient of $R_{H_2O}/[E]$ with hydrophobicity using the Engelman scale is 0.04 ± 0.05 , 0.15 again omitting the wild-type HCA III. It is not entirely clear why a correlation would be found between k_{cat} and hydrophobicity and not between R_{H_2O} and hydrophobicity.

Inhibition

The apparent inhibition constants K_I for ethoxzolamide and cyanate determined by inhibition of ^{18}O -exchange catalyzed by HCA III and six mutants show a strong dependence on the amino acid present at position 198 (Table 7). We have converted these apparent values of K_I to pH-independent binding constants by dividing each value of the apparent K_I by $(1 + K_a/[H^+])$ using the values of pK_a given in Table 6 or $pK_a = 5.2$ for the three enzymes with very low values of pK_a (see Table 6). These pH-independent values appear in parentheses in Table 7 and show a range on binding for cyanate caused by the changes at residue 198, but show only a small range of binding for ethoxzolamide caused by these

changes. This, however, excludes F198D HCA III. Eriksson et al. (1988) have shown that the thiadiazole ring of acetazolamide bound to HCA II is in van der Waals contact with the side-chain of Leu 198. From this observation on HCA II, they have suggested an unfavorable steric interaction between the thiadiazole ring of acetazolamide with Phe 198 to account for the weak binding of acetazolamide to HCA III. Our data show that the binding of ethoxzolamide is roughly the same for F198A, F198L, F198N, F198V, F198Y, and HCA III, suggesting that steric factors do not influence ethoxzolamide binding to HCA III and its mutants. The weak binding when aspartic acid is present at position 198 is most likely due to an unfavorable interaction of the charged side-chain and the aromatic component of ethoxzolamide.

The inhibition of the F198L and F198Y mutants by cyanate show little deviation from wild-type HCA III (Table 7). The replacement Phe 198 → Asp resulted in a mutant enzyme which is approximately 5×10^4 times (pH independent value) more weakly inhibited by cyanate. The most likely explanation for this decrease in binding of cyanate is an electronic repulsion of cyanate with the carboxylate of aspartic acid. This is illustrated by a difference of -1.78 kcal/mole in $\Delta\Delta G$ ($\Delta G_{\text{Asp}} - \Delta G_{\text{Asn}}$) for K_I cyanate between the mutants F198D and F198N HCA III. It is to be noted that binding of cyanate to HCA II has been found to occur at the backbone NH of Thr 199

and not at zinc (A. Liljas, personal communication), although thiocyanate does bind to the zinc and is in van der Waals contact with Leu 198 (Eriksson et al., 1988). Such information is not yet available for isozyme III. It is also worthy to note that a linear correlation (correlation coefficient 0.77) between $-\log (K_I)$ cyanate and the volume (Richards, 1977) of the amino acid present at position 198 was found. The same analysis for k_{cat}/K_m for CO_2 hydration yields a weaker correlation indicating that cyanate binding to these mutants is more sensitive to the size of the amino acid present at position 198 than CO_2 and HCO_3^- inter-conversion. This is supported with the observation that $\Delta\Delta G$ for k_{cat}/K_m between F198D HCA III and wild-type HCA III is -2.9 kcal/mole whereas $\Delta\Delta G$ for K_I cyanate between F198D HCA III and wild-type HCA III is -6.4 kcal/mole. These data suggest that the CO_2 and cyanate binding sites are probably separate in HCA III, and are complimentary to the findings of Fierke et al. (1991) where they conclude separate binding sites for CO_2 and cyanate in HCA II.

Conclusion

By replacing Phe 198 in HCA III with amino acids which probe the effect that size, charge, hydrogen bonding capability, and hydrophobicity have on the kinetic and inhibition constants we have confirmed the importance of this position as a major source for the unique catalytic and

inhibition properties of HCA III. Specifically, our results suggest that mutations at position 198 affect the proton transfer pathway possibly thru an alteration of active-site water structure. Furthermore, Asp at position 198 increases CO₂ hydration activity by a combination of effects predominated by electrostatic contributions which most likely act by increasing the nucleophilicity of the zinc center, and facilitating the release of HCO₃⁻.

CHAPTER 5 DISCUSSION AND CONCLUSIONS

The unifying goal of this project was to determine at the molecular level the importance of unique active-site residues in the catalytic mechanism of human carbonic anhydrase III and to account for the difference in catalytic and inhibition properties between HCA III and HCA II. A focal point of this interest was phenylalanine 198 in HCA III. To accomplish this task, a site-directed mutagenesis approach was used.

To a significant extent, we have achieved much of this goal. The triple mutant K64H-R67N-F198L HCA III had catalytic and inhibition properties similar to HCA II. The rate constant, k_{cat}/K_m , was increased 60-fold over wild-type HCA III, to a level that was only 8-fold less than HCA II. Furthermore, the triple mutant had a turnover number for CO_2 hydration which approximated that of HCA II in magnitude and pH profile. Additionally, the binding constant, K_I , for ethoxzolamide, and k_{cat}/K_m for the hydrolysis of 4-nitrophenyl acetate were approximately equal to that for HCA II. Therefore, the combination of mutations at positions 64, 67, and 198 in HCA III to their corresponding residues in HCA II gave a mutant HCA III almost identical to HCA II in catalytic and inhibition properties.

When only single point mutations were considered at position 198 in HCA III our results showed the replacement Phe 198 → Asp yielded a mutant enzyme which approached HCA II within 3-fold in catalytic activity and proton transfer activity further signifying the important role residue 198 plays in the catalytic function of HCA III. Indeed, all replacements at position 198 have shown Phe 198 to be a major contributor to the low CO₂ hydration activity, the low pK_a of zinc-bound water, and a major interactive binding site of inhibitors in HCA III.

Replacements at Phe 198 suggest several possible mechanisms for proton transfer in HCA III. For example, our data suggest that at low pH (6 to 8) proton transfer occurs presumably between zinc-bound water and water in the active site, is most likely diffusion controlled (Rowlett et al., 1991), and is not influenced by the effects of Lys 64. At high pH however, the enhancement of k_{cat} for the F198D and F198N HCA III is consistent with proton transfer from zinc-bound water to Lys 64. In addition, there may be alternate pathways involving other basic groups such as Tyr 7, which may act as proton acceptor along with Lys 64. Moreover, Tu et al. (1990) have shown that proton transfer in catalysis by HCA III can be enhanced 6-fold by the addition of 100 mM imidazole. Furthermore, we have observed at low pH that our mutants fall into two groups: those with hydrogen-bonding capability (Asn, Asp, Phe, Tyr) have k_{cat} near 10^3 s^{-1} , and those without hydrogen-bonding capability (Ala, Leu, Val)

have k_{cat} near 10^4 s^{-1} . For isozyme II, proton transfer is believed to proceed through at least two hydrogen-bonded water molecules (Venkatasubban and Silverman, 1980) and isozyme III is believed to have the same pathway. Thus, our data may suggest an altered active-site water structure caused by mutations at residue 198. Finally, it remains unclear why intramolecular proton transfer as illustrated by the following mutants: wild-type HCA II, F198D HCA III, F198N HCA III, and H64A HCA II + 100 mM imidazole is limited at 10^6 s^{-1} .

It has also been suggested from our data that both nucleophilic attack and the release of HCO_3^- from the enzyme have rate-limiting contributions towards CO_2 and HCO_3^- interconversion. It has not yet been established the degree to which each of these processes contributes to overall CO_2 and HCO_3^- interconversion, and to what extent it differs for the various mutants studied. Furthermore, these studies have not established a definitive CO_2 binding site and consequently do not reflect upon the possible rate-contributing aspects of CO_2 binding towards CO_2 and HCO_3^- interconversion.

These results raise the question: Why did isozyme III evolve in slow-oxidative muscle tissue to be catalytically less efficient both in its C hydration activity and its ester hydrolysis activity than its red blood cell counterpart isozyme II? One answer may be that isozyme III has evolved to have a low esterase activity rather than a high CO_2

hydration activity. This may serve the muscle tissue well considering the many indigenous glycolytic ester substrates and triacylglycerol present in these cells. CO₂ hydration occurs at the same catalytic center as ester hydrolysis in isozyme II. I suggest that CO₂ hydration activity is lower in isozyme III as a consequence of the evolutionary predisposition to have negligible ester hydrolysis activity. In turn, the muscle cell compensates for the low CO₂ hydration activity with increased enzyme concentrations which have been shown to be 0.5 mM (Carter et al., 1982). That is, the cell wants an enzyme with no esterase activity so indigenous esters needed for glycolysis are not hydrolyzed, but one that can still accelerate CO₂ hydration to facilitate CO₂ transport.

The data from our work supports this hypothesis. The replacement Phe 198 → Leu gives an HCA III mutant with considerable 4-nitrophenyl acetate hydrolysis activity as well as enhanced CO₂ hydration activity showing how closely these two activities are associated. Moreover, Ren et al. (1991) have shown little effect on either CO₂ hydration or 4-nitrophenyl acetate hydrolysis activity when Leu 198 is replaced with Phe in HCA II. In addition, the association of CO₂ hydration and 4-nitrophenyl acetate hydrolysis activity is further illustrated by replacements made at positions 121 and 143 in HCA II (Nair et al., 1991; Fierke et al., 1991) which showed corresponding decreases in CO₂ hydration activity and 4-nitrophenyl acetate hydrolysis activity.

Further support for this hypothesis comes from the mutant F198D HCA III which manages to separate CO₂ hydration activity and 4-nitrophenyl acetate hydrolysis activity. According to the hypothesis, this mutant would be the ideal enzyme for the muscle cell because it has a high CO₂ hydration activity but no esterase activity. The question then becomes, why did the enzyme evolve without aspartate at position 198. The most likely answer is that placing Asp in the hydrophobic region of position 198 in HCA III causes the enzyme to be highly unstable. Indeed, we have observed that F198D HCA III loses its catalytic activity in 25 mM Tris pH 8.1 buffer approximately 5-times faster than wild-type HCA III (unpublished observations). Accordingly, the muscle cell evolved an enzyme which functions most efficiently based on its stability, its cellular requirements, and cellular milieu. An ironic twist may indeed be that HCA III has evolved just as efficiently as HCA II considering its biological role.

Two experiments to test this hypothesis are: testing the esterase activity of wild-type HCA III, wild-type HCA II, F198L HCA III, and F198D HCA III on a variety of the glycolytic and triacylglycerol substrates. If the hypothesis is correct, F198L HCA III and wild-type HCA II will have esterase activity on some of these substrates. Further experimental support could come from measuring *in vivo* in our *E coli* expression system how glycolysis is affected by these four enzymes. Once again, F198L HCA III and wild-type HCA II

should interfere with the glycolytic pathway whereas wild-type HCA III and F198D HCA III should not effect glycolysis.

Lastly, no direct evidence has been reported that indicates HCA III has any other significant biological role. For example, the very weak phosphatase activity that has been reported (Koester et al., 1981) is believed to occur at a site different than for CO₂ hydration. More importantly, no physiological substrate for the phosphatase activity is known (Gros and Dodgson, 1988). Moreover, modifiers such as phosphate have been shown to have little effect on CO₂ and HCO₃⁻ interconversion (Paranawithana et al., 1990), but can effect k_{cat} approximately 3-fold (Paranawithana et al., 1990; Rowlett et al., 1991).

To fully understand in a quantitative manner the kinetic effects of site-specific mutants, they must be interpreted in conjunction with structural information as determined by nuclear magnetic resonance (NMR), and x-ray crystallography. With a prolific expression system in place for HCA III mutants, uniform isotopic labeling and the associated NMR experiments similar to those done on HCA II by Venters et al. (1991) are a logical extension of our current work. Moreover, the dynamics of aromatic residues of HCA III and F198Y HCA III can be investigated. Wuthrich and Wagner (1975) and Cambell et al. (1975) have studied the rotational freedom of aromatic amino acids in basic pancreatic trypsin inhibitor and hen lysozyme respectively. This approach can be applied to HCA III and the F198Y HCA III mutant to

determine if the aromatic ring of position 198 is constrained in an anisotropic environment. This in turn may give insights into the overall environment of position 198 and its associated water structure.

In conjunction with the NMR structural characterization, high-resolution crystal structures of HCA III 198-mutants is a second logical extension of our work. These crystal structures will potentially help us determine if the mutations at position 198 have indeed caused changes in hydrogen bonding distances and active-site water structure, and therefore allow us to quantitate the contribution that mutation has made towards lowering the energy barrier for proton transfer. Additionally, changes in backbone structure can be quantitated, and the effects on other key residues such as Thr 199, can be calculated. Initial attempts in this lab have been successful in crystallizing HCA III and mutants containing replacements at position 198. These crystals will be delivered to University of Lund, Sweeden, for x-ray diffraction studies.

LIST OF REFERENCES

- Ackers, G.K., & Smith, F.R. (1985). *Ann. Rev. Biochem.* 54, 597-629.
- Alexander, R.S., Nair, S.K., & Christianson, D.W. (1991). *Biochemistry* 30, 11064-11072.
- Behravan, G., Jonsson, B.-H., & Linskog, S. (1990). *Eur. J. Biochem.* 190, 351-357.
- Beychok, S., Armstrong, J. McD., Lindblow, C. & Edsall, J.T., (1966). *J. Biol. Chem.* 241, 5150-5160.
- Brady, H.J.M., Lowe, N., Sowden, J.C., Barlow, J.H. & Butterworth, P.H.W. (1987). *Biochem. Soc. Trans.* 17, 184-185.
- Campbell, I.D., Dobson, C.M., & Williams, R.J.P. (1975). *Proc. R. Soc. Lond. B* 189, 503-509.
- Carter, N., Jeffery, S., & Shiels, A. (1982). *FEBS Lett.* 139, 265-266.
- Carter, N.D., Shiels, A., Jeffery, S., Heath, R., Wilson, C.A., et al. (1984). *Ann. NY Acad. Sci.* 429, 287-301.
- Carter, P.J., Winter, G., Wilkinson, A.J., & Fersht, A.R. (1984). *Cell* 38, 835-840.
- Coleman, J.E. (1968). *J. Biol. Chem.* 243, 4574-4587.
- Craig, W.S., & Garber, B.P., (1977). *J. Am. Chem. Soc.* 99, 4130-4134.
- Davis, M.B., West, L.F., Barlow, J.H., Butterworth, P.H.W., Lloyd, J.C., & Edwards, Y.H. (1987). *Somat. Cell. Mol. Genet.* 13, 173-178.
- Dermietzel, R., Leibstein, A., Siffert, W., Zamboglou, N., & Gros, G. (1985). *J. Histochem. Cytochem.* 33, 93-98.
- Eigen, M. (1964). *Angew. Chem. Int. Ed. Engl.* 3, 1-72.
- Engberg, P., & Linskog, S. (1984). *FEBS Lett.* 170, 326-330.
- Engberg, P., Millqvist, E., Pohl, G. & Linskog, S. (1985). *Arch. Biochem. Biophys.* 241, 628-638.

- Engleman, D.M., Steitz, T.A., & Goldman, A. (1986). *Am. Rev. Biophys. Biophys. Chem.* 15, 321-353.
- Eriksson, A.E. (1988). *Doctoral Dissertation*, Uppsala University.
- Eriksson, A.E., Jones, T.A., & Liljas, A. (1988). *Proteins: Struct. Funct. and Genet.* 4, 274-282.
- Fauchere, J.-L., & Pliska, V. (1983). *Eur. J. Med. Chem.* 18, 369-375.
- Fersht, A. (1985). Enzyme Structure and Mechanism, W.H. Freeman & Company, New York.
- Fierke, C.A., Calderone, T.L., & Krebs, J.F. (1991). *Biochemistry* 30, 11054-11063.
- Gros, G., & Dodgson, S.J. (1988). *Ann. Rev. Physiol.* 50, 669-694.
- Gros, G., Forster, R.E., & Dodgson, S.J. (1987). In Mechanisms and Control of pH Homeostasis, D. Haussinger, ed. Academic Press, London.
- Henderson, L.E., Henricksson, D., & Nyman, P.O. (1973). *Biochem. Biophys. Res. Commun.* 52, 1388-1394.
- Hillenbrand, E.A., & Scheiner, S. (1986). *J. Am. Chem. Soc.* 108, 7178-7186.
- Jeffery, S., Carter, N.D., & Wilson, C. (1984). *Biochem. J.* 221, 927-929.
- Jeffery, S., Wilson, C.A., Mode, A., Gustafsson, J.-A., & Carter, N.A. (1986). *J. Endocrinol.* 110, 123-126.
- Jewell, D.A., Tu, C.K., Paranawithana, S.R., Tanhauser, S.M., LoGrasso, P.V., Laipis, P.J., & Silverman, D.N. (1991). *Biochemistry* 30, 1484-1490.
- Jonsson, B.-H., Steiner, H., & Lindskog, S. (1976). *FEBS Lett.* 64, 310-314.
- Kannan, K.K. (1980). In Biophysics and Physiology of Carbon Dioxide, C. Bauer, G. Gros, and H. Bartels, eds. Springer-Verlag, Berlin. pp. 184-189.
- Karali, T., & Silverman, D.N. (1985). *J. Biol. Chem.* 260, 3484-3489.
- Kato, K. (1990). *FEBS Lett.* 271, 137-140.

- Khalifah, R.G. (1971). *J. Biol. Chem.* 246, 2561-2573.
- Khalifah, R.G. (1973). *Proc. Natl. Acad. Sci. U.S.A.* 70, 1986-1991.
- Koester, M.K., Pullan, L. M., & Noltmann, E.A. (1981). *Arch. Biochem. Biophys.* 211, 632-642.
- Kunkel, T.A. (1985). *Proc. Natl. Acad. Sci. U.S.A.* 82, 488-492.
- Kunkel, T.A., Roberts, J.D., & Zabour, R.A. (1987). *Methods in Enzymology* 154, 367-382.
- Liljas, A., Kannan, K.K., Bergsten, P.-C., Waara, I., Fridborg, K., Strandberg, B., Carlbon, U., Jarup, L., Lovgren, S., & Petef, M. (1972). *Nature New Biol.* 235, 131-137.
- Lin, K.T.D., & Deutsch, H.F. (1974). *J. Biol. Chem.* 249, 2329-2337.
- Lindskog, S. (1966). *Biochemistry* 5, 2641-2646.
- Lindskog, S. (1982). *Adv. Inorg. Biochem.* 4, 115-170.
- Lindskog, S. (1984). *J. Mol. Catal.* 23, 357-368.
- Lindskog, S. & Coleman, J.E. (1973). *Proc. Natl. Acad. Sci. U.S.A.* 70, 2502-2508.
- Lindskog, S., & Thorslund, A. (1968). *Eur. J. Biochem.* 3, 453-460.
- Lloyd, J., McMillian, S., Hopkinson, D. & Edwards, Y. (1986). *Gene* 241, 233-239.
- LoGrasso, P.V., Tu, C.K., Jewell, D.A., Wynns, G.C., Laipis, P.J., & Silverman, D.N. (1991). *Biochemistry* 30, 8463-8470.
- Martin, R.B. (1974). *Proc. Natl. Acad. Sci. U.S.A.* 71, 4346-4347.
- Merz, K.A. Jr. (1991). *J. Am. Chem. Soc.* 113, 406-411.
- Mills, G.A., & Urey, H.C. (1940). *J. Am. Chem. Soc.* 62, 1019-1026.
- Montgomery, J.C. (1988). *Doctoral Dissertation*, University of Michigan.
- Nair, S.K., Calderone, T.L, Christianson, D.W., & Fierke, C.A. (1991). *J. Biol. Chem.* 266, 17320-17325.

- Nishita, T., & Deutsch, H.F. (1986). *Int. J. Biochem.* 18, 319-325.
- Paranawithana, S.R., Tu, C.K., Laipis, P.J., & Silverman, D.N. (1990). *J. Biol. Chem.* 265, 22270-22274.
- Pocker, Y. & Bjorkquist, D.W. (1977). *Biochemistry* 26, 5698-5707.
- Pocker, Y., & Sarkanen, S. (1978). *Adv. Enzymol. Relat. Areas Mol. Biol.* 47, 149-274.
- Ren, X., Jonsson, B.-H., & Lindskog, S. (1991). *Eur. J. Biochem.* 201, 417-420.
- Ren, X., Sandstrom, A., & Lindskog, S. (1988). *Eur. J. Biochem.* 173, 73-78.
- Richards, F.A. (1977). *Ann. Rev. Biophys. Bioeng.* 6, 151-176.
- Rosenberg, A.H., Lade, B.N., Chui, D.-S., Lin, S.-W., Dunn, J.J., & Studier, F.W. (1987). *Gene* 56, 125-135.
- Roughton, F.J.W. (1935). *Physiol. Rev.* 15, 241-296.
- Rowlett, R.S., & Silverman, D.N. (1982). *J. Am. Chem. Soc.* 104, 6737-6741.
- Rowlett, R.S., Gargiulo, N.J., Santoli, F.A., Jackson, J.M., & Corbett, A.H. (1991). *J. Biol. Chem.* 266, 933-941.
- Sanger, F., Nicklen, S., & Coulson, A.R. (1977). *Proc. Natl. Acad. Sci. U.S.A.* 74, 5463-5467.
- Sanyal, G., Swenson, E., Pessah, N., & Maren, T. (1982). *Mol. Pharmacol.* 22, 211-220.
- Scheiner, S., & Hillenbrand, E.A. (1985). *Proc. Natl. Acad. Sci. U.S.A.* 82, 2741-2745.
- Segel, I.H. (1975). Enzyme Kinetics, John Wiley & Sons, New York.
- Sharp, K.A., Nicholls, A., Friedman, R., & Honig, B. (1991). *Biochemistry* 30, 9686-9697.
- Shiels, A., Jeffery, S., Wilson, C., & Carter, N. (1984). *Biochem. J.* 218, 281-284.
- Shima, K., Tashiro, K., Hibi, N., Tsukada, Y., & Hirai, H. (1983). *Acta Neuropathol.* 59, 237-239.
- Siffert, W., & Gros, G. (1982). *Biochem. J.* 205, 559-566.

- Silverman, D.N., & Lindskog, S. (1988). *Acc. Chem. Res.* 21, 30-36.
- Silverman, D.N., & Tu, C.K. (1975). *J. Am Chem. Soc.* 97, 2263-2269.
- Silverman, D.N., & Tu, C.K. (1976). *J. Am. Chem. Soc.* 98, 978-984.
- Silverman, D. N., Tu, C.K., Lindskog, S., & Wynns, G.C. (1979). *J. Am. Chem. Soc.* 101, 6734-6740.
- Simonsson, I., & Lindskog, S. (1982). *Eur. J. Biochem.* 123, 29-36.
- Simonsson, I., Jonsson, B.H., & Lidskog, S. (1979). *Eur. J. Biochem.* 93, 409-417.
- Steiner, H., Jonsson, B.H., & Lindskog, S. (1975). *Eur. J. Biochem.* 59, 253-259.
- Studier, F.W., & Moffatt, B.A. (1986). *J. Mol. Biol.* 189, 113-130.
- Tanhauser, S.M., Jewell, D.A., Tu, C.K., & Laipis, P.J. (unpublished).
- Taoka, S., Chen, X., Tarnuzzer, R., Van Heeke, G., Tu, C.K., & Silverman, D.N. (unpublished).
- Tashian, R.E. (1989). *Bioessays* 10. 186-192.
- Tibell, L., Forsman, C., Simonsson, I., & Lindskog, S. (1984). *Biochem, Biophys. Acta* 789, 302-310.
- Timasheff, S.N., Susi, H., & Stevens, L. (1967). *J. Biol. Chem.* 242, 5467-5473.
- Tu, C.K., Paranawithana, S.R., Jewell, D.A., Tanhauser, S.M., LoGrasso, P.V., Wynns, G.C., Laipis, P.J., & Silverman, D.N. (1990). *Biochemistry* 29, 6400-6405.
- Tu, C.K., Sanyal, G., Wynns, G.C., & Silverman, D.N. (1983). *J. Biol. Chem.* 256, 9466-9470.
- Tu, C.K., & Silverman, D.N. (1982). *Biochemistry* 21, 6353-6360.
- Tu, C.K., & Silverman, D.N. (1985). *Biochemistry* 24, 5881-5887.
- Tu, C.K., Silverman, D.N., Forsman, C., Jonsson, B.H., & Lindskog, S. (1989). *Biochemistry* 28, 7913-7918.

- Tu, C.K., Thomas, H.G., Wynns, G.C., & Silverman, D.N. (1986). *J. Biol. Chem.* 261, 10100-10103.
- Venkatasubban, K.S., & Silverman, D.N. (1980). *Biochemistry* 19, 4984-4989.
- Venta, P.J., Montgomery, J.C., Hewett-Emmett, D., Wiebauer, K., & Tashian, R.E. (1985). *J. Biol. Chem.* 260, 12130-12135.
- Venters, R.A., Calderone, T.L., Spicer, L.D., & Fierke, C.A. (1991). *Biochemistry* 30, 4491-4494.
- Verporte, J.A., Mehta, S. & Edsall, J.T. (1967). *J. Biol. Chem.* 242, 4221-4229.
- Wells, J.A., Vasser, M., & Powers, D.B. (1985). *Gene* 34, 315-323.
- Wistrand, P.J., Carter, N.D., & Asmark, H. (1987). *Comp. Biochem. Physiol.* 86A, 177-184.
- Wuthrich, K., & Wagner, G. (1975). *FEBS Lett.* 50, 265-268.
- Yoshihara, C.M., Lee, J.D., & Dodgson, J.B. (1987). *Nucl. Acids Res.* 15, 753-770.

BIOGRAPHICAL SKETCH

The author was born in Whitestone, NY, on March 26, 1963, and spent most of his youth at Boosters Beach and playing baseball. Upon graduation from St. Francis Prep High School in 1981, the author and his family moved to Port St. Lucie, FL. The author attended New York University where he earned a B.A. in chemistry in 1985. He subsequently attended Florida State University where he earned an M.S. in chemistry in 1988. While in Gainesville, he worked for Habitat For Humanity. Throughout his life, he has enjoyed sports, the Beatles, and Elvis.

I certify that I have read this study and that in my opinion it conforms to acceptable standards of scholarly presentation and is fully adequate, in scope and quality, as a dissertation for the degree of Doctor of Philosophy.



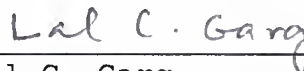
David N. Silverman, Chair
Professor of Pharmacology
and Therapeutics

I certify that I have read this study and that in my opinion it conforms to acceptable standards of scholarly presentation and is fully adequate, in scope and quality, as a dissertation for the degree of Doctor of Philosophy.



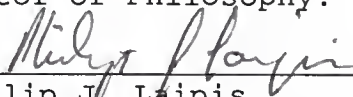
Ben M. Dunn
Professor of Biochemistry
and Molecular Biology

I certify that I have read this study and that in my opinion it conforms to acceptable standards of scholarly presentation and is fully adequate, in scope and quality, as a dissertation for the degree of Doctor of Philosophy.



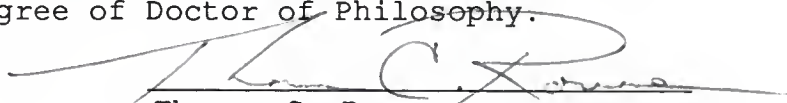
Lal C. Garg
Professor of Pharmacology
and Therapeutics

I certify that I have read this study and that in my opinion it conforms to acceptable standards of scholarly presentation and is fully adequate, in scope and quality, as a dissertation for the degree of Doctor of Philosophy.



Philip J. Laipis
Professor of Biochemistry
and Molecular Biology

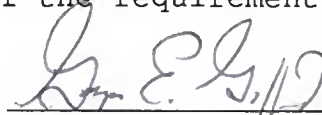
I certify that I have read this study and that in my opinion it conforms to acceptable standards of scholarly presentation and is fully adequate, in scope and quality, as a dissertation for the degree of Doctor of Philosophy.



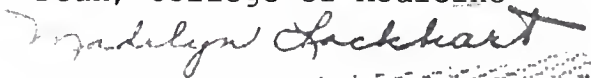
Thomas C. Rowe
Associate Professor of
Pharmacology and
Therapeutics

This dissertation was submitted to the Graduate Faculty of the College of Medicine and to the Graduate School and was accepted as partial fulfillment of the requirements for the degree of Doctor of Philosophy.

May, 1992



Dean, College of Medicine



Dean, Graduate School

UNIVERSITY OF FLORIDA



3 1262 08556 9902